Novel Hydrogels from Renewable Resources

by

Muzafer Ahmet Karaaslan

A dissertation submitted to the Graduate Faculty of
Auburn University
in partial fulfillment of the
requirements for the Degree of
Doctor of Philosophy

Auburn, Alabama
May 09, 2011

Keywords: Hydrogels, hemicellulose, chitosan, cellulose nanocrystals, semi-interpenetrating networks, nano-reinforcement

Approved by

Gisela Buschle-Diller, Chair, Professor of Polymer and Fiber Engineering
Peter Schwartz, Professor of Polymer and Fiber Engineering
Maria L. Auad, Professor of Polymer and Fiber Engineering
Xinyu Zhang, Professor of Polymer and Fiber Engineering

Abstract

The cell wall of most plant biomass from forest and agricultural resources consists of three major polymers, cellulose, hemicellulose and lignin. Of these, hemicelluloses have gained increasing attention as sustainable raw materials. In the first part of this study, novel pH-sensitive semi-IPN hydrogels based on hemicelluloses and chitosan were prepared using glutaraldehyde as the crosslinking agent. The hemicellulose isolated from aspen was analyzed for sugar content by HPLC, and its molecular weight distribution was determined by high performance size exclusion chromatography. Results revealed that hemicellulose had a broad molecular weight distribution with a fair amount of polymeric units, together with xylose, arabinose and glucose. The effect of hemicellulose content on mechanical properties and swelling behavior of hydrogels were investigated. The semi-IPNs hydrogel structure was confirmed by FT-IR, X-ray study and ninhydrin assay method. X-ray analysis showed that higher hemicellulose contents yielded higher crystallinity. Mechanical properties were mainly dependent on the crosslink density and average molecular weight between crosslinks. Swelling ratios increased with increasing hemicellulose content and were high at low pH values due to repulsion between similarly charged groups. In vitro release study of a model drug showed that these semi-IPN hydrogels could be used for controlled drug delivery into gastric fluid.

The aim of the second part of this study was to control the crosslink density and the mechanical properties of hemicellulose/chitosan semi-IPN hydrogels by changing the crosslinking sequence. It has been hypothesized that by performing the crosslinking step before introducing hemicellulose, covalent crosslinking of chitosan would not be hindered and therefore more and/or shorter crosslinks could be formed. Furthermore, additional secondary interactions and crystalline domains introduced through hemicellulose could be favorable in terms of mechanical stability of semi-IPN hydrogels.

In this last section of this study, the natural affinity of hemicellulose to cellulose was utilized to coat cellulose whiskers with chemically modified hemicellulose isolated from wood fiber. Surface modified cellulose nanowhiskers were used to prepare nanocomposite hydrogels using free radical polymerization of 2-hydroxyethyl methacrylate (HEMA), a biocompatible monomer. The effect of morphology and concentration of the incorporated nanocrystals on the hydrogel network was related to the mechanical properties, viscoelastic behavior and swelling of the hydrogels.

Acknowledgements

I would like express my sincere thanks to my advisor, Dr.Gisela Buschle-Diller, for her guidance, advice, encouragement and giving me the opportunity to complete my research work and dissertation. I am grateful to my committee members Dr. Peter Schwartz, Dr. Xinyu Zhang and Dr. Maria Auad for their help and suggestions. Many thanks go to Dr. Mandla Tshabalala for his collaboration and Dr. Brian Via for his service in my committee as the university reader. My sincere appreciation goes to the faculty, staff, graduate students of the Department of Polymer and Fiber Engineering, and group members of Dr. Buschle-Diller's lab for their help, support and friendship throughout my doctorate study. I owe thanks to Dr. Hasan B. Kocer for his help with NMR tests and ChemDraw software. I also would like to acknowledge the financial support of the Wood Education and Resource Center (WERC). Above all, I owe special thanks to my parents for their incredible encouragement, my wife and my son for being patient and supportive during my graduate work. Without their love, hope and prayers, I would not be where I am now.

Table of Contents

List of Tables

List of Figures

CHAPTER 1

Literature Review

1.1 Introduction

Polymers from renewable feedstock and biomass are viable substitutes for polymers derived from non-renewable and limited petrochemical resources. Unstable and rising oil prices and as well as environmental concerns on greenhouse emissions and landfill space are some of the driving forces for the use of polymers from renewable resources. Utilization, production, processing and new applications of these polymers have attracted increasing attention in the recent years.

In general, polymers from renewable resources can be categorized into three groups. The first group comprises natural polymers, such as polysaccharides and proteins, which exist in nature as in their polymeric form and can be extracted directly from biomass. The second group consists of synthetic polymers such as polylactic acid (PLA) synthesized by using monomers extracted from nature. The third group includes polyhydroxyalkonoates (PHA) and similar polymers that are synthesized by micro-organisms through fermentation of renewable monomers.[1]

In this study, hemicellulose, cellulose and chitosan, examples of first group of renewable polymers, have been utilized. The focus of Chapters 2 and 3 is hemicellulose

extracted from low value forest biomass via an alkaline process. Hemicellulose was blended with chitosan to synthesize hydrogel films for pH-responsive drug delivery applications. Rod-like shaped cellulose nanowhiskers isolated from aspen cellulose pulp were surface functionalized with chemically modified hemicellulose to synthesize nanoreinforced hydrogels for load bearing biomedical applications. This part of the study is presented in Chapter 4.

1.2 Hemicelluloses

Hemicelluloses are a class of hetero-polysaccharides present in the primary and secondary cell wall of wood and annual plants together with cellulose and lignin. They are considered to be the second most abundant polysaccharide in nature after cellulose, with an estimated production of 60 billion tons per year, representing about 20-35% of lignocellulosic biomass.[2,3] In general, hemicellulose is the non-crystalline alkali or water soluble material after removal of pectic substances from the constituents of the plant cell wall.[4] Hemicelluloses are considered to be found at the matrix or interphase between cellulose fibrils and other cell wall components. They are interconnected to each other through covalent bonds (such as ether and ester linkages with lignin) and secondary forces (such as hydrogen bonds with cellulose).

Unlike cellulose, which is a long and linear macromolecule that consists of approximately 10,000 D-glucose residues per molecule, hemicelluloses are low-molecular weight branched polysaccharides (DP=80-200) and may consist of various sugars such as D-xylose, L-arabinose, D-glucose, D-galactose, D-mannose, D-glucuronic

acid, D-galacturonic acid, L-rhamnose, L-fucose, and O-methylated neutral sugars in their repeating units. Depending on the plant species (e.g., grasses, cereals, hardwoods and softwoods) and cell wall type (primary or secondary), hemicellulose content, sugar content and structural patterns differ significantly. As an example, the weight percentages of the main constituents present in softwoods and hardwoods are shown in Table 1.1.

Table 1.1 Main constituents and their content in softwoods and hardwoods

Constituents	**% Weight**	
	Softwoods	**Hardwoods**
Cellulose	40-50	40-50
Hemicelluloses	20-30	25-40
Lignin	25-35	20-25
Extractives	0-25	0-25

Hemicelluloses can be categorized into four main groups; xyloglycans (xylans), mannoglycans (mannans), xyloglucans, and mixed linkage β-glucans.[5] Among all types of hemicelluloses, xylans are the predominantly biosynthesized polymer in plants and can be divided into several subclasses as follows: [5]

a) Homoxylans are linear polysaccharides including D-xylopyranosyl repeating units that are connected with β-(1→4), β-(1→3) and β-(1→3, 1→4) linkages. Figure 1.1 shows a partial chemical structure of their backbone.

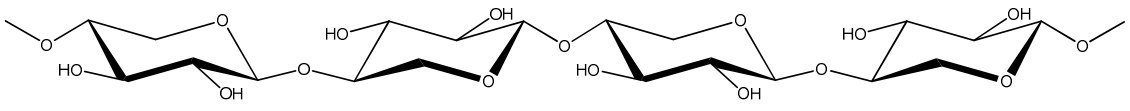

Figure 1.1 Partial chemical structure of β-(1→4) linked homoxylans

b) Glucoronoxylans have a backbone of β-(1→4)-linked D-xylopyranosyl residues, substituted with one α-(1→2)-linked 4-O-methyl-D-glucuronic acid and/or α-D-glucuronic acid. In their native form, they may also have some acetyl groups substituted from O-2 or O-3 positions. Approximately 90% of the hardwood hemicelluloses, which is the main focus of this study, belong to this type.[5] Figure 1.2 shows the partial structure of O-acetyl-(4-O-methylglucurono)xylans.

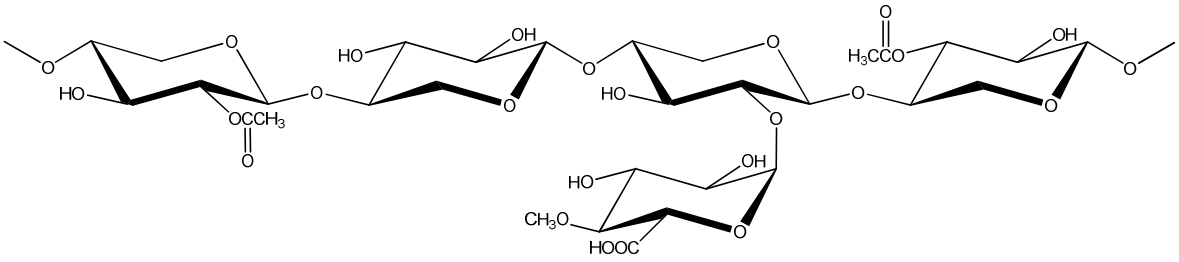

Figure 1.2 Partial chemical structure of O-acetyl-(4-O-methylglucurono)xylans

c) (Arabino)gluconoroxylans are common in softwoods and their structure is very similar to glucoronoxylans with additional α-L-arabinofuranosyl branches attached to D-xylopyranosyl backbone.

d) Arabinoxylans are found in grasses and cereal grains and consist of a β-(1→4)-linked D-xylopyranosyl backbone with α-L-arabinofuranosyl side units at O-2 or O-3 positions (see Figure 1.3).

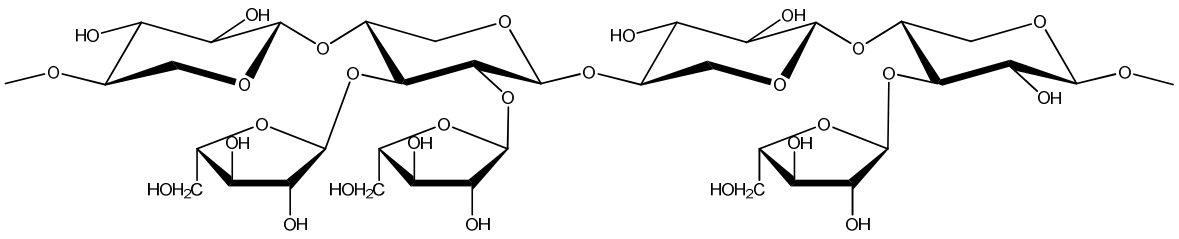

Figure 1.3 Partial chemical structure of L-arabino-D-xylan.

e) (Glucorono)arabinoxylans are also found in grasses and cereals. They consist of D-xylopyranosyl residues side units in addition to α-L-arabinofuranosyl branches.

f) Heteroxylans have a very complex structure and high degree of branching with oligomeric side chains.

Xyloglucans are another major group of hemicelluloses found in the primary cell wall of higher (dicotyledonous) plants whereas xylans are predominantly in the secondary cell wall of monocotyledonous plants and hardwoods.[6,7] Their backbone is different from xylans and consists of β(1→4)-glucopyranose units with α-D-xylopyranose residues attached. Figure 1.4 shows a typical partial structure of xyloglucans.

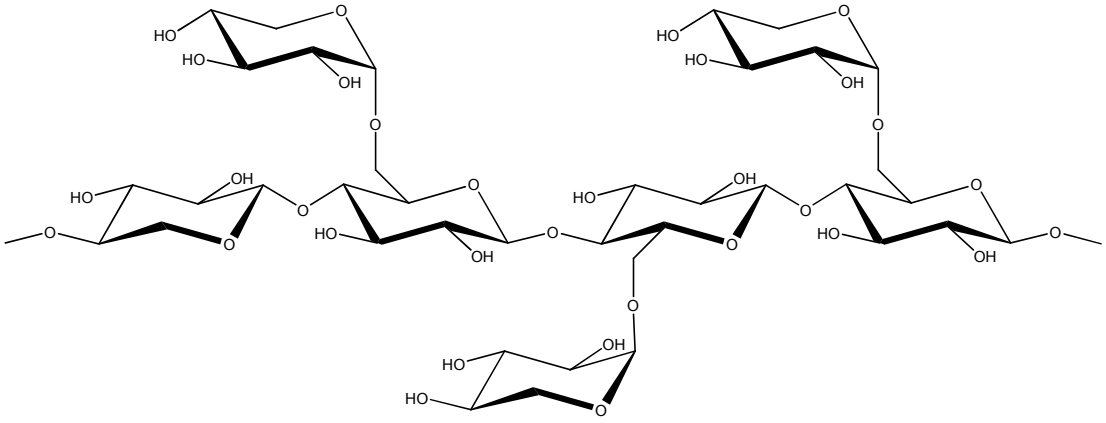

Figure 1.4 Partial chemical structure of D-xylo-D-glucan.

Hemicelluloses can be isolated from the lignocellulosic matrix of the plant cell wall by hydrolysis of ester linkages (deacetylation) which is commonly carried out through alkaline extraction or aqueous ammonia. To avoid saponification of ester linkages and to improve extraction yields, delignification treatments with sodium chloride and hydrogen peroxide prior to extraction can be performed. [8]

Hemicelluloses are amorphous in the native state because of the presence of acetyl groups in their structure, but can crystallize after removal of the acetyl groups by alkaline extraction.[9] Hardwood xylans are reported to crystallize in helical form and the crystallinity and interplanar spacings increase with increasing water content.[10] Compared to cellulose, xylans have weak intramolecular forces (van der Waals forces rather than hydrogen bonding) and need water to stabilize their structure. Therefore, xylans are less rigid than cellulose.[11]

The function of hemicelluloses in the plant cell wall has not yet been well understood. However, xylans are being suggested to have an important function in the aggregation pattern, for crystallinity and the dimensions of cellulose fibrils. [12,13] Another role assigned to hemicelluloses has been to provide linkages between cellulose fibrils and lignin matrix and hence to allow effective shear stress transfer throughout the cell wall. The shear and slip properties of hemicelluloses in the cell wall have been suggested as the mechanism for energy absorption in branches and stems of trees when resisting the wind.[14]

1.2.1 Applications

Hemicelluloses have not found many industrial applications like other plant polymers such as cellulose and lignin. To date, some of the common industrial uses were as sizing agents in papermaking and as the feedstock chemicals for xylitol, ethanol or lactic acid.[15] The reason for low utilization given was partial or complete degradation of hemicelluloses and loss of their polymeric properties during industrial pulping processes

which are mainly used to separate cellulose fibers from wood. However, recent studies showed that polymeric and oligomeric properties of hemicelluloses could be maintained with alkaline extraction processes.[16-18] So far, new potential uses for hemicelluloses can be divided into food and non-food applications. Hemicelluloses as food additives, viscosity enhancing thickeners, emulsifiers, adhesives, adsorbents, gelling agents, binder for charcoal/coal briquettes, and antitumor agents are some of the examples that have been suggested.[5,19,20]

Due to their hydrophilicity, biodegradability, biocompatibility and low toxicity, hemicelluloses have been studied by numerous research groups with respect to their use as hydrogels in biomedical applications. Blending with chitosan[16], polyvinyl alcohol[21] and copolymerization with 2-hydroxyethyl methacrylate[22] were some of the strategies investigated to prepare hydrogels. Oxygen barrier properties of hemicellulose-derived films for food packaging are found to be comparable with those of other commonly utilized biopolymers such as amylose, amylopectin and chitosan. B-glucan, arabinoxylan, glucuronoxylan, konjac glucomannan has been reported as examples of edible hemicellulose films for packaging uses.[23,24]

Recent research has been focused on use of hemicelluloses for the modification of cellulose fibers. Xylans have an inherent affinity to cellulose and irreversibly adsorb on cellulose surfaces.[25] For example, utilizing the strong hemicellulose-cellulose interaction, novel functionalities have been introduced on cellulose fibers without deteriorating its morphology and native structure. Chemically or enzymatically modified xyloglucan were

used for surface specific functionalization of cotton fiber, wood pulp fiber and regenerated cellulose.[26] Examples of inserted groups via xyloglucan were fluorescent optical brightening agents, nucleophiles such as amino groups and thiol groups, biomolecule capture agents and initiators for radical polymerization.[26] Mannans and xylans were shown to improve the tensile strength and wettability of kraft pulp/paper which was explained by increased cellulose fiber-fiber bonding ability in the presence of hemicellulose.[17]

1.3 Cellulose

Cellulose is the most abundant naturally occurring, renewable and biodegradable polymer available on earth biosynthesized by plants, green algae, bacteria and some sea animals at a total volume of over 10×10^{10} tons annually.[27] Owing to its ease of availability and low cost, it has been a commonly utilized resource as a natural fiber in textiles, paper making, and as food additive since the beginning of civilization. With increasing scientific knowledge and technological progress in the last century, the structure and chemistry of cellulose have been better understood. As a result, cellulose and its derivatives have found many new applications such as cellophane, regenerative fibers, adhesives, binders, thickeners, emulsifiers, lubricants, fillers, etc.[28] Moreover, due to the emerging field of nanotechnology, an emerging field of science dealing with the control of materials and devices in nanoscale (1 to 100 nm in at least one dimension), cellulose in the form of nanocrystals have attracted increasing attention as reinforcing filler for polymers and as templates for synthesis of nanostructures in last two decades.[29]

The chemical structure of cellulose was discovered in 1920s by Staudinger.[30] It is a high molecular weight linear polysaccharide consisting of D-anhydroglucopyranose monomeric units connected through β-(1,4) glycosidic linkages as shown in Figure 1.5.

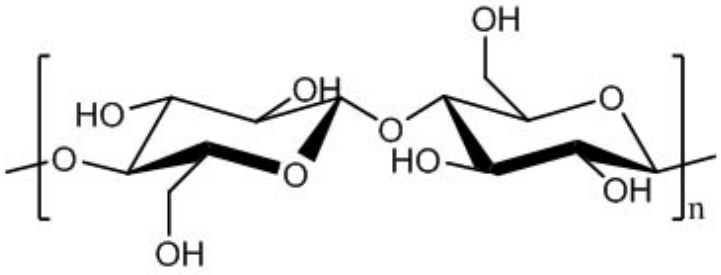

Figure 1.5 Chemical structure of cellulose

The degree of polymerization of cellulose depends on its source; and amounts to approximately 10,000 in wood and 15,000 in cotton.[31] In nature, cellulose does not exist in form of individual isolated molecule but as cellulose aggregates that form microfibrils which are long threadlike bundles of cellulose molecules with diameters ranging from 2 to 20 nm and lengths up to several tens of microns. Microfibrils are stabilized by intra- and intermolecular hydrogen bonds and van der Waals forces. As a consequence of this morphology, cellulose microfibrils have load-bearing capability and maintain the structural integrity of the plant cell wall. Cellulose fibers are further formed by aggregation of these microfibrils.[31] A representing scheme for the arrangement of cellulose fibrils and microfibrils in plant cell wall are shown in Figure 1.6.

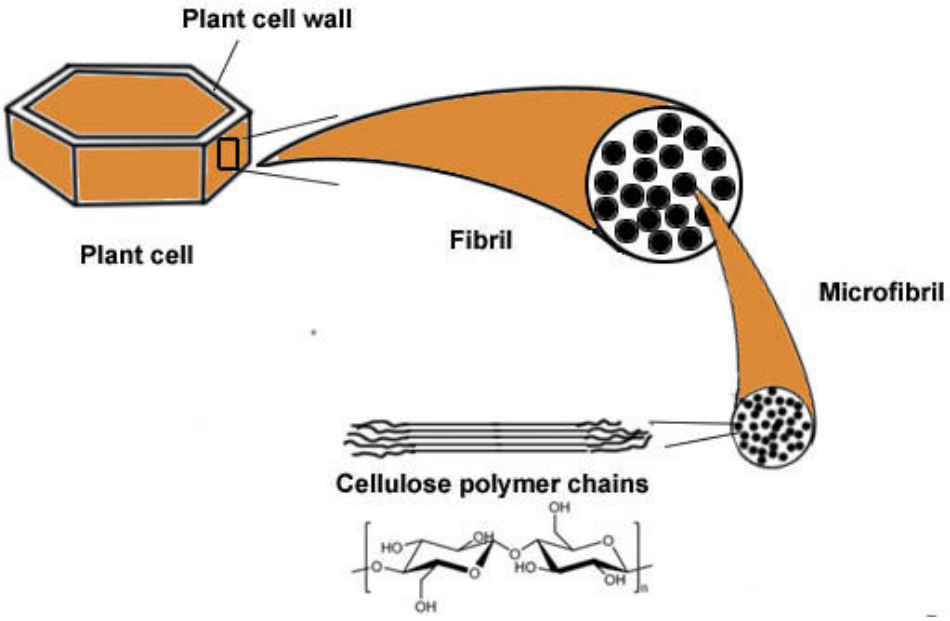

Figure 1.6 Cellulose, microfibrils and fibrils in the plant cell wall [32]

The crystalline structure of cellulose was first proposed in 1930s by Meyer and Misch.[33] Until now, six different crystal forms of cellulose have been described, however native cellulose (cellulose I) has been extensively studied. Depending on its origin and hydrogen bonding pattern native cellulose can occur in two different allomorphs; Iα and Iβ which correspond to triclinic and monoclinic unit cells, respectively. In addition to closely packed crystalline cellulose chains, native cellulose has less ordered amorphous domains as well. Degree of crystallinity or crystallinity index, the ratio of crystalline to amorphous regions, can be determined by using different techniques such as FT-IR, Raman, C-NMR, WAXS and SAXS.[34] X-ray crystallinity indices of some cellulosic materials obtained from various sources and in different forms are given in Table 1.2. When subjected to chemicals (acids, bases, water etc.), amorphous regions in cellulose are more susceptible to decomposition than the less accessible crystalline domains.

Table 1.2. X-ray crystallinity of some cellulosic materials[35]

	X-ray crystallinity (%)
Cotton linters	56-63
Sulfite dissolving pulp	50-56
Prehydrolyzed sulfate pulp	46
Viscose rayon	27-40
Regenerated cellulose film	40-45
Aspen Wood[36]	60-70
Microcrystalline cellulose[37]	77-90
Bacterial Cellulose[38]	81-87

1.3.1 Cellulose nanocrystals

Cellulose nanocrystals, which are also referred as cellulose whiskers or nanocrystalline cellulose, are rod-like highly crystalline nanoparticles prepared under controlled acid hydrolysis of cellulose microfibrils. Acid molecules can easily penetrate into randomly oriented amorphous regions and result in hydrolytic cleavage of glycosidic bonds. After hydrolysis and stabilization, a suspension of individual crystallites approximately 50nm-several μm in length and 3-10 nm in width can be formed.[29] The geometry and dimensions of these stiff nanoparticles depend on the hydrolysis conditions and the origin of the cellulose substrate. To date, the most common sources for preparing cellulose nanocrystals are cellulose fibers from cotton, hemp, sisal, ramie, wheat straw, palm, bleached softwood pulp, hardwood pulp, microcrystalline cellulose, sugar beet, bacterial cellulose and tunicates.[29,39] Table 1.3 shows the variation in dimensions of nanocrystals prepared from different cellulose sources.

Table 1.3 Dimensions of cellulose nanocrystals from various origins

Source	**Length (nm)**	**Width(nm)**
Cotton[40]	150-210	5-11
Ramie[42]	50-150	5-10
Tunicate[43]	1000-3000	15-30
Hardwood[39]	140-150	4-5
Softwood[44]	100-200	3-4
Bacterial cellulose[41]	100-1000	10-50
Algal(*Valonia*) [45]	>1000	10-20

Hydrolysis time, temperature, the type of acid, acid-to-pulp ratio and agitation are the parameters that most influence the resulting properties of cellulose nanocrystals.[31,39] For example, higher acid-to-pulp ratios and higher reaction temperature with longer reaction time generally result in shorter nanocrystals of the same origin of cellulose. Sulfuric acid and hydrochloric acid are the most extensively used acids for the hydrolysis. When sulfuric acid is used, negatively charged sulfate groups are introduced on the surface of the nanocrystals. Therefore, well-dispersed aqueous suspensions could be obtained by electrostatic repulsion forces among individual nanocrystals. A schematic of sulfuric acid hydrolysis of cellulose is shown in Fig.1.7. However, nanocrystals with no or minimal charge are formed in case of hydrolysis with hydrochloric acid, which results in limited dispersibility and unstable aqueous suspensions.

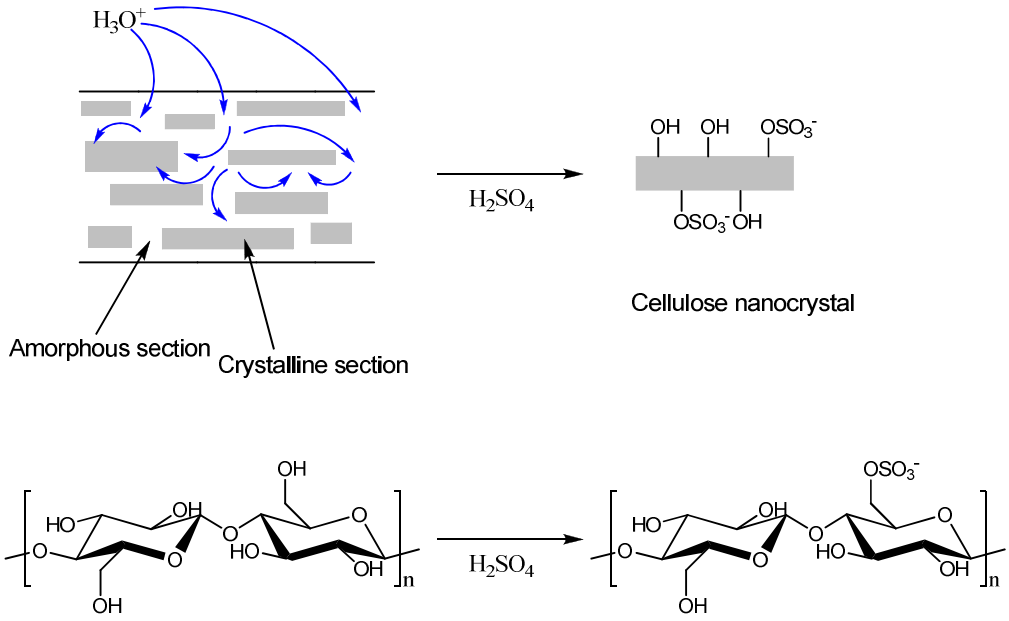

Figure 1.7 A Schematic representation of hydrolysis of cellulose with sulfuric acid

The ability to form stable suspensions, low cost, low density, abundance in nature, biodegradability, high specific modulus and strength, high specific surface area, the presence of reactive surface and easy processability are the main advantages of cellulose nanocrystals that make them promising candidates in nanocomposite applications.[31] Cellulose nanocrystals have been used as reinforcing fillers in numerous polymer matrices such as polyvinyl chloride, polypropylene, polyethylene, polyvinyl alcohol, polysulfonates, poly(styrene-co-butyl acetate), carboxymethyl cellulose, polyurethane, starch-based biopolymers, chitosan, polylactic acid etc.[29,31,46] It was reported that the reinforcing effect of cellulose nanocrystals on the mechanical, electrical and thermal behaviors of nanocomposites was dependent on the concentration of whiskers, their orientation and distribution in the matrix, their aspect ratio(length/width) and filler/matrix interactions.[29,46]

1.4 Chitosan

Chitosan is a polysaccharide derived from chitin by deacetylation. Chitin is the main structural component in the shells of crustaceans, mollusks and insects, and also occurs in the cell wall of some fungi. Commercially available chitin and chitosan are from waste of the seafood industry which abandons huge amount of crab and shrimp shells every year.[47] Chitin is extracted from ground shells by subsequent deproteination with HCl, demineralization with NaOH and decoloration with KMnO4 and oxalic acid treatments. Then chitosan is prepared by alkaline hydrolysis, using concentrated NaOH at high temperature.[48]

Chitin and chitosan are actually linear polysaccharides similar to cellulose. The difference is the glucosamine and N-acetyl glucosamine units attached to D-glucopyranose backbone (see Figure 1.8). Chitin consists of 2-acetamido-2-deoxy-β-D-glucopyranose, and chitosan of 2-amino-2-deoxy-β-D-glucopyranose. The ratio between the glucosamine units to N-acetyl glucosamine is referred as the degree of deacetylation (DD). Chitin and chitosan can form cationic charge when dissolved in slightly acidic solution and therefore have unique properties including chelating of metal ions and polyoxysalt formation. The molecular weight of chitosan ranges from 300 to over 1000kD with a degree of deacetylation from 30% to 95% depending on the source and preparation procedure. Unlike other polysaccharides, chitosan has a nitrogen content of about 5-8% depending on its DD; therefore chitosan can undergo reactions that are characteristic for primary amines.[48]

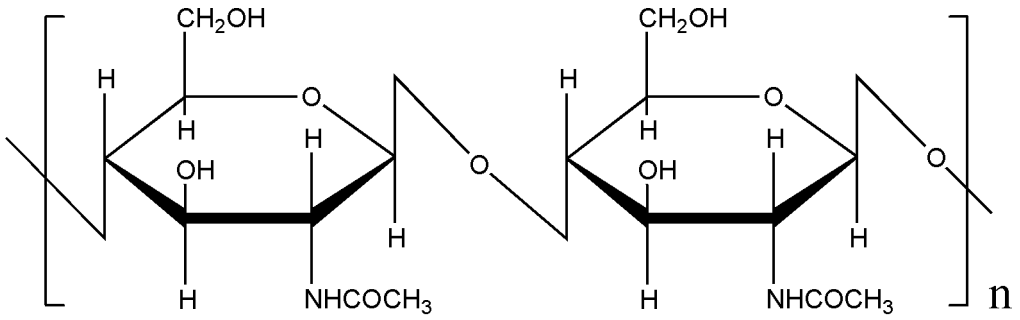

Chitin

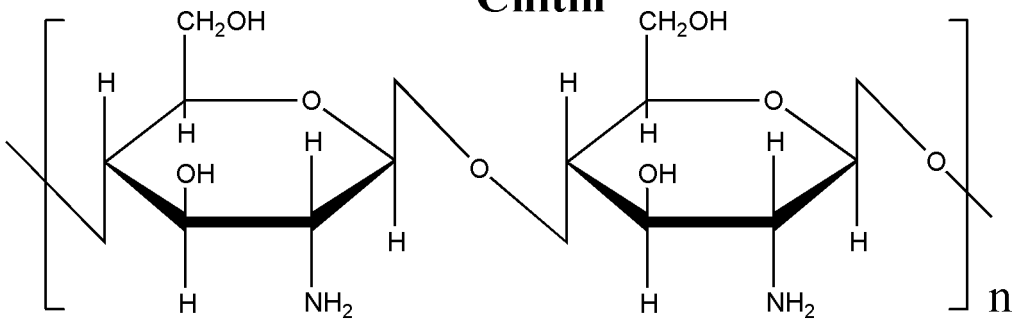

Chitosan

Figure1.8 Chemical Structures of repeating units of chitin and chitosan

Chitosan has a good chelating ability; the amine groups of chitosan can form complexes with heavy metal ions. Therefore, chitosan has found various applications in waste water treatments (e.g. textile dye effluents). The physical state of chitosan (powder, fiber, film, gel, etc.), the degree of deacetylation and the nature of the metal ions (affinity) are some factors that influence the efficiency of chitosan as a chelator.[49]

Chitosan is a hydrophilic, biocompatible, non-toxic, and biodegradable polymer which can be metabolized by certain human enzymes such as lysozyme.[50] In addition, it is physiologically inert, antibacterial, haemostatic, fungistatic, anti-tumoral, anti-cholesteremic and has notable affinity to proteins. Chitosan has gel-forming and film-

forming ability and can be used in the form of powder, beads, fibers, membranes, sponges, paste, and solutions. Therefore, chitosan has been safely used for biomedical, pharmaceutical and food applications.[51]

1.5 Hydrogels

Hydrogels made from biomaterials have attracted increasing attention in biology related applications since the 1960s due to the ability to retain large amounts of water in their structure. Hydrogels can be formed that show characteristic of natural living tissue and stimuli responsive swelling behavior. They are basically water-swollen networks at which polymer chains are connected to each other with chemical or physical junctions.[52]

In the literature, to better define their network structure, hydrogels are classified in different categories. For example, depending on the way that crosslinks are formed, they are divided into three classes. Chemical hydrogels consist of covalently crosslinked network. Physical hydrogels are formed by secondary interactions (such as hydrogen bonds, ionic bonds, hydrophobic interactions and crystallites etc.). A further option is entangled networks.

Covalently crosslinked hydrogels include polymer chains interconnected to an irreversibly formed three dimensional network. These networks behave as one large macromolecule and their molecular weight is nominally infinite. Crosslinkers used to form these networks are molecules with lower molecular weight than that of the chains between two consecutive crosslinks. Crosslinkers with two reactive functional groups

such as dialdehydes (glutaraldehyde, formaldehyde, glyoxal etc.) are commonly used for traditional chemical crosslinking of both synthetic and natural polymers (gelatin, chitosan, PVA etc.).[53] The advantage of using dialdehydes is to allow direct reaction in aqueous media under mild conditions without additional auxiliary molecules. However, these reagents are known to be toxic and mutagenic. The potential toxicity of residual unreacted molecules that can leach out is a great problem when these hydrogels are to be used *in vivo*. As an alternative to dialdehydes, non-toxic and environmentally-safe crosslinking agents (genipin, oxalic acid, etc.) with direct reaction pathways have been studied as well.[53] In addition, chemical crosslinking can be achieved by bulk or simultaneous copolymerization of a monomer with a crosslinking agent or by crosslinking of a polymer in solution by other means such as irradiation. These methods are carried out to form hydrogels from commonly studied synthetic polymers such as PVA, PHEMA, PAAm and PNIPAAm.[52]

Physical hydrogels are temporary or reversible networks that are formed by physical forces between polymer chains without using specific crosslinking agents. Secondary interactions such as Coulombic forces, dipole-dipole and van der Waals interactions, hydrophobic forces, hydrogen bonds, formation of crystallites or combinations of several of these forces are considered as physical crosslinks that ensure temporary integrity. Physical gels have a limited amount of non-covalent crosslinks and their number and position changes with time and temperature.[54] These hydrogels are usually weak, unstable and may disintegrate rapidly as compared to covalently crosslinked gels. However, physical hydrogels are advantageous where short term drug

delivery, biodegradability and *in situ* gel formation is required.[55] They are good candidates for applications where reversible sol-gel transition upon stimuli (temperature, pH, ionic strength, etc.) and responsive behavior are needed. A common way to prepare physical gels is to use repeated freeze-thaw cycles of a polymer solution. For example, polyvinyl alcohol has been extensively studied for its ability to form physical gels upon crystallite formation.[55-57] Swelling behavior and mechanical properties of PVA hydrogels can be tailored by varying the polymer concentration and number of freeze-thaw cycles. These hydrogels are particularity designed for artificial cartilage replacement and contact lens applications because of their enhanced mechanical strength, high elasticity, nontoxicity and biocompatibility.[55, 58]

Entanglement networks are formed by physical interactions of polymer chains twisting and wrapping around each other. These are formed either in the melt or in solution when the relative molecular weight becomes greater than the critical entanglement molecular weight of the polymer. Entanglement networks can dissolve with the addition of an excess amount of solvent. Current research on entangled networks is focused on forming so-called interpenetrating networks such as semi-IPNs or double network hydrogels.[59-62] These systems consist of two or more type of polymers. The first polymer network is chemically crosslinked while the second one is non-crosslinked and highly entangled, and filling the voids of the first network. The formation of physical entanglements act as soft continuous phase and enhance the energy dissipation of the entire network, resulting in enhanced mechanical strength and toughness. This kind of hydrogel can be used for load bearing biomedical applications such as articular cartilage

replacement.[63] Hydrogels including two or more components are designed not only to improve mechanical properties, but also to enhance swelling capacity, stimuli responsiveness, biocompatibility and morphology.[64, 65]

Hydrogels can be prepared from natural or synthetic polymers. The main advantages of natural polymers include low toxicity, inherent biocompatibility, biodegradability, low-cost and having biologically recognizable moieties that support cellular activities.[66, 67] Recently, the use of natural materials for hydrogel synthesis has attracted attention of many researchers. Polysaccharides (chitosan, alginate, hyaluronic acid, dextran, etc.) and proteins (fibrin, collagen, gelatin, etc.) are the two major classes of natural biopolymers that have been used as hydrogels for biomedical and pharmaceutical applications.[68] For example, chitosan is a promising polycationic biopolymer. It is biocompatible, antibacterial, and bioadhesive due to its positive charge in acidic medium and can be degraded by human enzymes (lysozyme). It is further said to promote wound-healing. Chitosan hydrogels prepared by chemical or physical ways are considered as pH-responsive and are suitable for controlled drug delivery.[69] In general, however, natural hydrogels are mechanically weak. Various methods such as chemical crosslinking and blending with synthetic polymers are used to enhance their mechanical stability.[70, 71]

Hydrogels prepared from synthetic polymers are often preferable for biomedical applications even though they do not have intrinsic bioactive properties like natural biopolymers. However, their ability to form well-defined hydrogel networks with

molecular-scale tune-ability and consistent properties are some of the advantages of synthetic hydrogels. For example, poly(2-hydroxyethyl-methacrylate) or PHEMA hydrogels are known to be the earliest hydrogels used for biomedical applications.[72] Good mechanical properties, optically transparency and stability in water allow PHEMA hydrogels to be used predominantly as contact lenses.[73] Chemical derivation and copolymerization of HEMA monomers has been studied in order to fine-tune PHEMA properties for drug delivery and tissue engineering applications.[74,75] Poly(vinyl alcohol) or PVA is another widely used synthetic polymer for hydrogel formation. PVA hydrogels are strong (tensile strength up to 17 MPa), non-adhesive to cells and proteins, show a low coefficient of friction and have similar structural properties to natural cartilage. Therefore, PVA gels have been suggested as a biomaterial for the replacement of diseased articular cartilage.[76, 77]

Hydrogels can also be classified as neutral, anionic or cationic according to the ionization of the pendant group. Hydrogel networks containing acidic (anionic) or basic (cationic) side groups can be responsive to the pH and ionic composition of the swelling medium. According to Donnan equilibrium swelling theory, the osmotic pressure gradient or ion concentration gradient between inside and outside of the hydrogel is the driving force for swelling. A hydrogel is referred to as pH-sensitive when swelling is a result of proton ionization and repulsion of charged groups.[78] For example, for ionic gels containing weakly acidic groups such as carboxyl (-COOH) in poly(acrylic acid), poly(methacrylic acid) or alginate, the degree of swelling increases as the pH of the swelling medium increases. Chitosan and poly(acrylamide) are as examples of ionic gels

containing weakly basic amine ($–NH_2$) groups that protonate and increase the degree of swelling as the pH of external solution decreases. The pH-sensitivity and drug release profile of hydrogels is tunable. For example, an increase in crosslink density, which can simply be adjusted by weight ratio of the crosslinker or monomer, induces a decrease in swelling and pH-sensitivity and improves the network stability.[79] pH-sensitive hydrogels are widely used in oral drug delivery where they can protect peptide/protein drugs in the digestive track.[80] There are several strategies that aim to improve pH-responsive swelling behavior of hydrogels. For example, some chemically crosslinked chitosan hydrogels have no pH-sensitive drug release in acidic conditions because most of the free amino groups are reacted with the crosslinker. pH and ion-sensitive drug release of such hydrogels could be improved by incorporating a second polymer which has different hydrophilicity from chitosan. Additional polymer chains decrease the crosslinking density and increase the amount of free amino groups available for protonization.[81]

Another group of widely studied stimuli-responsive hydrogels are temperature-sensitive hydrogels that have the ability to swell or deswell as a result of changing the temperature of the external swelling medium. There are two types of temperature-sensitive hydrogels; positive and negative. Positive hydrogels have an upper critical solution temperature (UCST) below which the network collapses upon cooling. Negative hydrogels have a lower critical solution temperature (LCST) above which the network collapses upon heating. In the latter one, below the LCST, water molecules form hydrogen bonds with polar groups of the polymer chain and organize around hydrophobic groups resulting in an increase in degree of swelling. Upon heating above the LCST,

bound water molecules are released and the polymer network collapses.[81] Poly(N-sopropylacrylamide) or PNIPAAm and its copolymers have been the most studied temperature sensitive hydrogels in the literature.[82] It has a LCST around 32ºC which is in the rage of human body temperature. PNIPAAm, can be used to prepare drug-delivery systems that exhibit a pulsatile release in response to temperature changes. PNIPAAm hydrogels are commonly being used for patterning cells studies because of their ability to be hydrophilic or hydrophobic depending on the temperature below or above its LCST.[83] By block copolymerizing PNIPAAm with an ionic polymer such as poly(acrylic acid), both pH- and temperature sensitive can be prepared. Such hydrogels are suggested to modulate the drug release kinetics of streptokinase.[84] In addition, hydrogels that can respond to various stimuli have also been reported. For example, hydrogels sensitive to biological analytes such as mono- and di-saccharides, enzymes, antigens and ions have been studied extensively for biomedical applications.[85] Physical stimuli such as light, magnetic field, electric current and ultrasound can be used to trigger hydrogels for controlled and targeted drug release as well.[86-89]

In order to design hydrogels with desired performance and structure, determination and characterization of hydrogel network parameters are of great significance. Theories used to describe the network structure of hydrogels are derived from equilibrium-swelling theory and rubber-elasticity theory.[90] The most important parameters used to characterize the network structure of hydrogels are the polymer volume fraction in the swollen state ($\upsilon_{2,s}$), the molecular weight of the polymer chain between two neighboring crosslinking points ($\overline{M}_C$), and the corresponding mesh size

(ζ). The polymer volume fraction in the swollen state is a measure of the amount of water or biological fluid retained by the hydrogel. In general, hydrogels with $\upsilon_{2,s}$>10 are defined as highly swollen systems, while 1<$\upsilon_{2,s}$<5 are lightly swollen hydrogels.[52] The average molecular weight between two consecutive crosslinks is a measure of crosslink density of the polymer network. The correlation length or distance between two adjacent crosslinks (mesh size, pore size) is a measure of the space available between the polymer chains. These parameters are related to each other and can be calculated theoretically and experimentally. By controlling these parameters, mechanical, responsive and diffusive properties of hydrogels can be adjusted for a particular application to a great extent.[90]

As above mentioned, the major drawback of hydrogels is their relatively poor mechanical properties which limit their use not only in load bearing but also in other biomedical applications. The reason for low mechanical stability of conventional hydrogels can be found in their network structure. Hydrogels with conventional chemical crosslinks tends to break under low stress due to inadequate energy dissipation to retard crack propagation. Irregular distribution of crosslinking points throughout the hydrogel network results in different chain lengths between crosslinking points and uneven stress distribution among polymer chains. This is the main reason for easy crack initiation and bulk fracture. Another aspect of this phenomenon is related to the degree of extensibility of a polymer chain which is governed by the relationship between relaxed end-to-end distance of a chain and its contour length. Before breakage, this parameter is low for short chains between two crosslinking points in comparison to long chains. When load is applied, short chains are susceptible to break first. The load has then to be shared by the

adjacent polymer chains present between the crosslinking points (see Fig. 1.9). This dramatic change in stress redistribution can result in multiple chain fractures and is followed by the formation of voids and microcracks.[91]

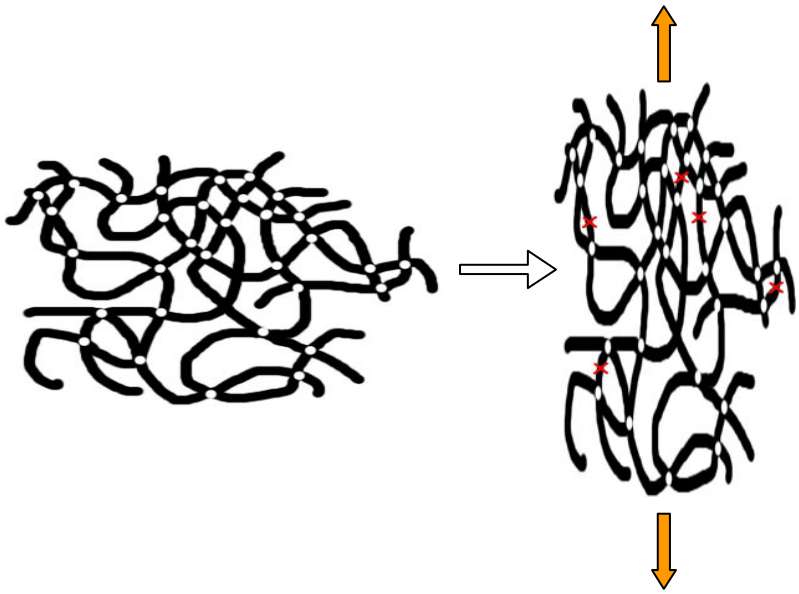

Figure 1.9 Schematic of the network in conventional hydrogels under applied load showing uneven stress distribution among polymer chains.

To improve their mechanical properties, various approaches such as the formation of interpenetrating networks, double-networks, formation of crystallites, and fiber reinforcement have been suggested. Recently, new hydrogels with unique network structure and excellent mechanical performance have been developed.[92,93] Haraguchi et al. developed nanocomposite hydrogels (NC gels) with unique organic-inorganic network structures that exhibit excellent mechanical performance as well as optical and swelling/deswelling properties.[94] In their study, water-swellable clay nanosheets (3 nm in

thickness and 30 nm in diameter) were used as highly multifunctional crosslinking sites. By performing *in situ* polymerization of specific monomers, initiators attached to nanoclay surfaces which were used as grafting sites for growing polymer chains. As a consequence to the formation of long and extensible polymer chains connecting the uniformly distributed nanoclay particles to each other, NC gels were strong, tough, highly extensible, and optically transparent and can absorb high amounts of water compared to conventional hydrogels.

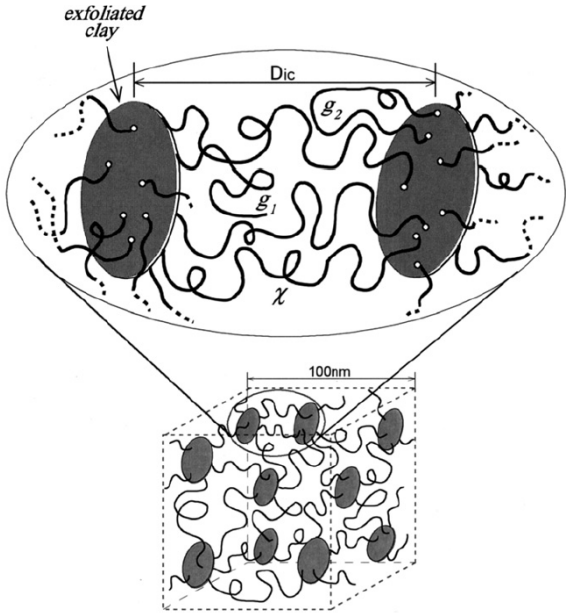

Figure 1.10 Schematic of the network structure of nanocomposite hydrogels showing exfoliated inorganic clay sheets and crosslinked polymer chains (Haraguchi, K.; Takehisa, T. Nanocomposite Hydrogels: A Unique Organic–Inorganic Network Structure with Extraordinary Mechanical, Optical, and Swelling/De-swelling Properties. Advanced Materials. 2002, 14, 1120–1124. Copyright Wiley-VCH Verlag GmbH & Co. KGaA. Reproduced with permission)

Huang et al.[91] have recently synthesized macromolecular microspheres composite hydrogels (MMC gels) with high strength and toughness using a similar approach to NC gels. In their study, a suspension of macromolecular microspheres (100 nm in diameter) carrying peroxide groups were irradiated to initiate polymerization of monomers and to synthesize hydrogels. By this way, macromolecular microspheres (MMS) acted as highly multifunctional crosslinking agents. Crosslink density and intercrosslinking distance can be easily adjusted by changing MMS concentration, monomer and initiator content. MMC hydrogels are about 120 times stronger than normal structure gels and compressible up to about 98% without fracture. They quickly recover their original shape.

In conclusion, hydrogels are promising biomaterials with a wide range of available materials and synthesis techniques. With optimized mechanical, responsive, diffusive and biological properties, hydrogels can play an even greater role in future biomedical applications and nanotechnology.

1.6 References

[1] Yua, L.; Dean, K.; Li, L. Polymer blends and composites from renewable resources. *Progress in Polymer Science*. **2006,** 31, 576–602.

[2] Timell, T.E. *Wood Science and Technology*, **1967**, l, 45.

[3] Gatenholm, P.; Tenkanen, M. *Hemicelluloses: Science and Technology*, **2004**, 15-16. Oxford University Press.

[4] Sun, R.; Sun, X. F.; Tomkinson, J. Hemicelluloses and Their Derivatives in Gatenholm, P.; Tenkanen, M. *Hemicelluloses: Science and Technology*, **2004**, 2-22. Oxford University Press.

[5] Ebringerova, A. Structural Diversity and Application Potential of Hemicelluloses. *Macromoecular Symposia*, **2006**, 232, 1.

[6] Hayashi, T. Xyloglucans in the Primary Cell Wall. *Annual Review of Plant Physiology and Plant Molecular Biology.* **1989**, 40, 139-168.

[7] Persson, S.; Caffall, K.H.; Freshour, G.; Hilley, M.T.; Bauer, S.; Poindexter, P.; Hahn, M.G.; Mohnen, D.; Somerville, C. The Arabidopsis irregular xylem8 mutant is deficient in glucuronoxylan and homogalacturonan, which are essential for secondary cell wall integrity. *The Plant Cell*. **2007**, 19, 237-55.

[8] Saake, B.; Erasmy, N.; Kruse, T.; Schmekal, E.; Puls, J. Isolation and Characterization of Arabinoxylan from Oat Spelts in Gatenholm, P.; Tenkanen, M. *Hemicelluloses: Science and Technology*, **2004**, 52-65. Oxford University Press.

[9] Gröndahl, M.; Eriksson, L.; Gatenholm, P. Material Properties of Plasticized Hardwood Xylans for Potential Application as Oxygen Barrier Films. *Biomacromolecules.* **2004**, 5, 1528–1535.

[10] Gröndahl, M.; Gatenholm, P. Role of Acetyl Substitution in Hardwood Xylan in Dumitriu, S. *Polysaccharides: Structural Diversity and Functional Versatility: Second Edition*. CRC Press**, 2004**, 509-514.

[11] Sundararajan, P. R.; Rao, V. S. R. Conformational studies of β-D-1,4′-xylan. *Biopolymers*. **1969**, 8, 305-312.

[12] Tokoh, C.; Takabe, K.; Sugiyama, J.; Fujita, M. Cellulose Synthesized by *Acetobacter xylinum* in the Presence of Plant Cell Wall Polysaccharides. *Cellulose*. **2002**, 9, 65-74.

[13] Reis, D.; Vian, B. Helicoidal Pattern in Secondary Cell Walls and Possible Role of Xylans in Their Construction. *Comptes Rendus Biologies*. **2004**, 327, 785-790.

[14] Walker, J. C. F. *Primary Wood Processing: Principles and Practice Second Edition*. Springer, **2007**, 40-41.

[15] Karimi, K.; Emtiazi, G.; Taherzadeh, M. J. Production of Ethanol and Mycelial Biomass from Rice Straw Hemicellulose Hydrolyzate by Mucor Indicus. *Process Biochemistry*. **2006**, 41, 653-658.

[16] Gabrielii, I.; Gatenholm, P.; Glasser, W. G.; Jain, R. K.; Kenne, L. Separation Characterization and Hydrogel-Formation of Hemicellulose from Aspen Wood. *Carbohydrate Polymers.* **2000,** 43, 367–374.

[17] Köhnke, T.; Pujolras, C.; Roubroeks, J. P.; Gatenholm, P. The Effect of Barley Husk Arabinoxylan Adsorption on the Properties of Cellulose Fibres. *Cellulose*. 2008, 15, 537-546.

[18] Karaaslan, M. A.; Tshabalala, M.; Buschle-Diller, G. Wood Hemicellulose/Chitosan-Based Semi-Interpenetrating Network Hydrogels: Mechanical Swelling and Controlled Drug Release Properties. Bioresources, 2010, 5, 1036.

[19] Popa, V.I. in Polysaccharides in Medicinal Applications, Dumitriu, S. Dekker, New York, 1996, 107.

[20] Lu, Z.X.; Gibson, P.R.; Muir, J. G.; Fielding, M.; O'Dea, K. Arabinoxylan Fiber from a By-Product of Wheat Flour Processing Behaves Physiologically like a Soluble, Fermentable Fiber in the Large Bowel of Rats. The Journal of Nutrition. 2000, 130, 1984.

[21] Tanodekaew, S.; Channasanon, S.; Uppanan, P. Xylan/polyvinyl alcohol blend and its performance as hydrogel. Journal of Applied Polymer Science. 2006, 100, 1914–1918.

[22] Lindblad, M. S.; Ranucci, E.; Albertsson, A. Biodegradable Polymers from Renewable Sources.New Hemicellulose-Based Hydrogels. Macromolecular Rapid Communications. 2001, 22, 962-967.

[23] Hansen, N. M. L.; Plackett, D. Sustainable Films and Coatings from Hemicelluloses: A Review. Biomacromolecules. 2008, 9, 1493-1505

[24] Kayserilioglu, B. S.; Bakir, U.; Yilmaz, L.; Akkas, N. Use of Xylan, An Agricultural By-Product, in Wheat Gluten Based Biodegradable Films: Mechanical, Solubility and Water Vapor Transfer Rate Properties. Bioresource Technology. 2003, 87, 239–246.

[25] Köhnke, T. Adsorption of Xylans on Cellulosic Fibres: Influence of Xylan Composition on Adsorption Characteristics and Kraft Pulp Properties. Dissertation, Chalmers University of Technology. Göteborg, 2010.

[26] Zhou, Q.; Rutland, M. W.; Teeri, T. T.; Brumer, H.. Xyloglucan in Cellulose Modification. *Cellulose*. **2007**, 14, 625-641.

[27] Hon, D. N. S. Cellulose: A Random Walk along Its Historical Path. *Cellulose,* **1994**, 1, 1-25.

[28] Lejeune, A.; Deprez, T. C*ellulose: Structure and Properties, Derivatives and Industrial Uses*. Nova Science Pub Inc, **2010**.

[29] Habibi, Y.; Lucia, L. A.; Rojas, O. J. Cellulose Nanocrystals: Chemistry, Self-Assembly, and Applications. *Chemical Reviews*. **2010**, 110 (6), 3479-3500.

[30] Staudinger, H. Die Chemie Der Hochmolekularen Organischen Stoffe Im Sinne Der Kekulèschen Strukturlehre. *Berichte der deutschen chemischen*. **1926**, 59, 3019-3043.

[31] Samir, M. A. S. A.; Alloin, F.; Dufresne, A. Review of Recent Research into Cellulosic Whiskers, Their Properties and Their Application in Nanocomposite Field. *Biomacromolecules*. **2005**, 6 (2), 612-626.

[32] http://www.mhhe.com/biosci/pae/botany/uno/graphics/uno01pob/vrl/, Botany Online Visual Resource Library **accessed** on 04/04/2011.

[33] Meyer, K. H.; Misch, L. L. Positions des atomes dans le nouveau modèle spatial de la cellulose. *Helvetica Chimica Acta*. **1937**, 20, 232−245.

[34] Agarwal, U. P.; Reiner, R. S.; Ralph, S. A. Cellulose I Crystallinity Determination Using FT–Raman Spectroscopy: Univariate and Multivariate Methods. *Cellulose*. **2010**, 17, 721–733.

[35] Klemn, D., Philipp, B., Heinze, T., Heinze, U., Wagenknecht, W., *Comprehensive cellulose chemistry. Fundamentals and analytical methods*. Vol. 1. **1998**, Weinhein,Germany: WILEY-VCH. 266.

[36] Jahan, M. S.; Mun, S.P. Effect of tree age on the cellulose structure of Nalita wood (Trema orientalis), *Wood Science and Technology.* **2005**, 39, 367-373

[37] Park, S.; Baker, J.O.; Himmel, M.E.; Parilla, P. A.; Johnson D.K. Cellulose Crystallinity Index: Measurement Techniques and Their Impact on Interpreting Cellulase Performance.*Biotechnology for Biofuels.* **2010**, 3, 1-10.

[38] Cai, Z.; Kim, J. Preparation and Characterization of Novel Bacterial Cellulose/Gelatin Scaffold for Tissue Regeneration Using Bacterial Cellulose Hydrogel. *Journal of Nanotechnology in Engineering and Medicine*. **2010**, 1, 1-6.

[39] Beck-Candanedo, S.; Roman, M.; Gray, D.G., Effect of Reaction Conditions on the Properties and Behavior of Wood Cellulose Nanocrystal Suspensions. *Biomacromolecules.* **2005**, 6*,* 1048-1054.

[40] Miller, A. F. and Donald, A. M. Imaging of Anisotropic Cellulose Suspensions Using Environmental Scanning Electron Microscopy. *Biomacromolecules.* **2003**, 4, 510

[41] Araki, J. and Kuga, S. Effect of Trace Electrolyte on Liquid Crystal Type of Cellulose Microcrystals. *Langmuir* **2001**, 17, 4493

[42] Junior de Menezes, A., Siqueira, G., Curvelo, A. A. S., and Dufresne, A. Extrusion and characterization of functionalized cellulose whiskers reinforced polyethylene nanocomposites. *Polymer.* **2009**, 50, 4552.

[43] Kimura, F., Kimura, T., Tamura, M., Hirai, A., Ikuno, M., and Horii, F. Magnetic Alignment of the Chiral Nematic Phase of a Cellulose Microfibril Suspension. *Langmuir* **2005**, 21,2034

[44] Araki, J., Wada, M., Kuga, S., and Okano, T. Influence of surface charge on viscosity behavior of cellulose microcrystal suspension. *Journal of Wood Science.* **1999**, 45, 258.

[45] Hanley, S. J.; Giasson, J.; Revol, J.-F.; Gray, D. G. Atomic force microscopy of cellulose microfibrils: comparison with transmission electron microscopy. *Polymer*. **1992**, 33, 4639−4642.

[46] Eichhorn, SJ; Dufresne, A; Aranguren, M; Marcovich, NE; Capadona, JR; Rowan, SJ; Weder, C; Thielemans W; Toman, M; Renneckar, S; Gindl, W; Veigel, S; Keckes, J; Yano, H; Abe, K; Nogi, M; Nakagaito, AN; Mangalam, A; Simonsen, J; Benight, AS; Bismarck, A; Berglund LA; Peijs, T. Review: current international research into cellulose nanofibres and nanocomposites. *Journal of Material Science*. **2010**, 45, 1–33.

[47] Dodane, V.; Vilivalam, V. D., Pharmaceutical applications of chitosan. *Pharmaceutical Science & Technology Today.* **1998,** 1, 246-253,

[48] Kumar, M.N.V.R. Chitin and chitosan fibres: A review. *The Bulletin of Materials Science.* **1999,** 22, 905-915.

[49] Rinaudo, M., Chitin and chitosan: properties and applications. *Progress in Polymer Science.* **2006**, 31, 603–632.

[50] George, M.; Abraham, T.E., Polyionic Hydrocolloids for the Intestinal Delivery of Protein Drugs: Alginate and Chitosan: A Review. *Journal of Controlled Release.* **2006**, 114, 1–14.

[51] Kim, I.Y.; Seo, S.J.; Moon, H.S.; Yoo, M.K.; Park, I.Y. Chitosan and Its Derivatives for Tissue Engineering Applications. *Biotechnology Advances*. **2008**, 26, 1–21.

[52] Peppas, NA; Moynihan, HJ; Lucht, LM. The structure of highly crosslinked poly(2-hydroxyethyl methacrylate) hydrogels. *Journal of Biomedical Materials Research* **1985**, 19, 397-411.

[53] Berger, J; Reist, M; Mayer, JM; Felt, O; Gurny R. Structure and interactions in covalently and ionically crosslinked chitosan hydrogels for biomedical applications. *European Journal of Pharmaceutics and Biopharmaceutics*. **2004** , 57, 19–34.

[54] Hoffman, A.S. Hydrogels for biomedical applications. *Advanced Drug Delivery Reviews*. **2002**, 43, 3 –12.

[55] Hassan, C.M.; Peppas, N.A. Structure and Morphology of Freeze/Thawed PVA Hydrogels. *Macromolecules*. **2000**, 33, 2472–2479.

[56] Nugent, M.J.D.; Hanley, A.; Tomkins, P.T.; Higginbotham, C.L. Investigation of a novel freeze-thaw process for the production of drug delivery hydrogels. *Journal of Materials Science: Materials in Medicine.* **2005**, 16, 1149–1158.

[57] Mitsumata, T.; Hasegawa, C.; Kawada, H.; Kaneko, T.; Takimoto, J.I. Swelling and viscoelastic properties of poly (vinyl alcohol) physical gels synthesized using sodium silicate. *Reactive and Functional Polymers.* **2008**, 68, 133–140.

[58] Bodugoz-Senturk, H.; Macias, C.E.; Kung, J.H.; Muratoglu, O.K. Poly(vinyl alcohol)–acrylamide hydrogels as load-bearing cartilage substitute. *Biomaterials.* **2009**, 30, 589-596.

[59] Myung, D.; Waters, D.; Wiseman, M.; Duhamel, P.E.; Noolandi, J.; Ta, C.N.; Frank, C.W. Progress in the development of interpenetrating polymer network hydrogels. *Polymers for Advanced Technologies*, **2008**, 19, 647 – 657.

[60] Calvert, P. Hydrogels for Soft Machines. *Advanced Materials.* **2009**, 21, 743–756.

[61] Gong, J.P.; Katsuyama, Y.; Kurokawa, T.; Osada, Y. Double-network hydrogels with extremely high mechanical strength. *Advanced Materials*. **2003**, 15, 1155 – 1158.

[62] Han, Y.A.; Lee, E.M.; Ji, B.C. Mechanical properties of semi-interpenetrating polymer network hydrogels based on poly (2-hydroxyethyl methacrylate) copolymer and chitosan. *Fibers and Polymers* **2008**, 9, 393-399.

[63] Yasuda, K.; Ping Gong, J.; Katsuyama, Y. Biomechanical properties of high-toughness double network hydrogels. *Biomaterials.* **2005**, (26):4468-4475

[64] Li, X.; Xu, S.; Wang, J.; Chen, X.; Feng, S. Structure and characterization of amphoteric semi-IPN hydrogel based on cationic starch. *Carbohydrate Polymers.* **2009**, 75, 688–693.

[65] Culin, J., Smit, I., Andreis, M., Veksli, Z., Anzlovar, A, Zigon, M., Motional heterogeneity and phase separation of semi-interpenetrating networks and mixtures based on functionalised polyurethane and polymethacrylate prepolymers. *Polymer.* **2005**, 46, 89–99.

[66] Lin, C.C.; Metters, A.T. Hydrogels in controlled release formulations: network design and mathematical modeling. *Advanced Drug Delivery Reviews*. **2006**, 58, 1379–1408.

[67] Barbucci, R.; Consumi, M.; Lamponi, S.; Leone, G. Polysaccharides based hydrogels for biological applications. *Macromolecular Symposia*. **2003**, 204, 37-58.

[68] Kadokawa, J.; Saitou, S.; Shoda, S. Preparation of polysaccharide–polymethacrylate hybrid materials by radical polymerization of cationic methacrylate monomer in the presence of anionic polysaccharide. *Polymers for Advanced Technologies.* **2007**, 18, 643–646.

[69] Berger, J.; Reist, M.; Mayer, J.M.; Felt, O.; Gurny, R. Structure and interactions in chitosan hydrogels formed by complexation or aggregation for biomedical applications. *European Journal of Pharmaceutics and Biopharmaceutics.* **2004**, 57, 35-52.

[70] Lee, C.; Grodzinsky, A.; Spector, M. Modulation of the Contractile and Biosynthetic Activity of Chondrocytes Seeded in Collagen–Glycosaminoglycan Matrices. *Tissue Engineering.* **2003**, 9, 27-36.

[71] Schoof, H.; Apel, J.; Heschel, I.; Rau, G. Control of pore structure and size in freeze-dried collagen sponges. *Journal Biomedical Materials Research* **2001**, 5, 352-357.

[72] Wichterle, O.; Lim, D. Hydrophilic gels in biologic use. *Nature.* **1960**, 185, 117-118.

[73] Kidane, A.; Szabocsik, J.M.; Park, K. Accelerated study on lysozyme deposition on poly (HEMA) contact lenses. *Biomaterials.* **1998**, 19, 2051.

[74] Bryant, S.J.; Cuy, J.L.; Hauch, K.D.; Ratner, B.D. Photo-patterning of porous hydrogels for tissue engineering. *Biomaterials.* **2007**, 28, 2978.

[75] Kirker, K.R.; Luo, Y.; Nielson, J.H.; Shelby, J.; Prestwich, G.D. Glycosaminoglycan hydrogel films as bio-interactive dressings for wound healing. *Biomaterials.* **2002,** 23, 3661.

[76] Slaughter, B.V.; Khurshid, S.S.; Fisher, O.Z.; Khademhosseini, A.; Peppas, N.A. Hydrogels in Regenerative Medicine. *Advanced Materials.* **2009**, 21, 1–23.

[77] Pan, Y.S.; Xiong, D.S.; Ma, R.Y. A study on the friction properties of poly (vinyl alcohol) hydrogel as articular cartilage against titanium alloy. *Wear* **2007**, 262, 1021.

[78] Gunasekaran, S.; Wang, T.; Chai, C. Swelling of pH-sensitive chitosan–poly(vinyl alcohol) hydrogels. *Journal of Applied Polymer Science* **2006**, 102, 4665–4671.

[79] Khare, A.R.; Peppas, N.A. Release behavior of bioactive agents from pH-sensitive hydrogels. *Journal of Biomaterials Science: Polymer Edition.* **1993**, 4, 275–289.

[80] Mi, F.L.; Shyu, S.S.; Lee, S.T.; Wong, T.B. Kinetic study of chitosan-tripolyphosphate complex reaction and acid-resistive properties of the chitosan-tripolyphosphate gel beads prepared by in-liquid curing method. *Journal of Polymer Science Part B: Polymer Physics* **1999**, 37, 1551–1564.

[81] Yao, K.D.; Peng, T.; Feng, H.B.; He, Y.Y. Swelling kinetics and release characteristic of crosslinked chitosan: Polyether polymer network (semi-IPN) hydrogels. *Journal of Polymer Science Part A: Polymer Chemistry.* **1994**, 32, 1213–1223.

[82] Sershen, S.; West, J. Implantable, polymeric systems for modulated drug delivery. *Advanced Drug Delivery Reviews.* **2002**, 54, 1225-1235.

[83] Yamato, M.; Konno, C.; Utsumi, M.; Kikuchi, A.; Okano, T. Thermally responsive polymer-grafted surfaces facilitate patterned cell seeding and co-culture. *Biomaterials*. **2002**, 23, 561-567.

[84] Vakkalanka, S.K.; Brazel, C.S.; Peppas, N.A.; Temperature- and pH-sensitive terpolymers for modulated delivery of streptokinase. *Journal of Biomaterials Science: Polymer Edition.* **1997**, 8, 119-129.

[85] Qiu, Y.; Park, K. Environment-sensitive hydrogels for drug delivery. *Advanced Drug Delivery Reviews.* **2001**, 53, 321–339.

[86] Kodzwa, M.G.; Staben, M.E.; Rethwisch, D.G. Photoresponsive control of ion-exchange in leucohydroxide containing hydrogel membranes. *Journal of Membrane Science.* **1999**, 158, 85-92.

[87] Zrinyi, M.; Szabo, A.D.; Kilian, H.G. Kinetics of the shape change of magnetic field sensitive polymer gels. *Polymers Gels and Networks.* **1998**, 6, 441-454.

[88] Lavon, I.; Kost, J. Mass transport enhancement by ultrasound in non-degradable polymeric controlled release systems. *Journal of Controlled Release.* **1998**, 54, 1-7.

[89] Gelbrich, T.; Feyen, M.; Schmidt, A.M. Magnetic Thermoresponsive Core− Shell Nanoparticles. *Macromolecules.* **2006**, 39, 3469–3472.

[90] Peppas, N.A.; Hilt, J.Z.; Khademhosseini, A.; Langer, R. Hydrogels in Biology and Medicine: From Molecular Principles to Bionanotechnology, *Advanced Materials*. **2006**, 18, 1345–1360.

[91] Huang, T.; Xu, H.; Jiao, K.; Zhu, L.; Brown, H. R.; Wang, H. A Novel Hydrogel with High Mechanical Strength: A Macromolecular Microsphere Composite Hydrogel. *Advanced Materials.* **2007**, 19, 1622–1626.

[92] Tanaka, Y.; Gong, J. P.; Osada, Y. Novel Hydrogels with Excellent Mechanical Performance. *Progress in Polymer Science*. **2005,** 30, 1-9.

[93] Schexnailder, P.; Schmidt, G. Nanocomposite Polymer Hydrogels. *Colloids and Polymer Science.* **2009,** 287, 1-11.

[94] Haraguchi, K.; Takehisa, T. Nanocomposite Hydrogels: A Unique Organic–Inorganic Network Structure with Extraordinary Mechanical, Optical, and Swelling/De-swelling Properties. *Advanced Materials.* **2002,** 14, 1120–1124.

CHAPTER 2

Wood Hemicellulose/Chitosan-Based Semi-Interpenetrating Network Hydrogels: Mechanical, Swelling and Controlled Drug Release Properties

2.1 Abstract

The cell wall of most plant biomass from forest and agricultural resources consists of three major polymers, cellulose, hemicellulose and lignin. Of these, hemicelluloses have gained increasing attention as sustainable raw materials. In the first part of this study, novel pH-sensitive semi-IPN hydrogels based on hemicelluloses and chitosan were prepared using glutaraldehyde as the crosslinking agent. The hemicellulose isolated from aspen was analyzed for sugar content by HPLC, and its molecular weight distribution was determined by high performance size exclusion chromatography. Results revealed that hemicellulose had a broad molecular weight distribution with a fair amount of polymeric units, together with xylose, arabinose and glucose. The effect of hemicellulose content on mechanical properties and swelling behavior of hydrogels were investigated. The semi-IPNs hydrogel structure was confirmed by FT-IR, X-ray study and ninhydrin assay method. X-ray analysis showed that higher hemicellulose contents yielded higher crystallinity. Mechanical properties were mainly dependent on the crosslink density and average molecular weight between crosslinks. Swelling ratios increased with increasing hemicellulose content and were high at low pH values due to repulsion between similarly

charged groups. In vitro release study of a model drug showed that these semi-IPN hydrogels could be used for controlled drug delivery into gastric fluid.

2.2 Introduction

Raw materials from renewable resources have gained increasing importance in recent years as fossil fuels become less available. Forest by-products from low-value trees, bark, and residue from sawmills offer an alternative as renewable resources. Products based on forest biomass find applications in areas where biocompatibility and biodegradability are of major importance. Careful extraction and fractionation of forest biomass can yield chemicals, which in turn can be converted into high-value products. An example of useful silvichemicals is hemicellulose, a class of hetero-polysaccharides present in the cell wall of wood and annual plants together with cellulose and lignin.[1] Hemicellulose is considered to be the second most abundant polysaccharide in nature, representing about 20-35% of lignocellulosic biomass.[2] Potential applications of hemicelluloses and their derivatives have been described in the literature.[3]

One such area of application is super-absorbent hydrogels. Hydrogels have attracted significant attention in biological and biomedical applications based on their high liquid up-take, their stimuli-responsive swelling-deswelling capabilities without disintegration, and their biocompatibility.[4-6] Hydrogels generally consist of three-dimensional hydrophilic polymeric networks. They owe their mechanical stability during swelling to chemical and/or physical cross-links between the macromolecular chains that allow for flexibility, yet render low, but sufficient strength.[7] Polysaccharides such as

chitosan and alginate have been widely used to prepare natural hydrogels that have the advantages of biocompatibility, biodegradability, low toxicity, and availability from renewable resources.[8]

Efforts have been made to improve their mechanical properties without impairing their sorption capabilities. Reinforcement with small fibers, formation into nano-composites, chemical crosslinking and formation of interpenetrating (IPN) or double networks are some of the strategies that have been employed.[9-11] Of those, semi-interpenetrating network hydrogels (semi-IPNs) have been extensively described.[12-14] Semi-IPNs are achieved by blending two polymers with one being crosslinked in the presence of the other (not crosslinked) polymer.[15] In semi-IPNs, additional interactions between the two polymers such as hydrogen bonds, crystallites, ionic, and hydrophobic interactions may participate in the hydrogel formation.[16] Moreover, each polymer might contribute to the final properties of semi-IPN hydrogels in terms of mechanical stability,[17] stimuli responsiveness to pH,[18] and temperature.[19]

Recent studies showed that agricultural and forestry by-products can also be incorporated into hydrogels. In this context, hemicelluloses have been explored by some research groups.[20-23] Gabrielii et al.,[21] for example, studied chitosan hydrogels that contained xylan for reinforcement. They concluded that crystalline arrangement and electrostatic interactions between two biopolymers were responsible for the relatively high stability of the hydrogels.

Chitosan is a cationic polysaccharide known for its good film forming ability. It is obtained from waste chitin, and as such can be considered a material from renewable resources. Amine groups attached to its backbone enable chitosan to become positively charged in acidic medium. Therefore, chitosan can serve as a biomaterial for pH-responsive hydrogel applications. However, these hydrogels generally lack mechanical stability unless they are crosslinked and/or reinforced by suitable compounds.

In this study, hemicelluloses isolated from aspen were evaluated for use as value-added biomaterials. For this purpose, novel semi-IPN hydrogels based on hemicellulose and chitosan were prepared and designed for application in pH-responsive drug delivery systems by using riboflavin as the model active agent. It has been hypothesized that alkaline extracted hemicellulose could be entrapped in a chemically crosslinked pH-responsive polymer network such as chitosan. If the hemicellulose was capable of crystallizing, it would act as a reinforcing component for enhancing the mechanical properties of this semi-IPN hydrogel. It is further hypothesized that such a semi-IPN hydrogel could be constituted into a potential controlled release drug delivery system.

2.3 Experimental

2.3.1 Materials

Chitosan with 190,000-310,000 g/mol viscosity average molecular weight and 75-85% degree of deacetylation was obtained from Sigma Aldrich. Glutaraldehyde, acetic acid, riboflavin, and other solvents and chemicals were purchased from Fisher Scientific

and used as received. For comparison, experiments with commercially available xylan from birch wood of known chemical composition (Sigma Aldrich) were also performed.

2.3.2 Isolation of hemicelluloses from wood flour

Hemicellullose, isolated from aspen by a novel alkaline extraction method, was provided by USDA Forest Products Laboratory, Madison, WI. Aspen chips were processed into flour in a Wiley mill to pass through a 1-mm mesh size screen attached to the mill. The flour was sieved on a 60-mesh screen. Fifty (50) grams of the fraction captured on the 60-mesh screen was treated with 500 mL 0.05 M HCl at 70ºC for 2 h. The suspension was allowed to cool to room temperature before adjusting its pH to 9.2 with approximately 6 mL concentrated NH_4OH. The suspension was stirred overnight at room temperature and filtered under suction on Whatman GF/A glass microfiber filter paper to extract pectins, starch, and fats. The filter cake was placed in 500 mL 0.025M NaOH in 70% ethanol at 75ºC and stirred for 2 h to solubilize lignin. The suspension was allowed to cool to room temperature before filtration under suction on Whatman GF/A glass microfiber filter paper to remove lignin. The remaining filter cake was transferred to 500 mL 0.1M NaOH, and stirred for 16 h at room temperature to solubilize hemicelluloses. At the end of this period the suspension was filtered under suction on Whatman GF/A glass microfiber filter paper, to isolate hemicelluloses in the filtrate. The filtrate was heated to 65°C, and 35 mL 30% H_2O_2 was added to the filtrate in 1-mL increments and it was allowed to react under constant stirring. When the filtrate had turned white, it was allowed to cool to room temperature. Its pH was adjusted to 5.3 with 32 mL concentrated HCl before transferring it to three-times its volume of 95% ethanol.

The mixture was left overnight to allow hemicellulose to precipitate. The supernatant liquid was carefully removed by vacuum suction, and the hemicellulose precipitate was reconstituted in 300-500 mL of reverse osmosis (RO) water. This hemicellulose solution was dialyzed in a Spectra/Por dialysis membrane, MWCO: 3500, against 3000 mL RO water. After overnight dialysis, the dialyzed hemicellulose solution was freeze-dried to yield hemicellulose powder. A sample of the hemicellulose powder was dissolved in 0.1M $NaNO_3$ for molecular weight determination by high performance size exclusion chromatography with refractive index (HPSEC-RI) and UV (HPSEC-UV) detection. Another sample of the hemicellulose powder was hydrolyzed, and the hydrolysate was analyzed for sugar content by HPLC with electrochemical detection (HPLC-ED).

2.3.3 Hydrogel preparation

Chitosan was dissolved in 2% v/v acetic acid aqueous solution to prepare 1% w/w chitosan solution. Hemicellulose was added to deionized water at 1% w/v and heated to 95°C for 20 minutes with stirring. The solution was cooled to room temperature. Blended hydrogels were prepared by mixing chitosan and hemicellulose solution for 8 h at 70:30 and 30:70 weight ratios with a total dry matter of 1%.

For crosslinking, glutaraldehyde was added at a set ratio (3% w/w) to the total dry weight of chitosan in the solution after stirring the mixtures for 8 h. Final solutions were cast into films in plastic petri dishes and dried in an oven at 40ºC for 24 h. The dry films were immersed in 0.1 N sodium hydroxide solution to neutralize acetic acid residues, then washed with ethanol to remove an excess NaOH. After rinsing with excess

deionized water, the films were dried in an oven at 40ºC for 24 h. The average crosslink density of samples reported in this paper was determined to be 22% unless otherwise noted. FT-IR spectra of crosslinked chitosan films did not show any traces of unreacted glutaraldehyde.

2.3.4 Hydrogel characterization

2.3.4.1 Crosslinking density

The effective crosslink density was estimated using the kinetic theory of rubbery elasticity (Eq. 2.1),[24-26]

$$G = RT\nu_e \upsilon_2^{1/3} \tag{2.1}$$

where G is the elastic modulus, ν_e is the effective crosslink density, υ_2 is the polymer volume fraction at equilibrium swollen state, R is the gas constant, and T is the temperature in Kelvin. The elastic modulus of swollen hydrogels, G, was determined from the linear portion of the stress-strain curve at low strains by using Eq. 2.2,

$$\tau = G\left[\alpha - \frac{1}{\alpha^2}\right] \tag{2.2}$$

where τ is the force per unit of initial cross-sectional area of swollen gel and α is the deformation ratio (deformed length/initial length) of the network by tensile force.

The average molecular weight between crosslinks ($\overline{M_C}$, g/mol) was calculated as follows (Eq. 2.3):[27]

$$\overline{M_c} = \frac{1}{\nu_e \overline{\upsilon}} \tag{2.3}$$

where ν_e is the effective crosslink density in mol/cm^3 obtained by Eq.2.1, and $\bar{\upsilon}$ is the specific volume of the polymer in cm^3/g.

In addition, the degree of crosslinking was also determined by the percent decrease of free amine groups in the hydrogels. The ninhydrin assay method, which is commonly used for quantitative determination of free amine (NH_2) groups in chitosan, was performed according to the standard procedure.[28, 29]

2.3.4.2 Mechanical Properties

The fiber-film geometry module of the RSAIII Dynamical Mechanical Analyzer with a 3.5 kg load cell was used to test the tensile properties of the dry hydrogel films. Crosshead speed and gauge length was 1 mm/min and 10 mm, respectively. Samples were cut into 7x30 mm strips. The thickness of the film sample was measured using a digital micrometer with 0.001 mm resolution at three locations and averaged. Samples were conditioned at 65% RH and 22ºC for about 48 h before testing. Replicate tests of at least three films were performed.

Tensile testing of the swollen hydrogel films at equilibrium was performed with an Instron Universal Tester with a 100 N load cell. Gauge length and crosshead speed were set to 10 mm and 2 mm/min, respectively. Samples were cut into 7x30 mm strips before immersing in deionized water. In order not to damage the swollen samples during the thickness measurements, they were gently sandwiched between microscope cover

slips. To prevent water loss during testing, hydrogel samples were coated with petroleum gel.[30]

2.3.4.3 Swelling Behavior

For the swelling experiments, dry films with an average thickness of 17 μm were cut into samples of 10 mm x 10 mm. Each sample weighed approximately 6 mg. The equilibrium swelling ratio of hydrogels, which signifies the expanding and retracting forces between crosslinks at equilibrium, was determined by water uptake measurements. Pre-weighed dry samples were immersed in deionized water at room temperature for 1 h, which was determined to be sufficient to reach the equilibrium state. The weight of the swollen samples was measured after blotting excessive water gently with filter paper. The equilibrium swelling ratio (S) was calculated by the following equation (Eq. 2.4),

$$S(\%) = \frac{W_s - W_d}{W_d} \times 100 \qquad (2.4)$$

where W_s and W_d are the swollen and dry weight of samples, respectively. Equilibrium swelling ratios at different pH buffers (2, 4, 6, 8, and 10) were determined as described above.

2.3.4.4 In vitro cumulative release study

In order to load the model drug into the hydrogels, riboflavin was added to chitosan/ hemicellulose solution before the crosslinking step. The amount of drug loaded was 20% (w/w) of total dry matter in the final solution. Solubility of riboflavin in DI water is low (<0.05%); however riboflavin is highly soluble in dilute alkaline solutions. To minimize the drug loss before the *in vitro* test, samples were immersed in DI water for

1 h, rinsed with excess water (without using sodium hydroxide and ethanol) and oven-dried. Drug loss from dried films was determined by measuring the absorbance of the rinse water at 445 nm with UV-vis. The amount of drug loaded (M_0) before the *in vitro* test was calculated by subtracting the amount of drug loss from the initial amount of drug loaded.

To simulate the release of riboflavin into physiological media, riboflavin loaded hydrogels with the same dimensions as used for the swelling experiments were incubated in 25 mL pH 2.2 and pH 7.4 phosphate buffer solutions with same concentration (0.1 M) and ionic strength (0.1 M) at 37ºC and shaken at 50 rpm. At different time intervals, 4 mL of test solution were extracted and 4 mL fresh buffer solution added. The concentration of riboflavin released was determined by measuring the absorbance at 445 nm with a UV-vis spectrophotometer. Cumulative release (M_t/M_0, %) was determined by the ratio of the amount of drug released (M_t) at time t to the initial amount of drug loaded (M_0).

2.3.4.5 Structural and morphological analysis

FTIR spectra of dry films were obtained with a Nicolet 6700 FT-IR spectrometer between 4000 and 400 cm^{-1} over 32 scans with a resolution of 4 cm^{-1}.

The crystallinity of the films was analyzed using a Bruker D8 X-ray diffactometer. Cu Kα radiation at 40 kV and 40 mA with a wavelength of 1.54 Å was used, and 2θ was varied between 5 and 30° at a rate of 2° per min and a step size of

0.01°. The degree of crystallinity (ϕ, Eq. 2.5) was calculated by TOPAS software. The amorphous baseline was determined by a first order Chebyshev polynomial fit to the experimental diffractogram according to Rogers et al.[31] The relationship of the intensity of amorphous background (ΣI_a) to the total intensity (ΣI_{exp}) was then calculated to yield the degree of crystallinity as follows:

$$\phi = (1 - \frac{\Sigma I_a}{\Sigma I_{\exp}}) \times 100 \tag{2.5}$$

The surface morphology of films was examined by a Zeiss EVO 50 scanning electron microscope (SEM) at 15 kV. Samples were sputter-coated with gold prior to examination. The appearance of the films was also evaluated by a Nikon SMZ-U optical light microscope with 10x zoom.

2.4 Results and Discussion

2.4.1 Hemicellulose extraction

Sugar analysis of hemicellulose fractions (see Table 2.1) from aspen wood showed that the fraction most suitable for hydrogel formation experiments contained mostly xylose (82%), arabinose (8%) and glucose (5%). For comparison, a commercially available xylan sample from birch wood was also hydrolyzed and analyzed for sugars. It was found to contain less xylose (75%) and glucose (1%) and basically no arabinose.

Table 2.1. Sugar Composition of Hydrolysates of Hemicellulose Fractions and Commercial Xylan (%)

	Arab	Gal	Rham	Glc	Xyl	Man	Residue	Total CHO
Hemicellulose	8.2	2.2	0.0	5.1	82.1	2.4	0.0	100.0
Commercial xylan	-	0.4	0.0	1.02	75.3	-	-	76.9

Size exclusion chromatography results revealed a fairly broad molecular weight distribution with large amounts of low and medium molecular weight, but also a fair amount of polymeric saccharides. Two peaks, detected by HPSEC-RI, and identified as Peak #1 and Peak #2 in Figure 2.1, showed apparent molecular weights of $MW_p \approx$ 401,000 and 391,000 $g.mol^{-1}$, respectively. The observed polydispersity, however, is not unusual for hemicellulose extracted from forest biomass.

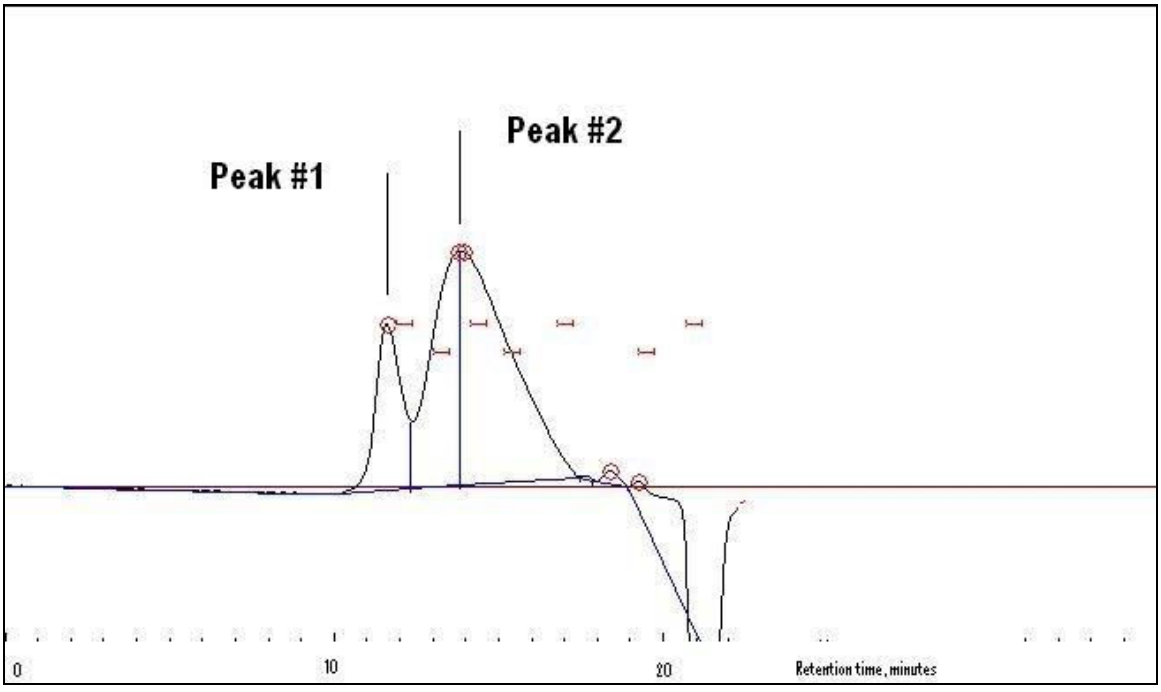

Figure 2.1 HPSEC-RI chromatogram of hemicellulose fraction: Peak #1 at retention time 11.5 min corresponds to $MW_p \approx 401{,}000$ g.mol^{-1}, and Peak #2 at retention time 13.8 min corresponds to $MW_p \approx 391{,}000$ g.mol^{-1}.

Although the chemical structure of the polysaccharides has not yet been determined in detail, it is reasonable to assume that the hemicellulose isolation procedure described in this paper yielded xylan-rich heteropolysaccharides with arabino-, gluco-, galacto-, and mannan- residues with some UV-absorbing moieties such as acetyl groups. The carboxyl group (–COOH) content was determined to be 0.01-0.02 mmol/g, which suggested the presence of –COOH carrying glucuronic acid residues.

Teleman et al.[32] performed extensive spectroscopic studies on hemicelluloses isolated from milled aspen chips and fractioned into oligomeric and polymeric components consisting mainly of O-acetyl-(4-O-methylglucurono)xylan. According to their research, the backbone of this structure is constituted of β-(1→4)-linked d-xylopyranosyl residues, substituted with one α-(1→2)-linked 4-O-methyl-d-glucuronic acid per approximately every tenth such residue.

2.4.2 Film formation

It was possible to cast films from aqueous solutions of hemicellulose on glass plates. However, the films were highly brittle with very low mechanical stability. Groendahl et al.[33] argued that the poor film-forming ability and brittleness of glucuronoxylans is a direct consequence of insufficient chain length of the polymer, high

glass transition temperature and poor solubility. Glucuronoxylan in its native state is amorphous but can crystallize to a certain extent after alkaline treatment due to partial removal of acetyl groups.[33, 34] The hemicellulose used in this study showed highly regular crystal formation when cast on glass plates from 1% w/v aqueous solutions. Figure 2.2 shows SEM micrographs of the observed highly regular crystallites. It is interesting to note that the commercial birch xylan could not be developed into films or flakes and did not demonstrate such crystal formations.

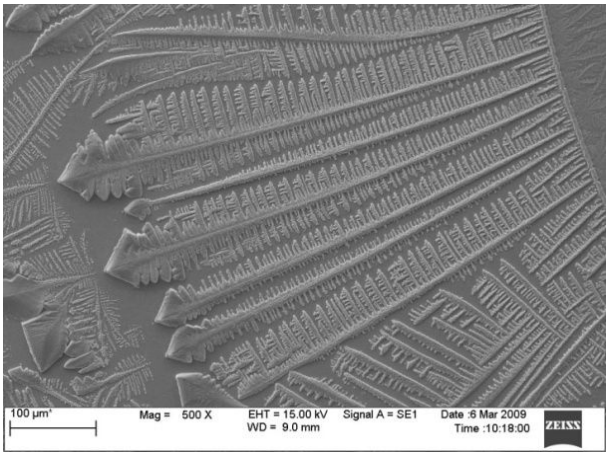

Figure 2.2 SEM images of macroscopic crystal formation in 1% (w/v) aqueous hemicellulose solutions cast on glass plates.

Chitosan, as an extensively studied polysaccharide due its non-toxicity and biocompatibility, has been demonstrated to have excellent film-formation ability.[35] As expected, the mechanical stability of the hemicellulose films improved with using chitosan as the supporting matrix. At a ratio of 70:30 hemicellulose to chitosan, stable films were produced that showed spherulite formation (Figure 2.3a) similar to those of hemicellulose samples without chitosan. With increasing chitosan content however, the form and size of the crystallites changed (Figure 2.3b). At a ratio of 50:50 hemicellulose

to chitosan, crystallite domains no longer overlapped, but rather showed space in-between separate domains without any interference.

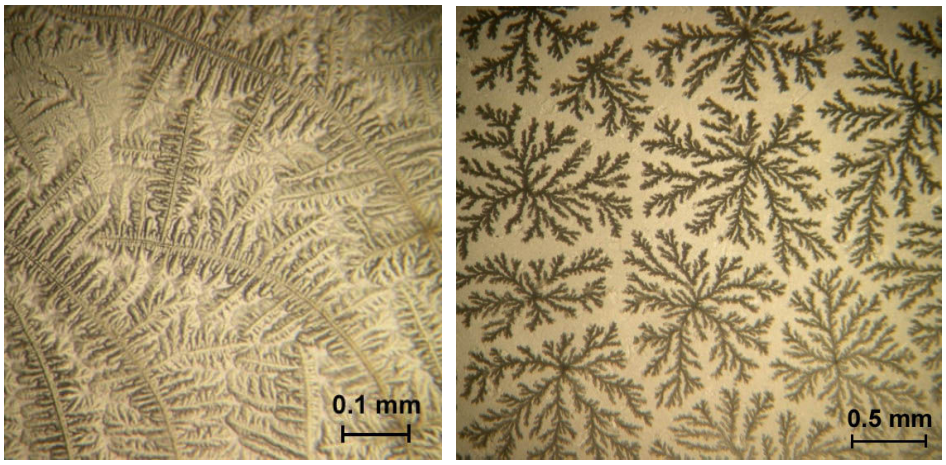

Figure 2.3 Optical microscopic images of the dendritic crystals formed in hemicellulose/chitosan films; (a) H:CS = 70:30 (b) H:CS = 50:50

At first, it was assumed that the crystallites primarily originated from the mono- or oligomeric components of hemicellulose. In this case these compounds would be removed upon exposure to repeated swelling/deswelling in distilled water. However, though less pronounced, crystallites similar to those shown in Figure 2.3 were repeatedly formed.

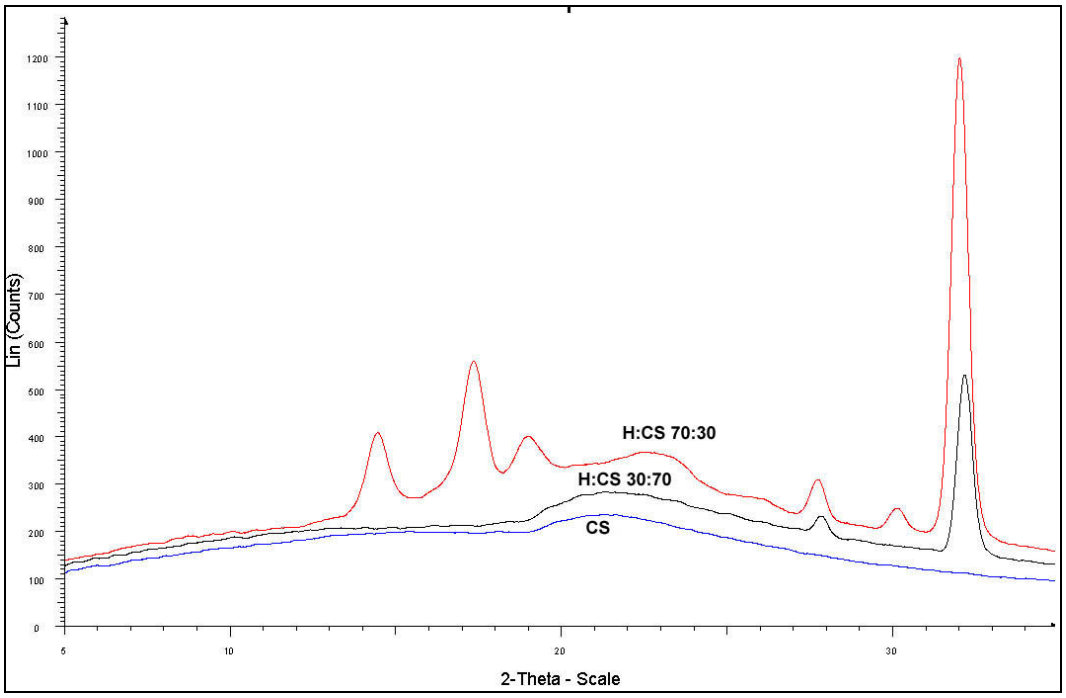

Figure 2.4 X-ray diffractograms of films before swelling-deswelling cycles (CS; CS:H 70:30; CS:H 30:70).

Figure 2.4 shows X-ray diffractograms of hemicellulose/chitosan films before swelling in water as well as of films from chitosan without hemicellulose for comparison. Clearly, higher hemicellulose contents yielded higher crystallinity. Major peaks were located at 2θ=14.1, 16.9, and 18.6, as found for hemicellulose. After swelling/deswelling, the crystallinity index of dry hydrogels was estimated to be 20.2% and 14.5% for 70:30 and 30:70 ratios of hemicellulose:chitosan, respectively. These results confirmed that the chitosan gel was able to entrap the crystallized water-insoluble polymeric portion of hemicellulose.

2.4.3 Semi-IPN formation

By crosslinking of chitosan in presence of hemicellulose, a semi-interpenetrating network (IPN) structure could be formed. Semi-IPN formation was confirmed by FTIR, X-ray diffraction and the ninhydrin assay method. Figure 2.5 presents the FTIR spectra of hemicellulose, crosslinked chitosan, and semi-IPN hydrogel film at 30:70 hemicellulose: chitosan ratio. The peak at 1637 cm^{-1} can be attributed to the imine bond (C=N stretching) in the semi-IPN due to the Schiff's base reaction between chitosan and glutaraldehyde.[36, 37] A decrease in the percentage of free amine groups was also confirmed by ninhydrin assay (see Table 2.2). In comparison to crosslinked chitosan without hemicellulose, peak shifts were detected in the semi-IPN at 1540 cm^{-1} (NH deformation-amide II) and 3400 cm^{-1} (OH/NH stretching). These band shifts could be attributed to intermolecular interactions between hemicellulose and chitosan such as H-bonding and hydrophobic attraction. In addition, as proposed by Gabrielii et al.,[20, 21] some ionic interaction between carboxyl groups in hemicellulose and free amino groups in chitosan may also occur, although the amounts of carboxyl groups in hemicellulose are quite low (see Table 2.2).

Although some of the dendritic crystals shown in Fig. 2.3 were removed during rinsing and neutralization steps, X-ray diffraction measurements showed that a crystallinity of 14.5% and 20.2% for H:CS 30:70 and 70:30, respectively, had been preserved. Taking the ionic and intermolecular interactions as well as crystallinity introduced by hemicellulose chains into account, the structure of the crosslinked H:CS semi-IPN hydrogel could be proposed as schematically presented in Figure 2.6.

Interspersed crystalline regions and chemical crosslinks form the major support of the structure, while additional weaker interactions also contribute to the mechanical stability of the hydrogel.

Table 2.2 Amount of carboxyl groups in hemicellulose

	Carboxyl groups (mmol/g)	Free amino groups (mmol/g)
Hemicellulose	0.01-0.02	-
Commercial xylan	0.05-0.06	-
Chitosan	-	2.05**
Chitosan***	-	1.60**

** averages determined by ninhydrin assay method described in experimental methods

***crosslinked with 3% w/w glutaraldehyde, degree of crosslinking was ~22%.

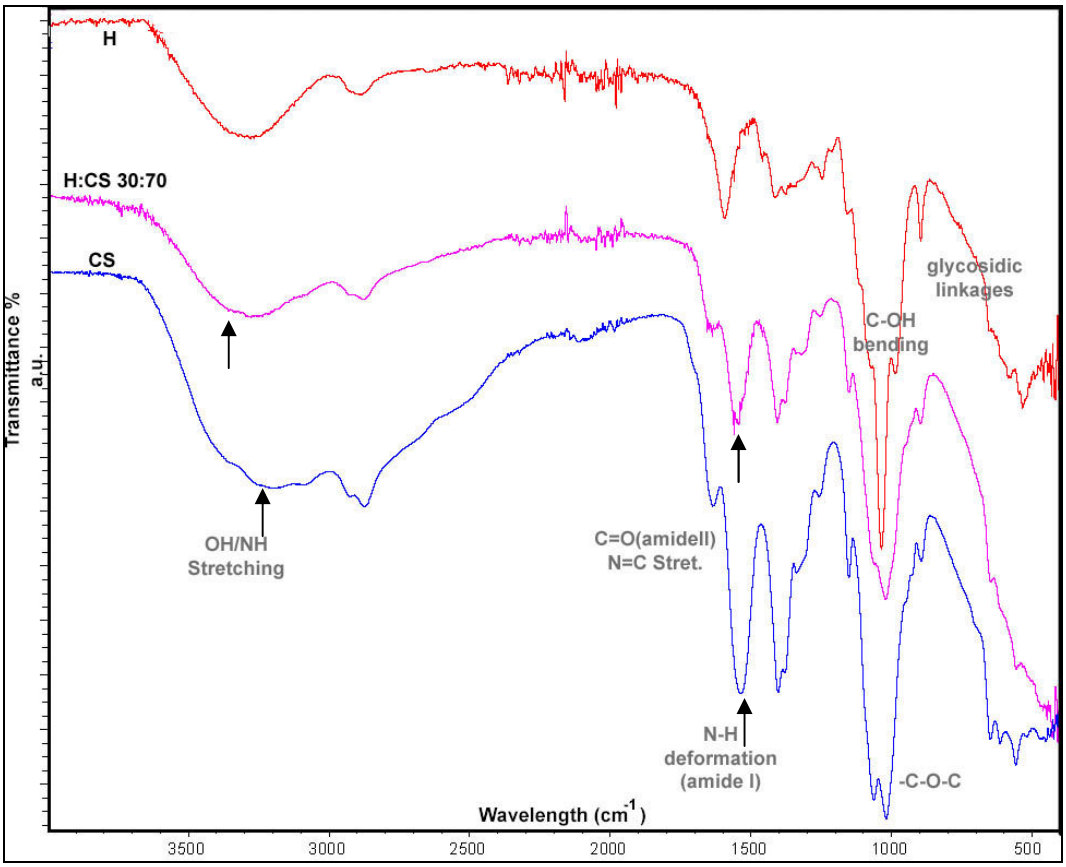

Figure 2.5 FTIR spectra of dry hydrogel films (arrows point at shifted peaks)

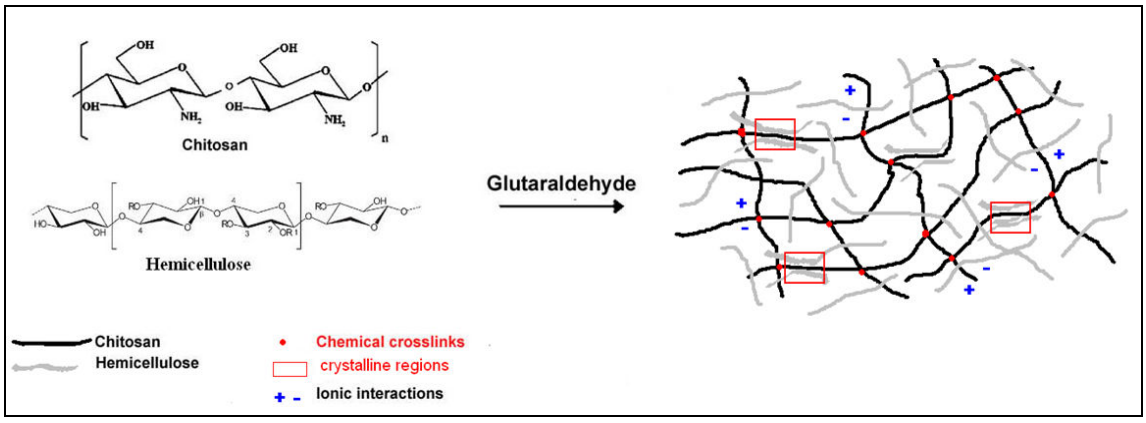

Figure 2.6 Possible semi-interpenetrating network of crosslinked chitosan and entrapped hemicellulose with weak interactions to chitosan

2.4.4 Mechanical properties of hydrogel films

The gelling properties of chitosan are well-documented.[16] However, chitosan gels without chemical or ionic crosslinks cannot be considered for controlled drug delivery due to their low shape retention and low mechanical stability in the swollen state. In this study, it was hypothesized that the addition of hemicellulose might have a sufficiently high stabilizing effect due to the introduction of crystallites and the interaction between the functional groups of hemicellulose and chitosan.

The mean and standard deviation values of elastic modulus, ultimate strength and strain to failure (standard deviations in brackets) are given in Table 2.3. Dry and water-swollen hemicellulose films without admixture of chitosan were too brittle to test. In the dry state of the films, hemicellulose did not enhance their mechanical properties, and crosslinked chitosan films were clearly stronger. However, in the swollen state the difference in strength between pure chitosan and chitosan/hemicellulose semi-IPN films was less. Absorbed water acted as a plasticizer and reduced the strength and modulus of swollen semi-IPN gels significantly, while slightly increasing the elongation. Strain to failure values were lower in both the swollen and dry state with increasing hemicellulose content. This might be attributed to the higher crystallinity of the semi-IPN films in comparison to the purely amorphous chitosan matrix. On the other hand, the crystallites formed in H:CS films showed little overlap, if at all (see Fig. 2.3). Instead, more or less isolated crystallites were observed.

Even though hemicellulose incorporation did not enhance the mechanical properties, observed values in regard to the tensile strength, elastic modulus and strain to failure for H:CS films in the dry state were comparable to those of biodegradable films reported in the literature.[38] The similarity of mechanical properties of semi-IPN gels that contained hemicellulose and commercially available xylan showed that hemicellulose extracted for this study could compete with the products currently on the market.

Table 2.3 Mechanical properties of dry and water-swollen hydrogel films with different hemicellulose compositions

Films	Modulus (MPa)	Ultimate Strength (MPa)	Strain to Failure (%)
H	Too brittle to test	Too brittle to test	Too brittle to test
H:CS 70:30-dry film	1390± 50	29.27±1.83	3.65±0.46
H:CS 30:70-dry film	2160±180	54.90±15.50	5.03±2.28
CS-dry film	2460±250	71.15±13.37	11.07±1.75
H:CS 30:70-swollen film	4.79±0.21	0.46±0.23	12.67±4.74
X[a]:CS 30:70-swollen film	5.33±1.08	0.45±0.08	11.23±1.37
CS-swollen film	7.74± 1.01	1.46±0.32	23.15±4.51

[a] X: commercial xylan

It can be hypothesized that the decrease in modulus and strength values is a consequence of lower crosslink density and a simultaneous increase in average chain length between crosslinks ($\overline{M_C}$, g/mol) with hemicellulose inclusion into chitosan matrix (see Table 2.4). Effective crosslinking density was reduced from 15.3 x10^{-4} mol/cm^3 to 9.3 x10^{-4} mol/cm^3, while the average molecular weight of the chain length between crosslinks increased from 1074 g/mol to 1326 g/mol for semi-IPN gels with 30%

hemicellulose content. The decrease in crosslink density and increase in $\overline{M_C}$ may have resulted in a more effortless movement of the chain segments within the network and thus led to a reduction in mechanical properties.

The crosslink density of H:CS 70:30 samples could not be determined because the tensile testing of these hydrogel films at swollen state was impossible. Even though these samples stayed intact in the swelling medium, samples were easily broken when taken out from the swelling medium for tensile testing.

Berger et al.[16] suggested that an additional polymer whose hydrophilicity is different than chitosan might disturb the covalent crosslinking of chitosan chains, which then results in lower crosslink density. It is possible that glutaraldehyde formed fewer and/or longer crosslinks due to the strong intermolecular interactions between chitosan and hemicellulose. Although crystalline domains and additional secondary interactions were introduced with hemicellulose inclusion, it can be suggested that covalent crosslinks were the predominant factor that influenced the overall crosslinking density and resulted in lower modulus and strength.

Table 2.4 Crosslink density and $\overline{M_C}$ values calculated form elastic modulus of swollen hydrogels and equilibrium swelling ratios

	Crosslink density (mol/cm^3)	$\overline{M_C}$ (g/mol)	S (%)
CS	15.3± 1.6 x10^{-4}	1074±114	126±4
H:CS 30:70	9.3± 0.6 x10^{-3}	1326±96	136 ±13
H:CS 70:30	-	-	148±10

2.4.5 Swelling behavior

The percentage equilibrium swelling ratios of semi-IPN hydrogels are listed in Table 2.4. As compared to crosslinked chitosan without hemicellulose, semi-IPN hydrogels had slightly higher swelling ratios with increasing hemicellulose content. Higher equilibrium swelling ratios can be attributed to lower crosslink density and higher $\overline{M_C}$ (g/mol), which resulted in more space for water molecules.

It might have been expected that swelling ratios would be reduced with addition of hemicellulose into the chitosan matrix due to the formation of water-impermeable crystalline domains. Additionally, intermolecular interactions might be considered as physical crosslinks.[16] However, as discussed previously, the reaction of glutaraldehyde could have been impaired by hemicellulose, and therefore higher swelling ratios were observed as a consequence of lower crosslink density and higher $\overline{M_C}$ (g/mol).

2.4.6 pH-dependant swelling

According to Donnan equilibrium swelling theory, the osmotic pressure or ion concentration gradient between the inside and outside of a hydrogel is the driving force for swelling. If swelling/deswelling occurs in a narrow pH range and is caused by ionization and repulsion of charged groups, the hydrogel is considered to be pH-sensitive. Such hydrogels are very useful as drug carriers. The swelling behavior of crosslinked chitosan and semi-IPN hydrogels containing hemicellulose is shown in Figure 2.7. At pH 4, the swelling ratios of semi-IPN hydrogels were fairly high. At pH 2, the observed slight decrease could be due to a shielding effect caused by excess H^+. At basic pH values, swelling was clearly reduced since the hydrogel contracted.

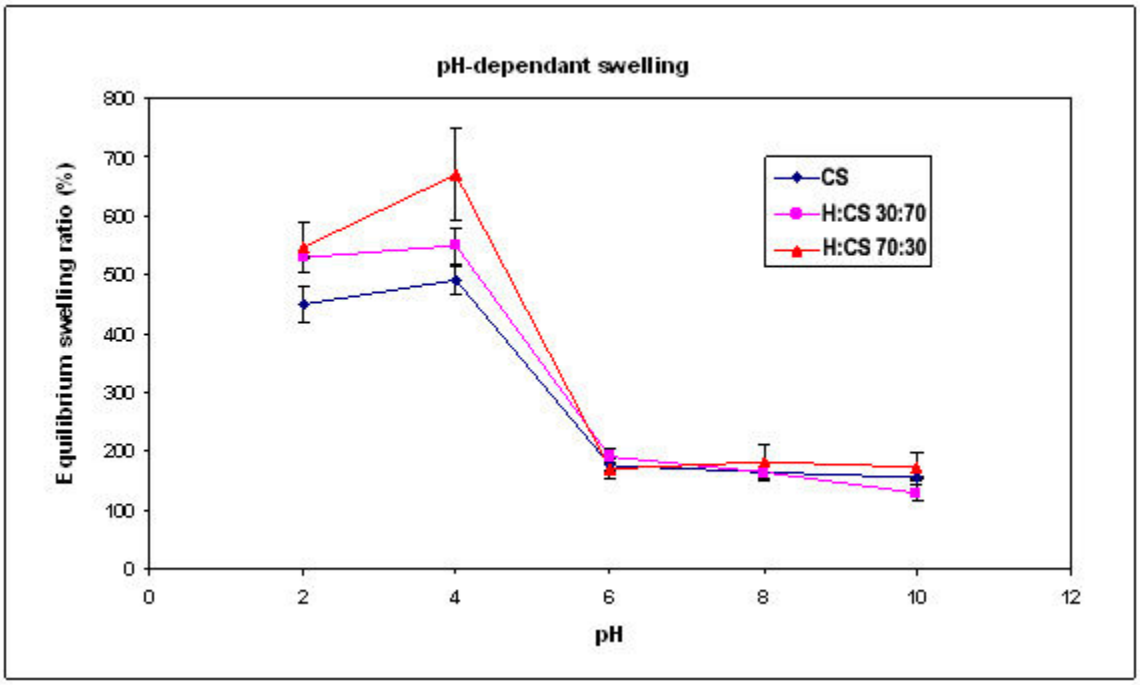

Figure 2.7 Effect of pH on the swelling behavior of CS and CS/H hydrogels.

2.4.7 In vitro release study

Release systems depend on the matrix, the drug to be discharged, and its solubility in both the matrix and the release medium. Riboflavin has been chosen as a model drug for this study due to its different solubility at different pH ranges and the aspect that it does not significantly interfere with the functional groups of the matrix. Due to the fact that it is not soluble under acidic conditions, the evaluation of the gel matrix becomes possible, separate from effects that occur due to drug solubility. Chitosan-based hydrogels have been reported for oral sustained delivery of antibiotics/ antiulcer drugs in the stomach.[39] The semi-IPN gels reported in this study could be an alternative for this purpose.

At pH 2.2, the gel matrix was highly swollen (Fig. 2.7, room temperature), and the cumulative release of riboflavin from both CS and H:CS 70:30 gels was higher and faster than at pH 7.4 (Fig. 2.8). At this pH value, raising the temperature to 37°C caused an additional increase in equilibrium swelling ratio by 30% on the average. Therefore it was not surprising that within 3 h approximately 95% of the drug was released, although riboflavin is little soluble at this pH. Therefore, it can be assumed that in this case riboflavin was discharged mainly as a consequence of the fairly open gel structure. The matrix most likely presented only a physical impediment for the release, and the interaction of riboflavin with release medium was of minor importance.

The total amount of riboflavin liberated at pH 7.4 was lower for both H:CS 70:30 (70%) and CS gels (85%) after 3 h exposure. Here the temperature did not play a major role in regard to the equilibrium swelling ratio. At 37°C the fairly collapsed gels showed

only approximately 10% higher swelling. However, with increasing alkalinity riboflavin becomes significantly more soluble. In this case, the higher solubility of riboflavin might have contributed to the still fairly fast release from a far less swollen gel matrix at this pH value (Fig. 2.7).

The presence of hemicellulose in H:CS 70:30 gels, however, clearly reduced the release rate compared to pure CS gels. In order to interpret the experimental results better, drug release mechanisms were determined by fitting the first 60% of the release profiles into the following equation (Eq. 2.6)[40],

$$\frac{M_t}{M_\infty} = kt^n \tag{2.6}$$

where M_t/M_∞ is the fractional release of drug in time t, k is the constant characteristic of the drug–polymer system, and n is the diffusion exponent characteristic of the release mechanism.

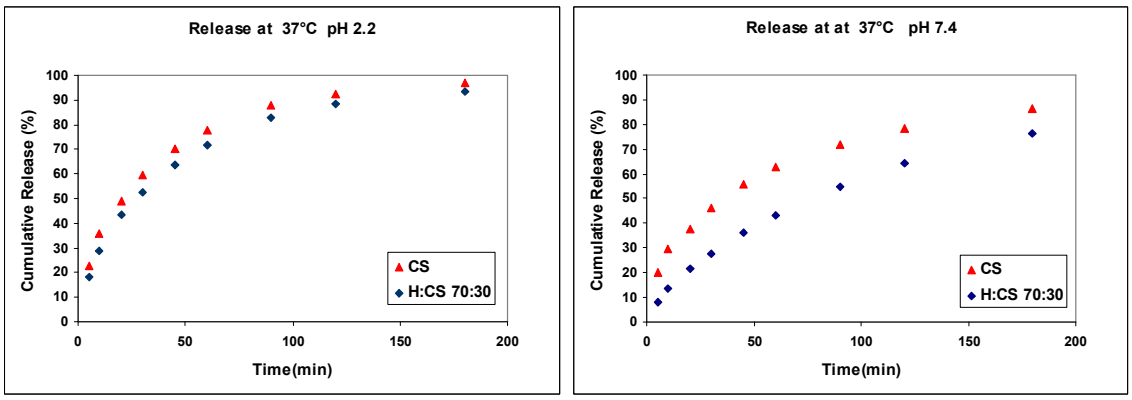

Figure 2.8 Release of riboflavin from semi-IPN hydrogels as a function of time in (a) pH 2.2 and (b) pH 7.4 buffer solutions at 37°C.

Table 2.5. Kinetic Constants (k), Release Exponents (n) and Determination Coefficients (r^2) Obtained from the First 60% of Cumulative Release Data (Eq.2.6)

Films	n	k	r^2
CS at pH 2.2	0.52	0.101	0.990
CS at pH 7.4	0.45	0.099	0.993
H:CS 70:30 at pH 2.2	0.60	0.070	0.995
H:CS 70:30 at pH 7.4	0.66	0.287	0.998

According to Eq.2.6, for polymer films, the value of n=0.5 implies that the drug release is controlled mostly by diffusion, while swelling- (or chain relaxation) controlled drug release occurs in case of n=1.0. The values between 0.5 and 1.0 are indicative of the release behavior being controlled by both phenomena. H:CS 70:30 hydrogels at both pH levels showed non-Fickian behavior ($0.5<n<1$), indicating that the drug release was due to both drug diffusion and chain relaxation of the hydrogel matrix (see Table 2.5). However, n values for CS hydrogels were relatively close to n=0.5 (for thin film), suggesting that the release was dominated by Fickian diffusion.[12, 41] At pH 7.4 CS gels begin to lose their swelling capacity. It can therefore be argued that n values drop below 0.5, implying a beginning transformation from a gel to a solid material.

Further, equilibrium swelling of the gel matrix was reached after approximately one hour; however, the drug continued to be discharged into the release medium for additional two hours, which is one more indication for the release to follow a combined mechanism of diffusion and chain relaxation.

2.5 Conclusions

An innovative alkaline extraction technique was used to separate hemicellulose from low-value aspen biomass. Although the isolated hemicellulose was fairly polydisperse, a sufficiently large amount of polymeric polysaccharides could be preserved. Novel pH-sensitive semi-IPN hydrogels were developed based on the extracted high molecular weight hemicellulose and crosslinked chitosan as a matrix. Crystallites introduced through hemicellulose enhanced the coherence of the swollen semi-IPN hydrogels. It is assumed that although covalent crosslinks predominantly influenced the mechanical stability, fewer and/or longer crosslinks were formed in presence of hemicellulose, thus improving the response to pH-induced swelling. Higher swelling ratios were observed with increasing hemicellulose content. Swelling ratios were high at low pH due to repulsion of the charged groups in the chitosan gel and low at the physiological pH of 7.4. Riboflavin was selected as a model drug due to its low solubility and minimal interference with the gel matrix. An *in vitro* release study of riboflavin showed that these semi-IPNs could have potential for application as pH-sensitive controlled drug delivery vehicles in physiological environments, e.g., for antibiotics or antiulcer drugs in the stomach. At low pH the highly swollen hydrogel matrix would fairly easily discharge the drug, while at higher pH values the gel matrix is collapsed, and the release is dominated by the solubility of the drug in the release medium.

2.6 References

[1] Timell, T.E. Recent Progress in the Chemistry of Wood Hemicelluloses. *Wood Science and Technology.* **1967**, l, 45-70.

[2] Gatenholm, P.; Tenkanen, M. *Hemicelluloses: Science and Technology*, **2004**, 15-16. Oxford University Press.

[3] Ebringerova, A. Structural Diversity and Application Potential of Hemicelluloses. *Macromolecular Symposia.* **2006,** 232, 1-12.

[4] Peppas, N.A.; Hilt, J. Z.; Khademhosseini, A.; Langer, R. Hydrogels in Biology and Medicine: From Molecular Principles to Bionanotechnology. *Advanced Materials*. **2006,** 18, 1345–1360.

[5] Slaughter, B. V.; Khurshid, S. S.; Fisher, O. Z.; Khademhosseini, A.; Peppas, N. A. Hydrogels in Regenerative Medicine, *Advanced Materials*. **2009,** 21, 1-23.

[6] Hoare, T. R.; Kohane, D. S. Hydrogels in Drug Delivery: Progress and Challenges. *Polymer*. **2008,** 49, 1993-2007.

[7] Peppas, N.A.; Bures, P.; Leobandung, W.; Ichikawa, H. Hydrogels in Pharmaceutical Formulations. *European Journal of Pharm. and Biophar.* **2000,** 50, 27–46.

[8] Coviello, T.; Matricardi, P.; Marianecci, C.; Alhaique, F. Polysaccharide Hydrogels for Modified Release Formulations. *Journal of Controlled Release*. **2007,** 119, 5-24.

[9] Tanaka, Y.; Gong, J. P.; Osada, Y. Novel Hydrogels with Excellent Mechanical Performance. *Progress in Polymer Science*. **2005,** 30, 1-9.

[10] Schexnailder, P.; Schmidt, G. Nanocomposite Polymer Hydrogels. *Colloid and Polymer Science.* **2009,** 287, 1-11.

[11] Myung, D.; Waters, D.; Wiseman, M.; Duhamel, P.E.; Noolandi, J.; Ta, C.N.; Frank, C.W. Progress in the development of interpenetrating polymer network hydrogels. *Polymers for Advanced Technologies*, **2008**, 19, 647 – 657.

[12] Liu, C.; Chena, Y.; Chena, J. Synthesis and Characteristics of pH-Sensitive Semi-Interpenetrating Polymer Network Hydrogels Based on Konjac Glucomannan and Poly (Aspartic Acid) for in Vitro Drug Delivery. *Carbohydrate Polymers.* **2010,** 79, 500-506.

[13] Jin, S.; Liu, M.; Zhang, F.; Chen, S.; Niu, A. Synthesis and Characterization of pH-Sensitivity Semi-IPN Hydrogel Based on Hydrogen Bond Between Poly(N-Vinylpyrrolidone) and Poly(Acrylic Acid). *Polymer.* **2006**, 47, 1526–1532.

[14] Zhao, Y.; Kang, J.; Tan, T.W. Salt-, pH- and Temperature-Responsive Semi-Interpenetrating Polymer Network Hydrogel Based on Poly(Aspartic Acid) and Poly(Acrylic Acid). *Polymer.* **2006,** 47, 7702–7710.

[15] Čulin, J.; Šmit, I.; Andreis, M.; Veksli, Z.; Anžlovar, A.; and Žigon, M. Motional Heterogeneity and Phase Separation of Semi-Interpenetrating Networks and Mixtures Based on Functionalised Polyurethane and Polymethacrylate Prepolymers. *Polymer.* **2005,** 46, 89–99.

[16] Berger, J.; Reist, M.; Mayer, J. M.; Felt, O.; Gurny, R. Structure and Interactions in Covalently and Ionically Crosslinked Chitosan Hydrogels for Biomedical Applications. *European Journal of Pharmaceutics and Biopharmaceutics.* **2004**, 57, 19-34.

[17] Zugic, D.; Spasojevic, P.; Petrovic, Z.; Djonlagic, J. Semi-Interpenetrating Networks Based on Poly(N-Isopropyl Acrylamide) and Poly(N-Vinylpyrrolidone). *Journal of Applied Polymer Scence.* **2009**, 113, 1593-1603.

[18] Zhang, G.Q.; Zha, L.S.; Zhou, M.H.; Ma, J.H.; Liang, B.R. Preparation and Characterization of pH- and Temperature- Responsive Semi-Interpenetrating Polymer Network Hydrogels Based on Linear Sodium Alginate and Crosslinked Poly(N-Isopropylacrylamide). *Journal of Applied Polymer Science.* **2005,** 97, 1931–1940.

[19] Guo, B.L.; Gao, Q.Y. Preparation and Properties of a pH/Temperature-Responsive Carboxymethyl Chitosan/Poly(N-Isopropylacrylamide)Semi-IPN Hydrogel for Oral Delivery of Drugs. *Carbohyrate Polymers.* **2007,** 342, 2416-2422.

[20] Gabrielii, I.; Gatenholm, P. Preparation and Properties of Hydrogels Based on Hemicellulose. *Journal of Applied Polymer Science.* **1998,** 69, 1661–1667.

[21] Gabrielii, I.; Gatenholm, P.; Glasser, W. G.; Jain, R. K.; Kenne, L. Separation Characterization and Hydrogel-Formation of Hemicellulose from Aspen Wood. *Carbohyrate Polymers.* **2000,** 43, 367–374.

[22] Lindblad, M.S.; Albertsson, A.C.; Ranucci, E.; Laus, M.; Giani, E. Biodegradable Polymers from Renewable Sources: Rheological Characterization of Hemicellulose-Based Hydrogels. *Biomacromolecules.* **2005,** 6, 684-690.

[23] Lindblad, M.S.; Ranucci, E.; Albertsson, A.C. Biodegradable Polymers from Renewable Sources. New Hemicellulose-Based Hydrogels. *Macromolecular Rapid Communications.* **2001,** 22, 962-967.

[24] Yui, N. *Supramolecular Design for Biological Applications*. **2002**. CRC Press, Boca Raton.

[25] Ma, P. X.; Elisseeff, J. H. *Scaffolding in Tissue Engineering*, **2005.** CRC Press, Boca Raton.

[26] Lou, X.; Coppenhagen, C. Mechanical Characteristics of Poly(2-Hydroxyethyl Methacrylate) Hydrogels Crosslinked With Various Difunctional Compounds. *Polymer International.* **2003,** 50, 319-325.

[27] Yu, H.; Lu, J.; Xia, C. Preparation and Properties of Novel Hydrogels from Oxidized Konjac Glucomannan Cross-Linked Chitosan for in Vitro Drug Delivery. *Macromolecular Bioscience.* **2007,** 7, 1100 – 1111.

[28] Curotto, E.; Aros, F. Quantitative Determination of Chitosan and the Percentage of Free Amino Groups. *Analytical Biochemistry.* **1993,** 211, 240-241.

[29] Mi, F.L.; Tan, Y.C.; Liang, H.C.; Huang, R.N.; Sung, H.W. In Vitro Evaluation of a Chitosan Membrane Cross-Linked with Genipin. *Journal of Biomaterial Science Polymer Edition.* **2001,** 12, 835–850.

[30] Anseth, K. S.; Bowman, C. N.; Bannon-Peppas, L. Mechanical Properties of Hydrogels and their Experimental Determination. *Biomaterials.* **1996,** 17, 1647-1657.

[31] Rogers, K.; Etok, S.; Broadhurst, A.; Scott, R. Enhanced analysis of biomaterials by synchrotron diffraction. *Nuclear Instruments and Methods in Physics Research.* **2005**, 548, 123-128.

[32] Teleman, A.; Lundqvist, J.; Tjerneld, F.; Stalbrand, H.; Dahlman, O. Characterization of Acetylated 4-O-Methylglucuronoxylan Isolated from Aspen Employing H- and C-NMR Spectroscopy. *Carbohyrate Research*. **2000,** 329, 807−815.

[33] Gröndahl, M.; Eriksson, L.; Gatenholm, P. Material Properties of Plasticized Hardwood Xylans for Potential Application as Oxygen Barrier Films. *Biomacromolecules.* **2004**, 5, 1528–1535.

[34] Dumitriu, S. *Polysaccharides: Structural Diversity and Functional Versatility: Second Edition*. **2004**, pp.509-510, CRC Press.

[35] Kumar, M. N. V. R.; Muzzarelli, R. A. A.; Muzzarelli, C.; Sashiwa, H.; Domb, A. J. Chitosan Chemistry and Pharmaceutical Perspectives. *Chemical Reviews.* **2004,** 104, 6017–6084.

[36] Guan, Y. L.; Shao, L.; Yao, K. D. A Study on Correlation between Water State and Swelling Kinetics of Chitosan-Based Hydrogels. *Journal of Applied Polymer Science***.** **1996**, 61, 2325–2335.

[37] Wang, T.; Turhan, M.; Gunasekaran, S. Selected Properties of pH-sensitive, Biodegradable Chitosan–Poly(Vinyl Alcohol) Hydrogel. *Polymer International.* **2004**, 53, 911–918.

[38] Hansen, N. M. L.; Plackett, D. Sustainable films and coatings from hemicelluloses: A review. *Biomacromolecules.* **2008***,* 6, 1493-1505

[39] Shu, X. Z.; Zhu, K. J.; Song, W. Novel pH-sensitive citrate cross-linked chitosan film for drug controlled release. *International Journal of Pharmaceutics*. **2001**, 212, 19-28.

[40] Ritger, P.L.; Peppas, N.A. A Simple Equation for Description of Solute Release I. Fickian and Non-Fickian Release from Swellable Devices. *Journal Controlled Release.* **1987,** 5, 37–42.

[41] Lynch, I.; Dawson, K. A. Release of Model Compounds from Plum-Pudding– Type Gels Composed of Microgel Particles Randomly Dispersed in a Gel Matrix. *Journal of Physical Chemistry B.* **2004,** 108, 10893–10898.

CHAPTER 3

Hemicellulose/Chitosan-Based Hydrogel Networks: Effect of Hemicellulose on Crosslink Density, Swelling and Mechanical Properties

3.1 Abstract

Semi-interpenetrating network hydrogel films were prepared using hemicellulose and chemically crosslinked chitosan. Hemicellulose, which was extracted from aspen by using a novel alkaline treatment and characterized by HPSEC, consisted of a mixture of high and low molecular weight polymeric fractions. Their major constituent sugar, which was determined by hydrolysis and HPLC analysis, was found to be xylose. X-ray analysis showed that the relative crystallinity of hydrogels increased with increasing hemicellulose content up to 31.3%. Strong intermolecular interactions between chitosan and hemicellulose were evidenced by FT-IR analysis. Quantitative analysis of free amino groups showed that hemicellulose could interrupt the chemical crosslinking of chitosan macromolecules. Mechanical testing and swelling experiments were used to define the effective network crosslink density and average molecular weight between crosslinks. Swelling ratios increased with increasing hemicellulose content and were mainly caused by H-bonding of bound water. Results revealed that by altering the hydrogel preparation steps and hemicellulose content, crosslink density and swelling behavior of semi-IPN hydrogels could be controlled without deteriorating their mechanical properties.

3.2 Introduction

Hemicelluloses are a class of hetero-polysaccharides present in the cell wall of wood and annual plants together with cellulose and lignin. They are considered to be the second most abundant polysaccharide in nature, representing about 20-35% of lignocellulosic biomass.[1] Increasing interest in materials derived from renewable resources has rekindled intensive research with focus on new applications for hemicelluloses. Due to their inherent hydrophilicity, low toxicity, biodegradability and biocompatibility, the formation of hydrogels is a potential area of application for hemicelluloses and their derivatives.[2, 3]

Hydrogels are crosslinked networks of hydrophilic polymers that are capable of retaining considerable amounts of water or biological fluids without disintegration. In addition to their high liquid up-take, stimuli-responsive swelling capabilities and biocompatibility are some of the features that render them suitable for biological and biomedical applications.[4-6] However, most hydrogels show relatively low mechanical stability. Efforts focused on improving the chemical and/or physical crosslinks between the macromolecular chains without impairing their sorption capabilities.[7-9] The formation of semi-interpenetrating networks (semi-IPNs) - blending two polymers with one being crosslinked in the presence of the other (not crosslinked) polymer - is a possible strategy that has been widely studied.[10-12] In addition to chemical crosslinks, additional interactions including hydrogen bonds, crystallites, ionic, and hydrophobic interactions, may contribute to the characteristics of the resulting hydrogel.[13]

In our previous study, we synthesized semi-interpenetrating network hydrogel films from aspen hemicellulose and chitosan and investigated their potential applications as pH-sensitive controlled drug delivery vehicles.[14] The mechanical stability of hydrogels was predominantly influenced by covalent crosslinks rather than crystallites introduced through hemicellulose. Aspen hemicelluloses had been freeze-dried and contained some acetyl groups. As discussed by Berger et al.[13], strong intermolecular interactions between chitosan and an additional hydrophilic polymer, hemicellulose in our case, was suggested to be the interfering factor for covalent crosslinking of chitosan chains and resulted in the reduction of overall crosslink density, lower modulus and strength. For the current study, extraction of hemicellulose from fresh aspen chips was performed under conditions that resulted in substitution of the acetyl groups with hydroxyl groups, which in turn enabled additional hydrogen bonding within the hydrogel.

The aim of the present work was to control the crosslink density and the mechanical properties of hemicellulose/chitosan semi-IPN hydrogels by changing the crosslinking sequence. It has been hypothesized that by performing the crosslinking step before introducing hemicellulose, covalent crosslinking of chitosan would not be hindered and therefore more and/or shorter crosslinks could be formed. Furthermore, additional secondary interactions and crystalline domains introduced through hemicellulose could be favorable in terms of mechanical stability of semi-IPN hydrogels.

3.3 Experimental

3.3.1 Materials

Chitosan with 190,000-310,000 g/mol viscosity average molecular weight with 75-85% degree of deacetylation and ninhdyrin solution (2%) were obtained from Sigma Aldrich. Glutaraldehyde, acetic acid, and other solvents and chemicals were purchased from Fisher Scientific and used as received.

3.3.2 Isolation of Hemicelluloses

Hemicellullose, isolated from fresh aspen chips extracted by a novel alkaline extraction method and milled by a commercial blender, was provided by USDA Forest Products Laboratory, Madison, WI (See Figure 3.1). Details of the isolation procedure are described in Karaaslan et al.[14] The sugar content analyzed by HPLC with electrochemical detection is given in Table 3.1.

Table 3.1 Sugar composition of hydrolysates of hemicellulose fractions (%) from fresh aspen chips

Arab	Gal	Rham	Glc	Xyl	Man	Lignin ash	Klason Lignin	Unknowns
ND*	0.48	0.26	0.93	69.70	0.29	0.35	0.7	27.29

ND = Not detected*

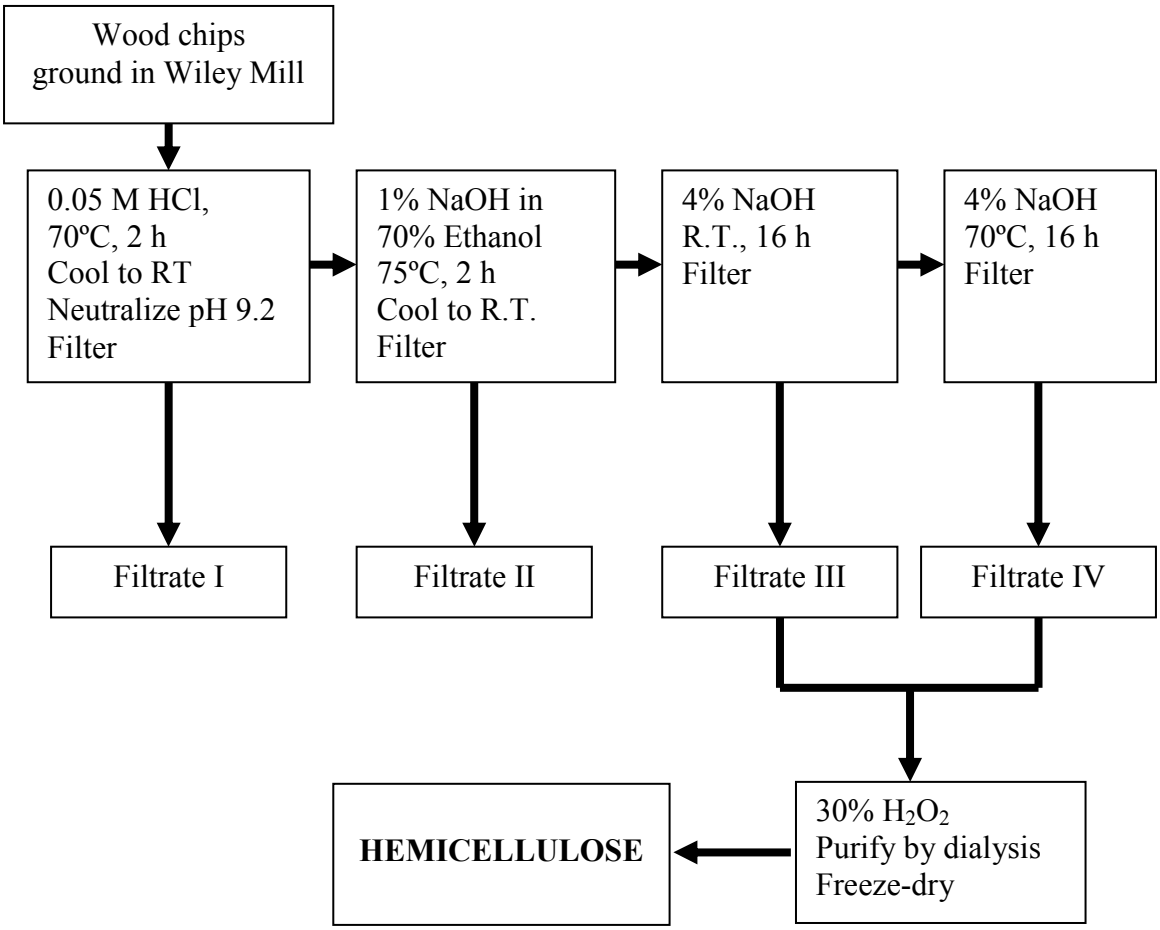

Figure 3.1. Schematic view of hemicellulose fractionation process

3.3.3 Hydrogel Preparation

Chitosan was dissolved in 2% v/v acetic acid aqueous solution to prepare 1% w/w chitosan solution. Hemicellulose was added to deionized water at 1% w/v and heated to 95°C for 20 min with stirring. The solution was cooled to room temperature.

In order to evaluate the effect of the order of sequential blending, semi-IPN hydrogels were prepared in two ways. In the first method (semi-IPN-1), chitosan and hemicellulose solutions at 70:30 and 30:70 weight ratios with a total dry matter of 1%

were stirred for 8h. For crosslinking, glutaraldehyde was added at a set ratio (3% w/w) to the total dry weight of chitosan and stirred for additional 8h. In the second method (semi-IPN-2), crosslinking of chitosan solution was performed first, and then hemicellulose solution was added subsequently at the same weight ratio. The mixture was stirred for 8h. Crosslinked chitosan control samples (CS) were prepared accordingly without addition of hemicellulose.

Final solutions were cast into films in petri dishes and dried in an oven at 40ºC for 24 h. The dry films were immersed in 0.1 N sodium hydroxide solution to neutralize acetic acid residues, then washed with ethanol to remove excess NaOH. After rinsing with deionized water, the films were dried in an oven at 40ºC for 24 h.

3.3.4 Hydrogel characterization

3.3.4.1 Mechanical Properties

Tensile testing of the swollen hydrogel films at equilibrium was performed with an Instron Universal Tester with a 2.5 N load cell. Gauge length and crosshead speed were set to 10 mm and 2 mm/min, respectively. Samples were cut into 7x30 mm strips before immersing in deionized water. In order not to damage the swollen samples during the thickness measurements, they were gently sandwiched between microscope cover slips. To prevent water loss during testing, hydrogel samples were coated with petroleum gel.[15] Mean values and 95% confidence intervals of at least ten replicates were reported.

3.3.4.2 Swelling Behavior

Pre-weighed dry films were immersed in deionized water at room temperature for 1 h, which was previously determined to be sufficient to reach the equilibrium state. The weight of the swollen samples was measured after blotting excessive water gently with filter paper. The equilibrium swelling ratio (*S*) was calculated by the following equation (Eq. 3.1),

$$S(\%) = \frac{W_s - W_d}{W_d} \times 100 \tag{3.1}$$

where W_s and W_d are the swollen and dry weight of samples, respectively. Equilibrium volume swelling ratio (Q) was determined according to (Eq.3.2),

$$Q_s = \frac{Vs}{Vd} = 1 + \frac{\rho_p}{\rho_s}(q-1) \tag{3.2}$$

where V_s is the volume of the swollen hydrogel, V_d is the volume of the dry hydrogel, ρ_p is the density of the polymer, ρ_s is the density of deionized water and q is the ratio of equilibrium swollen weight to dry weight of the films (W_s / W_d). The density of semi-IPN films was determined by the floating method with carbon tetrachloride and n-heptane as described by Jagadish et al.[16]

Differential scanning calorimetry (DSC) was used to study the state of water in the swollen hydrogels. A piece of equilibrium swollen sample (2-4 mg) was sealed in an aluminum pan. After equilibrating for 3 min at -50°C, the sample was heated to 25°C at a rate of 5°C/min. The non-freezing bound water and free water of the hydrogels were determined by using Eq. 3.3,

$$W_b(\%) = S(\%) - (\Delta H_m / \Delta H_0) \times 100 \quad (3.3)$$

where W_b is the percentage of bound water, $S(\%)$ is the equilibrium swelling ratio; ΔH_m and ΔH_0 (334 J/g) are the melting endothermic heat of measured free water in the hydrogel and pure water, respectively. [17]

3.3.4.3 Hydrogel structure analysis

The amount of free amino groups (NH_2) in semi-IPN hydrogels were determined by ninhydrin assay according to the standard procedure. FTIR spectra of dry films were obtained with a Nicolet 6700 FT-IR spectrometer in transmission mode between 4000 and 400 cm^{-1} over 64 scans with a resolution of 4 cm^{-1}. The crystallinity of the films was analyzed by using a Rigaku Miniflex X-ray diffractometer. Cu Kα radiation at 30 kV and 15 mA with a wavelength of 1.54 Å was used, and 2θ was varied between 5 and 30° at a rate of 1° per min and a step size of 0.02°. The relative crystallinity of films was determined by the percent ratio of area under the peak at about $2\theta=18°$ to the total area under the peak. [18]

3.4 Results and Discussion

3.4.1 Hemicellulose Extraction

Sugar analysis of hemicellulose fractions (see Table 3.1) isolated for this study yielded xylan-rich (70%) heteropolysaccharides with gluco-, galacto- mannan- and rhamnan-residues. NMR analysis showed that the sugar residues did not carry any acetyl groups. The carboxyl group (–COOH) content was estimated by acid-base titration of hemicellulose solution and found to be 0.02-0.025 mmol/g. HPSEC results revealed a fair

amount of polymeric saccharides with apparent peak molecular weights at $MW_p \approx$ 401,000 and 391,000 $g.mol^{-1}$ which is relatively high as compared to other xylans mentioned in the literature (e.g., oat spell xylan and commercially available birchwood xylan).[19, 20]

Aqueous hemicellulose solution (1% w/v) casted onto a glass plate did not produce films but brittle flakes which might be attributed to its fairly low molecular weight and high glass transition temperature.[21] X-ray analysis (See Figure 3.2) showed that the hemicellulose used in this study had a crystallinity of 42.9%, which is comparable to data reported in the literature for alkaline extracted hemicelluloses. [18, 21] The crystallinity of semi-IPN films with 70% and 30% hemicellulose content was determined to be 31.3% and 15.4%, respectively.

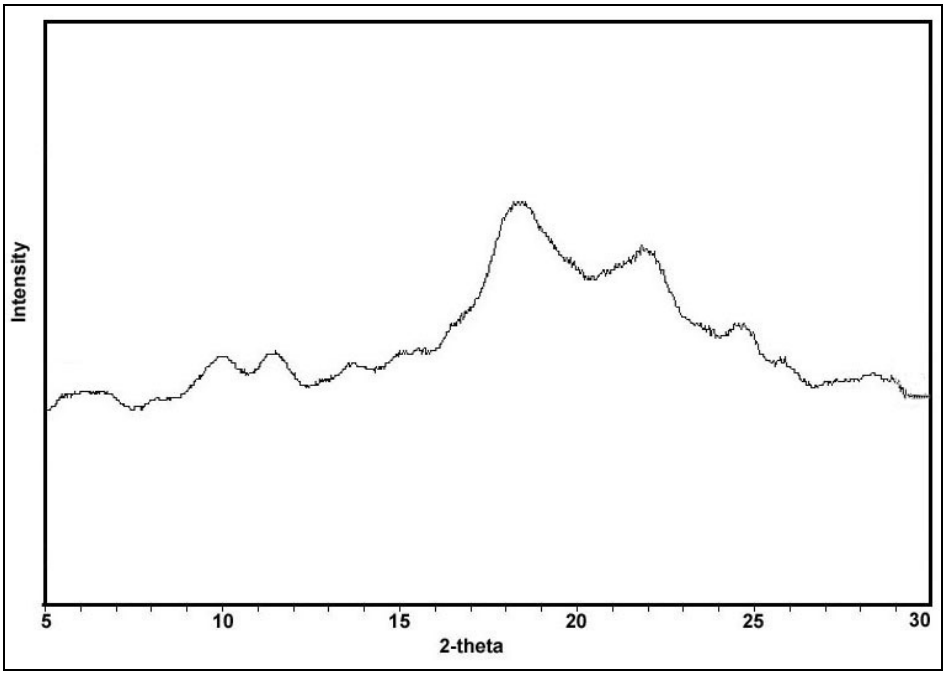

Figure 3.2 X-ray diffractogram of hemicellullose flakes

3.4.2 Effect of crosslinking sequence on the formation of semi-IPNs – FT-IR analysis

Figure 3.3 shows FT-IR spectra of semi-IPN-2 hydrogel films in comparison to crosslinked chitosan film (CS) and hemicellulose flakes (H) as the control samples. All spectra were normalized using 2880 cm^{-1} as the reference peak as described by Kolhe and Kannan.[22] Data for semi-IPN-1 films were very similar to semi-IPN-2 films.

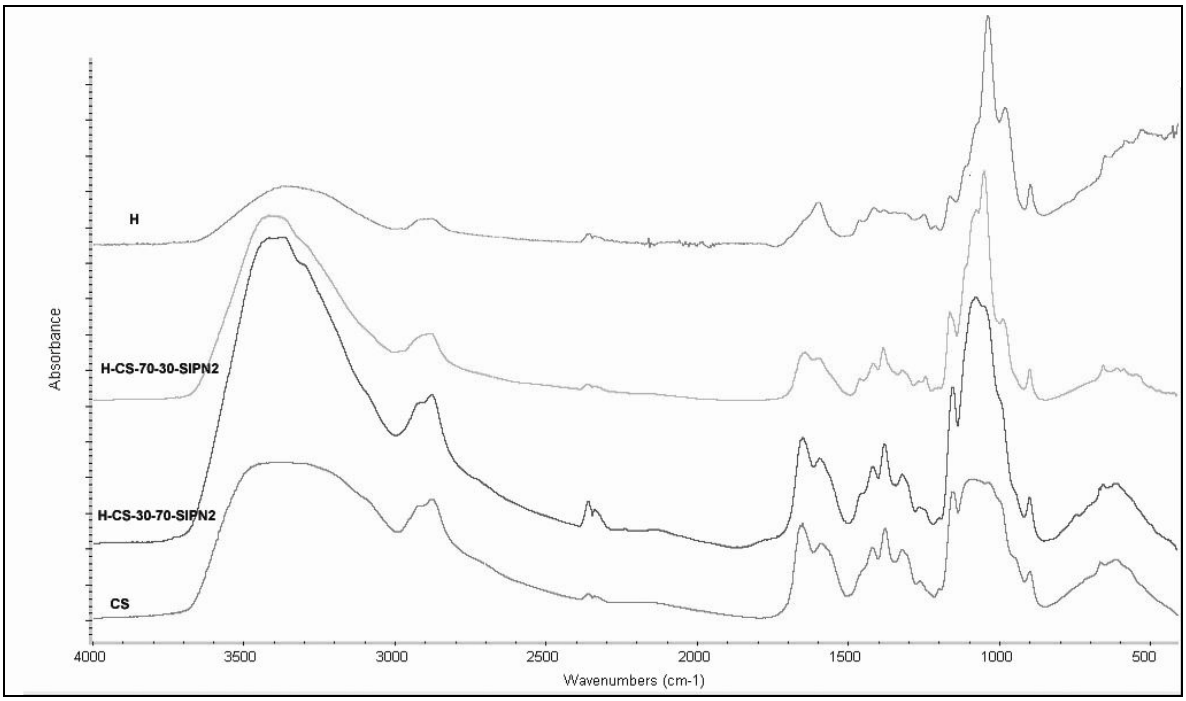

Figure 3.3 FT-IR spectra of semi-IPN-2 films, chitosan (CS) and hemicellulose (H) control samples

Major absorbance bands for the CS control sample were at 1651 cm^{-1} for imide (C=N stretching) and amide I bond (C=O stretching); 1590 cm^{-1} for amide II (N-H deformation); and a broad peak at 3200-3500 cm^{-1} for N−H and O−H stretching. These bands could be seen in both semi-IPN-1 and semi-IPN-2 hydrogel films with 30% and 70% hemicellulose content. Major peaks for hemicellulose were a broad O-H stretching band at about 3400cm^{-1}, and vibrations belonging to glycosidic linkages and saccharide

ring at 1070, 1035, 981 and 898 cm^{-1}. Unfortunately, these bands overlapped with chitosan peaks and were difficult to distinguish in semi-IPN films. For both semi-IPN-1 and -2 films, peak shifts were observed at the NH deformation band (from 1590 cm^{-1} to 1601 cm^{-1}) and O-H/N-H stretching band (from 3360 to 3410 cm^{-1}). In addition, absorbance bands at 1070 and 1035 cm^{-1} became more pronounced and narrower with increasing hemicellulose content. These differences in both semi-IPNs might be attributed to the strong intermolecular interactions such as H-bonding and hydrophobic attractions between hemicellulose and chitosan chains.

The quantitative FT-IR analysis (Fig. 3.4) did not show any significant difference between semi-IPN-1 and -2, except for the normalized N-H deformation band at 1590 cm^{-1}. This band is characteristic for amino groups attached to the chitosan backbone [23, 24] and could be used to evaluate the amount of free amino groups which did not undergo a crosslinking reaction with glutaraldehyde. As shown in Fig. 3.4, semi-IPN-2 films had lower absorbance values than those of semi-IPN-1 films for both hemicellulose compositions. The mean values for semi-IPN-2 films were relatively similar to crosslinked control CS films.

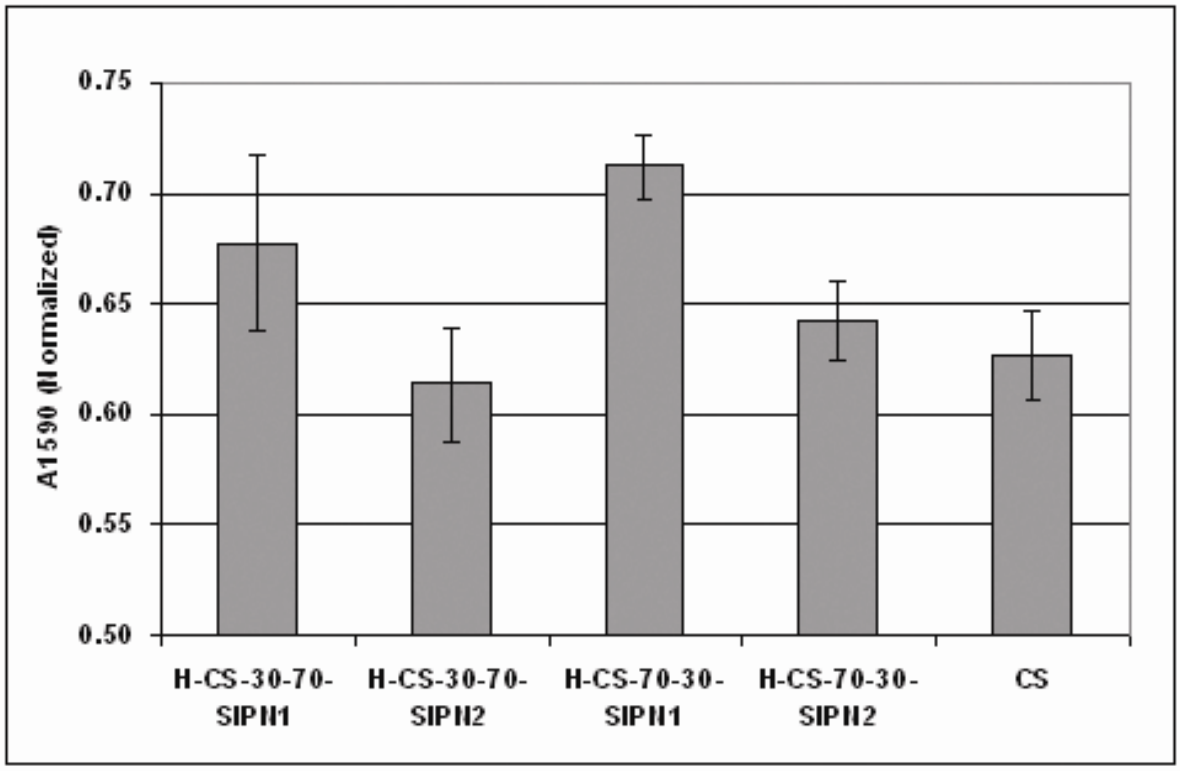

Figure 3.4 Comparison of the normalized N-H deformation absorbance band at 1590 cm^{-1} for semi-IPN-1 and -2 films (mean values and 95% confidence intervals reported, n=5)

The ninhydrin analysis (Fig. 3.5) of available amine groups showed that hemicellulose interfered in the covalent crosslinking reaction of chitosan chains with glutaraldehyde. This assay method is commonly used for quantitative determination of free amino groups in chitosan.[25, 26] Fig. 3.6 shows the average molar quantity of free amino groups ($-NH_2$) per unit chitosan weight and its dependence on hemicellulose composition in semi-IPN-1 and -2 hydrogels. Apparently, the amount of free amino groups in semi-IPN-1 hydrogels was fairly high compared to semi-IPN-2 hydrogels. Moreover, it increased slightly with increasing hemicellulose content for semi-IPN-1 hydrogels, suggesting that the interference with the crosslinking reaction was also dependant on the hemicellulose content. Available amine groups for semi-IPN-2

hydrogels were at comparable level to the CS control sample and did not seem to depend on the hemicellulose content. In this case there was no obvious interference of hemicellulose with the crosslinking reaction of chitosan.

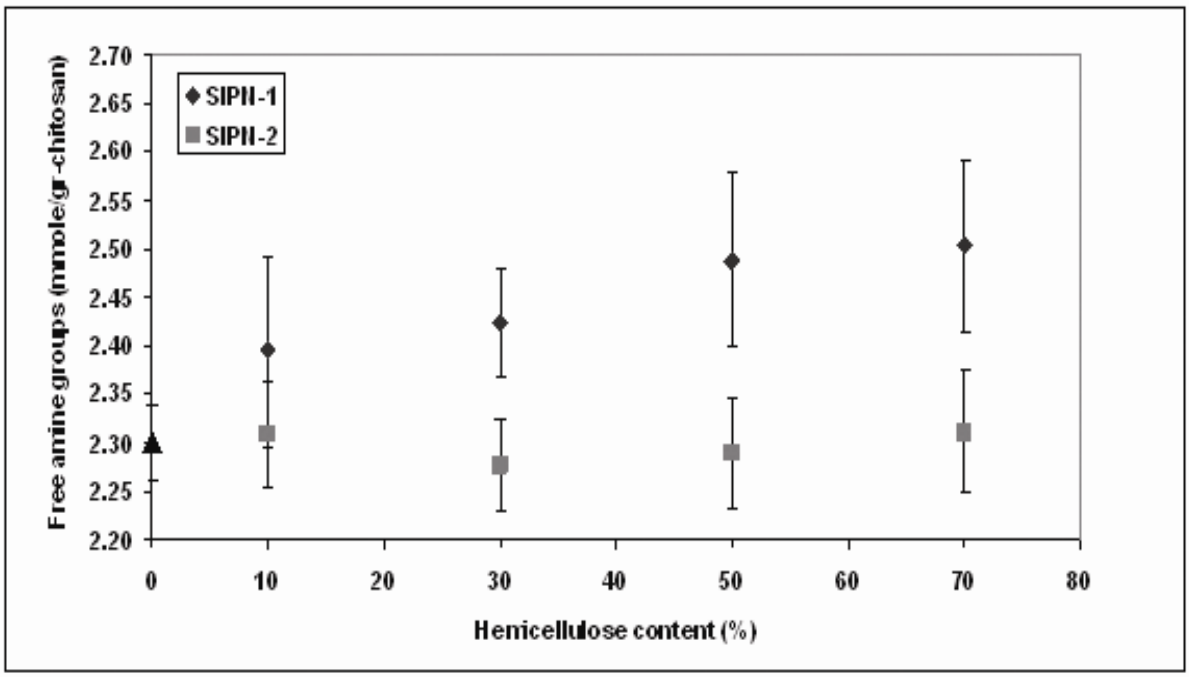

Figure 3.6 The amount of free amine groups determined by ninhydrin method and its dependence on hemicellulose content for semi-IPN-1 and -2 hydrogels (triangle represents the CS control sample).

3.4.3 Mechanical properties and network parameters

Stress-strain curves of swollen semi-IPN hydrogel films obtained from uniaxial tensile testing showed two regions with different slopes. To estimate the elastic modulus and network parameters, Flory's statistical rubber elasticity and Mooney-Rivlin theory were used for low and high elongations, respectively.

Elastic moduli of hydrogels, *G*, at low elongations were determined from the slope of stress-strain curves obtained by using Eq. 3.4,

$$\tau = G\left[\lambda - \frac{1}{\lambda^2}\right] \tag{3.4}$$

where τ is the force per unit of initial cross-sectional area of swollen gel and λ. is the deformation ratio (deformed length/initial length) of the network. According to Flory's statistical rubber elasticity theory, the number of effectively cross-linked chains per unit volume (ν_e, effective crosslink density) was calculated by using Eq. 3.5, [27-29]

$$\nu_e = \frac{RT\upsilon_2^{1/3}}{G} \tag{3.5}$$

where ν_e is the effective crosslink density in mol/cm^3, υ_2 is the polymer volume fraction at equilibrium swollen state, *R* is the gas constant, and *T* is the temperature in Kelvin. The average molecular weight between crosslinks ($\overline{M_C}$, g/mol) was calculated by using Eq.3.6,

$$\overline{M_c} = \frac{1}{\nu_e \bar{\upsilon}} \tag{3.6}$$

where $\bar{\upsilon}$ is the specific volume of the polymer in cm^3/g.

Mooney-Rivlin theory can be expressed by the following equation;

$$\tau = 2\left(C_1 + \frac{C_2}{\lambda}\right)\left(\lambda - \frac{1}{\lambda^2}\right) \tag{3.7}$$

where C_1 and C_2 are the elastic parameters. They can be obtained by plotting $\tau/(\lambda - \lambda^{-2})$ versus λ^{-1}, using the linear portion of the plots.[30] These constants are independent of

elongation and $G^* = 2C_1$ can be taken as an estimate of the high-elongation modulus.[31] In the present study, for **ε**>15%, $G^* = 2C_1$ was used to estimate the modulus, the effective crosslink density (ν_e^*, Eq.3.8) and the average molecular weight between the crosslinks ($\overline{M_c}^*$, from Eq.6).

$$\nu_e^* = \frac{2C_1}{RT} \tag{3.8}$$

The elastic modulus, tensile strength, elongation at break data and hydrogel network parameters calculated are given in Tables 3.2 and 3.3. Although calculated network parameters and modulus values from both sets of equations were significantly different, they followed the same trend. This showed that both theories could be applied to define the semi-IPN network structure prepared in the present study.

Table 3.2 Mechanical properties of swollen CS, semi-IPN-1 and -2 hydrogels. Low elongation modulus calculated using Flory's statistical rubber elasticity theory (G, for ε≤15%), high elongation modulus calculated using Mooney-Rivlin constants (G*, for ε>15%), tensile strength at break (σ) and elongation at break (ε) given in averages and 95% confidence intervals brackets (n>10).

	G (MPa)	**G* =2C$_1$ (MPa)**	**σ (MPa)**	**ε (%)**
CS	1.65±0.21	6.30±1.14	1.07±0.25	26.89±4.10
H-CS 30-70 SIPN-1	1.63±0.13	7.06±0.85	1.22±0.24	26.51±3.21
H-CS 30-70 SIPN-2	1.74±0.18	7.83±0.85	1.23±0.21	26.32±2.72
H-CS 70-30 SIPN-1	1.02±0.20	4.77±0.92	0.67±0.24	24.94±3.90
H-CS 70-30 SIPN-2	0.87±0.10	4.41±0.67	0.37±0.09	20.61±2.40

G and G* of samples at H-CS 30-70 ratio were comparable to those of CS. The results show that at a ratio of 30-70 H-CS, a denser network structure with shorter/more crosslinks was formed which might be the main reason for enhanced modulus and strength (higher G^* values and higher tensile strength at break, higher ν_e, ν_e^* and lower $\overline{M_c}$, $\overline{M_c}^*$ compared to CS samples).

In regard to the preparation sequence of H-CS 30-70 hydrogels, semi-IPN-2 samples showed slightly higher ν_e, ν_e^* and lower $\overline{M_c}$, $\overline{M_c}^*$ (Table 3.3), most likely due to a lower amount of free amino groups and more covalently crosslinked chains as determined by quantitative FT-IR analysis and ninhyrin assay.

Table 3.3 Effective crosslink density and average molecular weight between crosslinks calculated from elastic modulus of swollen hydrogel films. ν_e and $\overline{M_c}$ from ε≤15%, and ν_e^* and $\overline{M_c}^*$ from ε>15%.

	ν_e (10^4 mol/cm^3)	ν_e^* (10^4 mol/cm^3)	$\overline{M_c}$ (g/mol)	$\overline{M_c}^*$ (g/mol)
CS	9.8	25.7	1415	627
H-CS 30-70 SIPN-1	10.2	28.8	1360	506
H-CS 30-70 SIPN-2	10.8	31.9	1286	460
H-CS 70-30 SIPN-1	6.5	20.5	2097	732
H-CS 70-30 SIPN-2	5.5	18.0	2472	810

Obviously, H-CS 70-30 samples were fairly brittle. Increasing the amount of hemicellulose in the hydrogels did not improve the modulus and strength values (semi-IPNs with H-CS 70-30). This might be related to a decrease in effective crosslink density and simultaneous increase in average molecular weight between crosslinks (see Table 3.3). Overall the mechanical stability was reduced as a result of a more open network structure with longer/fewer crosslinks. Mechanical properties similar to CS samples could not be maintained (Table 3.2) regardless of the preparation sequence.

3.4.4 Swelling behavior

It was expected that the crosslink density and the average length of the crosslinks has an effect on hydrogel swelling. The percentage equilibrium swelling ratios of semi-IPN hydrogels are listed in Table 3.4.

Table 3.4 Equilibrium swelling ratios (S) of semi-IPN and CS hydrogels. Bound water (non-freezing) and free water (freezing bound water and freezing free water) in swollen hydrogels.

	S (%)	**Bound water (%)**	**Free water (%)**
CS	153±17	103	50
H-CS 30-70 SIPN-1	191±20	149	42
H-CS 30-70 SIPN-2	181±18	135	44
H-CS 70-30 SIPN-1	207±23	160	47
H-CS 70-30 SIPN-2	210±18	159	51

With increasing hemicellulose content, swelling ratios increased compared to hydrogels made from 100% CS, indicating a higher capacity for water uptake. With the help of DSC analysis, the amount of free water and non-freezing bound water was estimated. Non-freezing water represents water that is bound by hydrogen bonding to the polymer chains and can be calculated by the difference between the total amount of water held by the gel and free water. Free water includes the freezing water which is determined from the endothermic peak of the DSC curve at 0ºC.[17]

As shown in Table 3.4, the main percentage of water inside the swollen hydrogels was bound water. The amount of bound water was higher in all semi-IPNs and increased with increasing hemicellulose content compared to CS samples. The results clearly demonstrated the impact of longer crosslinks at H-CS 70-30 ratios with higher potential for interaction of water molecules with polymer chains.

3.5 Conclusions

Alkaline extracted aspen hemicellulose was used to prepare semi-interpenetrating (semi-IPN) hydrogel films with chitosan. The molecular weight of the hemicellulose was fairly high. Crystallinity of hydrogel films increased with increasing hemicellulose content. Hemicellulose showed to interfere with the crosslinking reaction of chitosan during semi-IPN formation. This effect could be controlled by altering the sequence of the hydrogel preparation steps. Increasing hemicellulose content increased the amount of H-bonded water and enhanced the overall swelling capacity of hydrogel films. Overall, the mechanical properties of semi-IPN hydrogels did not deteriorate.

3. 6 References

[1] Timell, T.E. *Wood Science and Technology*, **1967**, l, 45.

[2] Coviello, T.; Matricardi, P.; Marianecci, C.; Alhaique, F. Polysaccharide Hydrogels for Modified Release Formulations. *Journal of Controlled Release*. **2007,** 119, 5-24.

[3] Ebringerova, A. Structural Diversity and Application Potential of Hemicelluloses. *Macromolecular Symposia.* **2006,** 232, 1-12.

[4] Peppas, N. A.; Hilt, J. Z.; Khademhosseini, A.; Langer, R. Hydrogels in Biology and Medicine: From Fundamentals to Bionanotechnology. *Advanced Materials*, **2006**, 18, 1345.

[5] Slaughter, B. V.; Khurshid, S. S.; Fisher, O. Z.; Khademhosseini, A.; Peppas, N. A. Hydrogels in Regenerative Medicine. *Advanced Materials*, **2009**, 21, 1-23.

[6] Hoare, T. R.; Kohane, D. S. Hydrogels in Drug Delivery: Progress and Challenges. *Polymer*. **2008,** 49, 1993-2007.

[7] Schexnailder, P.; Schmidt, G. Nanocomposite Polymer Hydrogels. *Colloids and Polymer Science.* **2009,** 287, 1-11.

[8] Tanaka, Y.; Gong, J. P.; Osada, Y. Novel Hydrogels with Excellent Mechanical Performance. *Progress in Polymer Science*. **2005,** 30, 1-9.

[9] Myung, D.; Waters, D.; Wiseman, M.; Duhamel, P.E.; Noolandi, J.; Ta, C.N.; Frank, C.W. Progress in the development of interpenetrating polymer network hydrogels. *Polymers for Advanced Technologies*, **2008**, 19, 647 – 657.

[10] Liu, C.; Chena, Y.; Chena, J. Synthesis and Characteristics of pH-Sensitive Semi-Interpenetrating Polymer Network Hydrogels Based on Konjac Glucomannan and Poly (Aspartic Acid) for in Vitro Drug Delivery. *Carbohydrate Polymers*. **2010,** 79, 500-506.

[11] Jin, S.; Liu, M.; Zhang, F.; Chen, S.; Niu, A. Synthesis and Characterization of pH-Sensitivity Semi-IPN Hydrogel Based on Hydrogen Bond Between Poly(N-Vinylpyrrolidone) and Poly(Acrylic Acid). *Polymer.* **2006**, 47, 1526–1532.

[12] Zhao, Y.; Kang, J.; Tan, T.W. Salt-, pH- and Temperature-Responsive Semi-Interpenetrating Polymer Network Hydrogel Based on Poly(Aspartic Acid) and Poly(Acrylic Acid). *Polymer.* **2006,** 47, 7702–7710.

[13] Berger, J; Reist, M; Mayer, JM; Felt, O; Gurny R. Structure and interactions in covalently and ionically crosslinked chitosan hydrogels for biomedical applications. *European Journal of Pharmaceutics and Biopharmaceutics*. **2004** , 57, 19–34.

[14] Karaaslan, M. A.; Tshabalala, M.; Buschle-Diller, G. Wood Hemicellulose/Chitosan-Based Semi-Interpenetrating Network Hydrogels: Mechanical Swelling and Controlled Drug Release Properties. *Bioresources*, **2010**, 5, 1036.

[15] Anseth, K. S.; Bowman, C. N.; Bannon-Peppas, L. Mechanical Properties of Hydrogels and their Experimental Determination. *Biomaterials.* **1996,** 17, 1647-1657.

[16] Jagadish, R.S.; Raj, B.; Parameswara, P.; Somashekar, R. Effect of glycerol on structure–property relations in chitosan/poly(ethylene oxide) blended films investigated using wide-angle X-ray diffraction .*Polymer International*, **2010**, 59, 931-936.

[17] Ostrowska-Czubenko, J.; Gierszewska-Druzynska, M. Effect of ionic crosslinking on the water state in hydrogel chitosan membranes. *Carbohydrate Polymers*, **2009**, 77, 590-598.

[18] Gabrielii, I.; Gatenholm, P.; Glasser, W. G.; Jain, R. K.; Kenne, L. Separation Characterization and Hydrogel-Formation of Hemicellulose from Aspen Wood. *Carbohydrate Polymers.* **2000,** 43, 367–374.

[19] Henriksson, A.; Gatenholm, P. Controlled assembly of glucuronoxylans onto cellulose fibres. *Holzforschung*, **2001**, 55, 494-502.

[20] Kabel, M.A.; Bornea, H.; Vincken, J.P.; Voragen, A.G.J.; Schols H.A. Structural differences of xylans affect their interaction with cellulose. *Carbohydrate Polymers*, **2007**, 69, 94.

[21] Gröndahl, M.; Eriksson, L.; Gatenholm, P. Material Properties of Plasticized Hardwood Xylans for Potential Application as Oxygen Barrier Films. *Biomacromolecules.* **2004**, 5, 1528–1535.

[22] Kolhe, P.; Kannan, R.M. Improvement in Ductility of Chitosan through Blending and Copolymerization with PEG: FTIR Investigation of Molecular Interactions. *Biomacromolecules*, **2003**, 4, 173-180.

[23] Qu, X.; Wirsen, A.; Albertsson, A. C. Effect of lactic/glycolic acid side chains on the thermal degradation kinetics of chitosan derivatives. *Polymer*, **2000**, 41, 4841-4847.

[24] Osman, Z.; Arof, A. K. FTIR studies of chitosan acetate based polymer electrolytes. *Electrochimica Acta*, **2003**, 48, 993-999.

[25] Curotto, E.; Aros, F. Quantitative Determination of Chitosan and the Percentage of Free Amino Groups. *Analytical Biochemistry.* **1993,** 211, 240-241.

[26] Mi, F.L.; Tan, Y.C.; Liang H.C.; Huang R.N.; Sung H.W. In vitro evaluation of a chitosan membrane cross-linked with genipin. *Journal of Biomaterials Science Polymer Edition*, **2001**, 12, 835-850.

[27] Yui, N. *Supramolecular Design for Biological Applications*; CRC Press:Boca Raton, **2002**.

[28] Ma, P. X.; Elisseeff, J. H. *Scaffolding in Tissue Engineering*; CRC Press:Boca Raton, **2005**.

[29] Lou, X.; Coppenhagen, C. Mechanical Characteristics of Poly(2-Hydroxyethyl Methacrylate) Hydrogels Crosslinked With Various Difunctional Compounds. *Polymer International.* **2003,** 50, 319-325.

[30] Jiang, G.; Liu, C.; Liu, X.; Chen, Q.; Zhang, G.; Yang, M.; Liu, F. Network structure and compositional effects on tensile mechanical properties of hydrophobic association hydrogels with high mechanical strength. *Polymer*, **2010**, 51, 1507-1515.

[31] Mark, J. E.; Erman, B. *Rubberlike elasticity: a molecular primer*; John Wiley & Sons Inc: USA, **1988**.

CHAPTER 4

Nanoreinforced Biocompatible Hydrogels from Wood Hemicelluloses and Cellulose Nanowhiskers

4.1 Abstract

Nanoreinforced hydrogels with a unique network structure were prepared from wood cellulose whiskers coated with chemically modified wood hemicelluloses. The hemicelluloses were modified with 2-hydroxyethylmethacrylate prior to adsorption onto the cellulose whiskers in aqueous medium. Synthesis of the hydrogels was accomplished by in situ radical polymerization of the methacrylic groups of the adsorbed coating to form a network of poly(2-hydroxyethylmethacrylate) (PHEMA) matrix reinforced with cellulose whiskers. The mechanical, swelling and viscoelastic properties, of water-swollen hydrogels were investigated. Results indicated that the number of effective crosslinks between polymer chains and the average chain length between crosslinking points was significantly different from PHEMA hydrogels that had been crosslinked by a conventional chemical method, using a cross-linking agent. The resulting hydrogels had enhanced toughness, increased viscoelasticity, and improved recovery behavior. With respect to the mechanical and swelling properties, it can be hypothesized that these nanoreinforced PHEMA hydrogels have potential for use in load-bearing biomedical applications such as articular cartilage replacement.

4.2 Introduction

Polymers from renewable resources have received tremendous attention in the scientific community because of the projected unavailability of petroleum based raw materials in the near future. Recently, there has been a great effort to develop new materials and processes that could make bio-based renewable polymers viable alternative for synthetic polymers that would be readily available on the market.

Polysaccharides have been used in a wide range of applications such as food, packaging, agricultural and biomedical purposes where biodegradability, non-toxicity, biocompatibility and biofunctionality are required. Cellulose and its derivatives have been utilized extensively since the early ages as textile fibers, chemical precursors and for paper making and food additives. Nanowhiskers (nanocrystals) are a novel form of application for cellulose in nanocomposites. Whiskers are produced by hydrolysis with acid. The amorphous regions of cellulose are dissolved, leaving crystalline rod or whisker shape nanoparticles with a diameter of 3 to 20 nm and a length of 100nm to several μm behind.[2] These whiskers have high modulus, high aspect ratio, and low density. They may carry reactive functional groups on their surface, which might lead to further high-value applications. [3]

Hemicelluloses are hetero-polysaccharides present in the cell wall of wood and annual plants together with cellulose and lignin. They represent about 20-35% of lignocellulosic biomass.[4] Despite their abundance in nature, they have been under-utilized commercially. Recent research efforts are focused on their application in hydrogels for

biomedical applications because of their biodegradability and hydrophilicity.[5] A recent research direction has been focused on their use in the modification of cellulose surfaces by using biomimetic approach. Utilizing the strong hemicellulose-cellulose interaction, novel functionalities have been introduced on cellulose surfaces without deteriorating its morphology and native structure. [6]

The aim of this study is to design novel hydrogels with improved mechanical properties by utilizing hemicellulose and cellulose nanowhiskers isolated from forest biomass. Hydrogels are crosslinked networks of hydrophilic polymers that are capable of retaining considerable amounts fluids without disintegration. In addition to their high liquid up-take, stimuli-responsive swelling capabilities and biocompatibility are some of the features that render them suitable for biological and biomedical applications.[7, 8] However, one major obstacle with hydrogels is their poor mechanical properties. It has been a challenge to fabricate mechanically strong hydrogels with conventional chemical crosslinking pathways without compromising their other properties such as water uptake and stimuli responsiveness. [9] Recently, Haraguchi et al. developed nanocomposite hydrogels (NC gels) with unique organic-inorganic network structures that exhibit excellent mechanical performance as well as optical and swelling/deswelling properties. [10] In their study, water-swellable clay nanosheets (3 nm in thickness and 30 nm in diameter) were used as highly multifunctional crosslinking sites. By performing *in situ* polymerization of specific monomers, initiators attached to nanoclay surfaces are being used as grafting sites for growing polymer chains. As a consequence to the formation of long and extensible polymer chains connecting the uniformly distributed nanoclay

particles to each other, NC gels were strong, tough, highly extensible, optically transparent and can absorb high amounts of water compared to conventional hydrogels. Huang et al. have recently synthesized novel high strength hydrogels using a similar approach to NC gels.[11] In their study, a suspension of macromolecular microspheres (100 nm in diameter) carrying peroxide groups were irradiated to initiate polymerization of monomers and to synthesize hydrogels. These hydrogel network structures showed similarities to NC gels.

In this study, a novel approach was developed to prepare nanocomposite hydrogels using cellulose nanowhiskers and hemicellulose extracted from forest by-products. In order to possess methacrylic functionality, hemicellulose isolated from aspen wood was chemically modified. The natural affinity of hemicellulose to cellulose was utilized for surface modification of cellulose nanowhiskers. Surface modified cellulose nanowhiskers were used to prepare nanocomposite hydrogels using free radical polymerization of 2-hydroxyethyl methacrylate (HEMA), a widely used biocompatible monomer. The effect of morphology and concentration of the incorporated nanocrystals on the hydrogel network was related to the mechanical properties, viscoelastic behavior and swelling of the hydrogels.

4.3 Experimental

4.3.1 Materials

2-Hydroxyethyl methacrylate (HEMA, 96%) monomer was purchased from Acros Chemicals. To remove impurities such as ethylene glycol dimethacrylate, a commonly

used chemical crosslinking agent for poly(HEMA), further purification was performed as described in Bryant et al.[12] Dimethyl sulfoxide (DMSO), chloroform, acetone, sulfuric acid, ethyl acetate, ammoniumpersulfate, sodium pyrosulfite, ethylene glycol dimethacrylate (EGDMA), N,N‘-carbonyldiimidazole (CDI) and triethylamine was used as received.

4.3.1.1 Hemicellulose extraction from aspen

Hemicellulose, isolated from fresh aspen chips and milled by a commercial blender, extracted by a novel alkaline extraction method, was provided by USDA Forest Products Laboratory, Madison, WI. A more detailed isolation procedure has been described in Karaaslan et al.[13]

4.3.2 Methods

4.3.2.1 Preparation of cellulose nanowhiskers (CNW)

Cellulose nanowhiskers (CNW) were prepared using acid hydrolysis of cellulose from two different sources; aspen wood cellulose pulp and from Whatman No.1 filter paper. Hydrolysis was performed according to the procedure described in the literature with slight modifications.[14, 15] After grinding in a Wiley mill, cellulose powder was hydrolyzed under constant stirring at 45 ºC for 45 minutes using sulfuric acid (64 wt %) at 17.5 mL/g acid-to-pulp ratio. To stop the hydrolysis reaction, 10-fold excess of deinozed (DI) water was added. The suspensions were centrifuged and the acid residue was decanted. After washing the precipitate and redispersing in DI water, the CNW suspension was dialyzed against DI water using a dialysis membrane with 13,000 molecular weight cut-off for at least 3-5 days until the pH of the solution was above pH 5

and remained constant. Finally, aqueous CNW suspensions were sonicated for 10 min at 30% output control in an ice-cold water bath to prevent over heating and cleavage of surface sulfate groups. 10 μL chloroform was added to aqueous stock suspensions to avoid bacterial growth. The stock solutions were stored in a refrigerator. The concentrations of CNW suspensions were determined gravimetrically by evaporating the water in an oven heated to 105º C. To increase the CNW concentration, the water was evaporated by heating the CNW dispersion at 40-45ºC under a hood. The morphology of CNW was evaluated by Transmission Electron Microscopy (TEM). 20 μL of diluted CNW dispersion (0.01% w/v) was placed on a 300 mesh carbon film coated copper grid and air dried. Before TEM analysis, negative staining with uranyl acetate was carried out to obtain enhanced image contrast. Length (L), diameter (d) and aspect ratio (L/d) of CNW were determined by using an image processing software. Average values of at least 15 individual whiskers were reported.

4.3.2.2 Chemical modification of hemicellulose

2-[(1-Imidazolyl)formyloxy]ethyl methacrylate (HEMA-Im), the precursor for chemical modification of hemicellulose was prepared by reacting HEMA and CDI in chloroform at room temperature as described by Ranucci et al.[16] HEMA-Im product was confirmed by FT-IR analysis (see Figure 4.1)

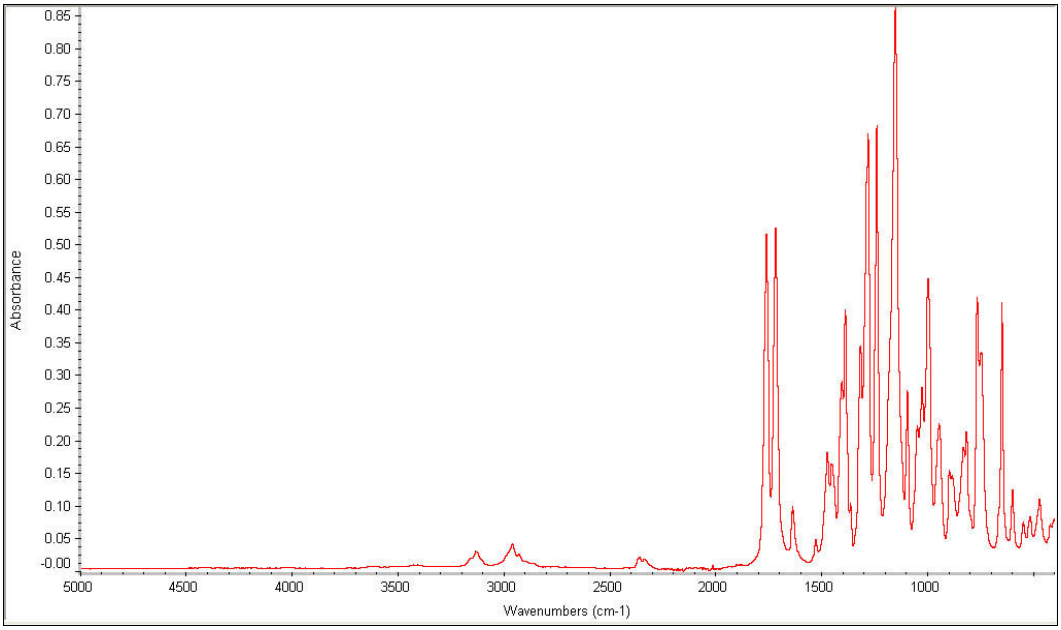

Figure 4.1 FTIR spectra of HEMA-Im precursor. Peaks: 3130 (ν heteroaromatic C-H); 2962, 2930 (ν aliphatic C-H); 1765 (ν imidazole C=O); 1722 (ν ester C=O); 1637, 1527 (ν C=C); 1450 (δ CH2); 1300-1160 (ν CO-O); 767 (γ heteroaromatic C-H); 650 (γ heteroaromatic C-H) cm^{-1}.

Hemicellulose with methacrylic functionality was synthesized according to Lindblad et al.[17] with slight modifications. (The reaction mechanism is outlined in Figure 4.2) Briefly, 286 mg aspen hemicellulose and 456 mg HEMA-Im were dissolved in DMSO. Triethylamine (40.5 mg) was used as the catalyst. Two different batches were prepared at which the reaction was kept at 45 °C under stirring for 10 and 25 hours, respectively. 10h and 25h batches are hereafter referred to as MH-10 and MH-25. The product was precipitated two times in ethyl acetate, centrifuged, the solvent was decanted and the final precipitate was freeze-dried overnight.

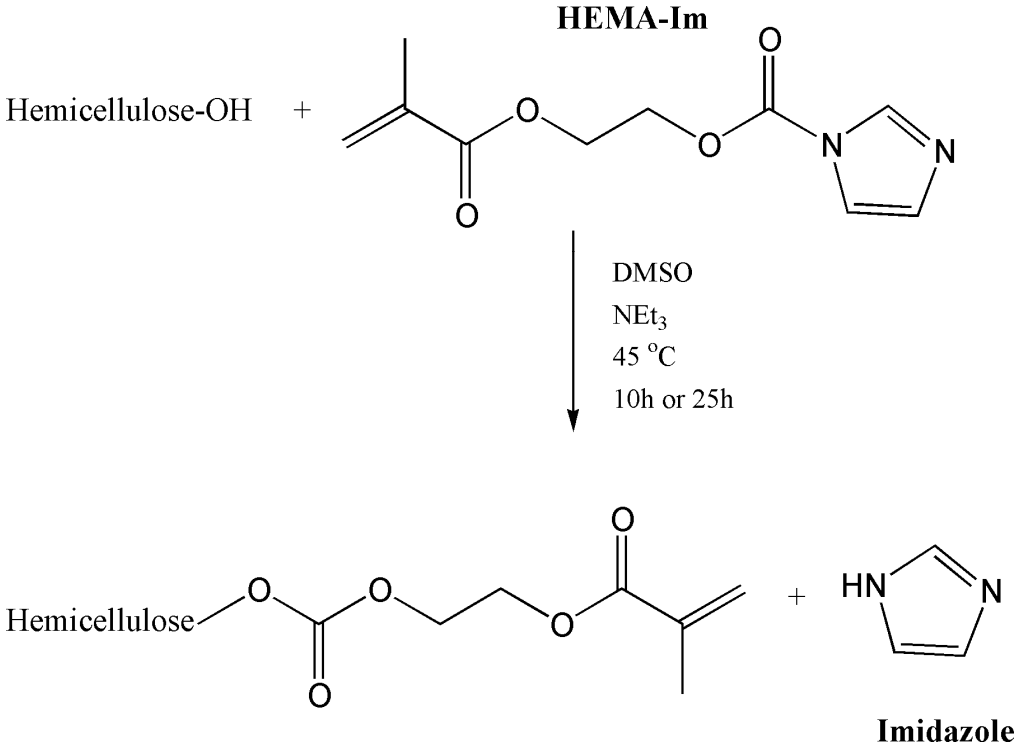

Figure 4.2 Proposed reaction mechanism for the methacrylation of hemicelluloses(Reproduced from: Ref. [16])

Degree of modification was evaluated by using specific chemical shifts of the ^{1}H-NMR spectrum in accordance with the method used for acetylated hemicelluloses[18] as follows;

$$D_m = \frac{\text{Sum of integrals of methacrylated hydroxyl groups } (\delta = 5.7 \text{ ppm and } 6.07 \text{ ppm})/2}{\text{Sum of integrals of all carbohydrate signals } (\delta = 3.2 - 5.5 \text{ ppm})/6}$$

4.3.2.3 Adsorption of modified hemicellulose to CNW

Adsorption experiments were performed by slightly modifying the method described for the adsorption of cationized glucoronoxylans on softwood cellulose

fibers.[19] 2 mL CNW suspension (1%w/v) and adequate amount of aqueous methacrylated hemicellulose (MH) solutions (ranging 0.5% to1% w/v) and 0.5 M NaCl were mixed in a vial giving a final concentration of 10 mM NaCl and 200mg/g MH to CNW ratio. The vials including the final mixtures were sealed with parafilm and incubated in an oven at 45 ºC for 24h. At the end of the adsorption experiments, to separate the non-adsorbed MH from CNW suspensions and to estimate the quantity of adsorbed MH, a typical solvent exchange procedure with acetone was performed as described by Capadona et al.[20] When a mechanically coherent CNW organogel layer had been formed, the acetone/water mixture at the top of CNW layer was collected and stored in a beaker. Finally, the separated mixture was flushed with nitrogen to remove acetone. The remaining aqueous solution was further used to determine the non-adsorbed and the adsorbed amount of MH based.

Iodine complexation, a commonly used method for the quantitative determination of xylans, [19, 21] was used to estimate the amount of methacrylated hemicellulose adsorbed to cellulose nanowhiskers. 0.1 mL of separated MH solution was mixed with 0.4 mL of DI water, 4 mL of 4.62 M $CaCl_2$ and 0.5 mL of triiodine stock solution (0.5% I_2 + 2.1% KI). Absorbance of this mixture at 610 nm was recorded with an UV-Vis spectrophotometer after 90 min at which the absorbance value remained constant. The amount of adsorbed MH was calculated from the difference in the absorbance at 610 nm before and after the adsorption test using a standard curve of known concentrations of MH aqueous solutions. To evaluate the contribution of CNW to the absorbance at 610 nm of MH solutions, control samples of CNW suspensions with and without MH were

tested with iodine complexation method. CNW suspensions did not form colored iodine complexes and the contribution to the absorbance band at 610 nm of MH solutions was negligible.

4.3.2.4 Hydrogel synthesis

Free radical polymerization of HEMA in water via redox initiators was performed to synthesize hydrogels following the monomer/water/initiator ratios reported in a recent study.[22] Methacrylated hemicellulose (MH) adsorbed CNW in the form of organogels (acetone gels) were redispersed in deionized water and nitrogen flushed to remove acetone. 500 mg of HEMA monomer was added into 250 μl of modified CNW suspension at different compositions (0.2-2% w/v) and vortexed. After adding the redox initiators (12.5 μL of each 4% w/v ammoniumpersulfate and sodium pyrosulfite aqueous solution, respectively), the polymerizing solution was vortexed again, immediately poured into a glass vial, flushed with nitrogen and sealed with parafilm. *In situ* polymerization was maintained for 3h in an oven heated at 40 ºC. To remove unreacted monomers and initiators and allow hydrogels to reach their equilibrium swelling, as-synthesized hydrogels were immersed in an excess amount of deionized water for 5 days by exchanging with fresh water 1-2 times daily. Final CNW weight fraction (w/w %) in hydrogels were calculated by the ratio of CNW with respect to the initial monomer used for polymerization. Control samples, normal structure (NS)-PHEMA hydrogels which were crosslinked by a conventional chemical crosslinking agent, EGDMA, were prepared. The weight fraction (w/w %) of the crosslinker (EGDMA) was 1 % with respect to the amount of HEMA.

4.3.2.5 Hydrogel characterization

Mechanical testing of the swollen hydrogels at equilibrium was performed with the parallel plate compression geometry of the RSAIII Dynamical Mechanical Analyzer (DMA) with a 3.5 kg load cell. Samples were cut into cylindrical shapes with a cork borer and had a diameter of 6.7 mm and thickness of approximately 1 mm. The thickness of the film sample was measured using a digital micrometer with 0.001 mm resolution at three locations and averaged. Equilibrium swollen samples were kept in deionized water until mechanical testing. To prevent water loss during testing, hydrogel samples were immersed in deinozed water. DMA experiment setup for compression tests is shown in Figure 4.3.

Figure 4.3 DMA experimental setup for testing the compressive mechanical properties of swollen hydrogels immersed in deionized water at room temperature

Frequency dependent storage modulus (E') and loss modulus (E'') of each hydrogel were evaluated at room temperature, at a compression frequency in the range of

of 0.1 to 80 Hz with 0.1% strain amplitude. 0.2 N static force was applied to ensure the surface contact between hydrogel and the upper compression plate.

Compressive stress relaxation tests were carried out to evaluate time-dependant properties of equilibrium swollen hydrogels. Equilibrium swollen hydrogel disks immersed in DI water bath were instant compressed to 20% strain for 20 min and relaxation stress as a function of time was recorded.

The equilibrium swelling ratio (S) was calculated by the following equation (Eq. 4.1),

$$S(\%) = \frac{W_s - W_d}{W_d} \times 100 \tag{4.1}$$

where W_s and W_d are the swollen and dry weight of samples, respectively. Pre-weighed dry films were immersed in deionized water at room temperature for 5 days. The weight of the swollen samples was measured after blotting excessive water gently with filter paper.

4.4 Results and Discussion

4.4.1 Cellulose nanocrystals

TEM images of cellulose nanowhiskers (CNW) isolated from aspen wood and filter paper by sulfuric acid hydrolysis are shown in Figures 4.4 and 4.5. Hydrolysis of aspen wood under same conditions yielded in shorter nanocrystals but with slightly higher aspect ratios than that of filter paper (cotton) CNW. Average length and diameter

of CNW from aspen wood was L = 156±19 nm and d = 11±3 nm. Compared to CNW from cotton (L = 177±33 nm, d = 15±3 nm), aspen wood CNW were slightly shorter in length and in diameter. The reason for shorter crystals might be due to the lower crystallinity of cellulose (I=53-80%) obtained from wood microfibrils in comparison to cotton.[14] The average aspect ratio (A = L/d) was 14 and 12 for aspen wood and cotton CNW, respectively. The aspect ratio of rod-like or needle-like nanocrystals has been reported as an important factor in terms of the critical nanocrystal volume fraction (X_c) needed for percolation. According to the percolation theory [23], to form a percolating network at which nanofillers strongly interact with each other and resulting in significant reinforcement of the soft matrix, lower volume fraction is needed with higher aspect ratio fillers. For example, in this study, X_c defined as 0.7/A for cellulose nanowhiskers, was 5% v/v and 5.83% v/v for aspen wood and cotton CNW, respectively. Results showed that the two types of whiskers had comparable dimensions and morphology; however, aspen wood CNW could be expected to have a slightly higher reinforcing capability.

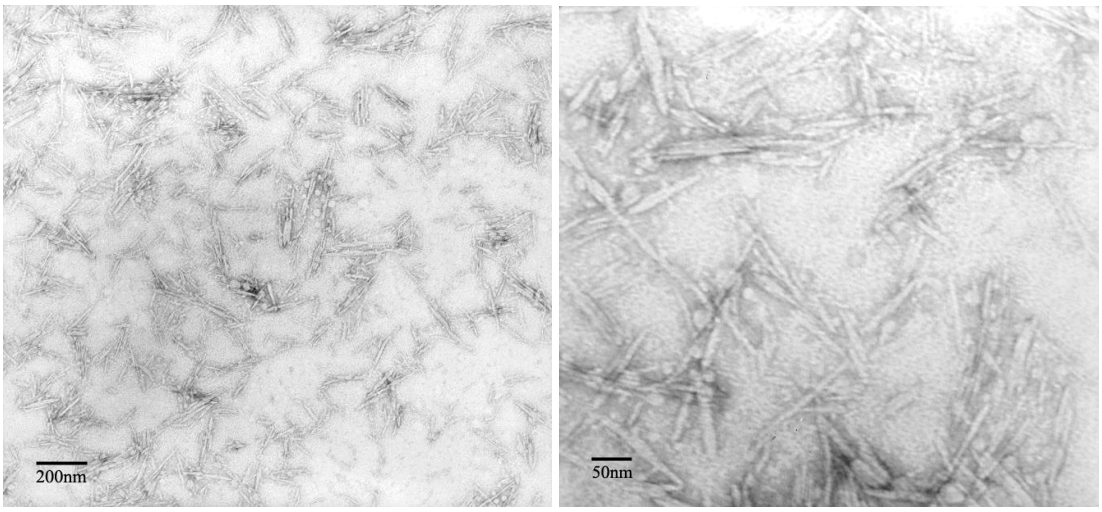

Figure 4.4 Cellulose nanowhiskers isolated from aspen wood pulp

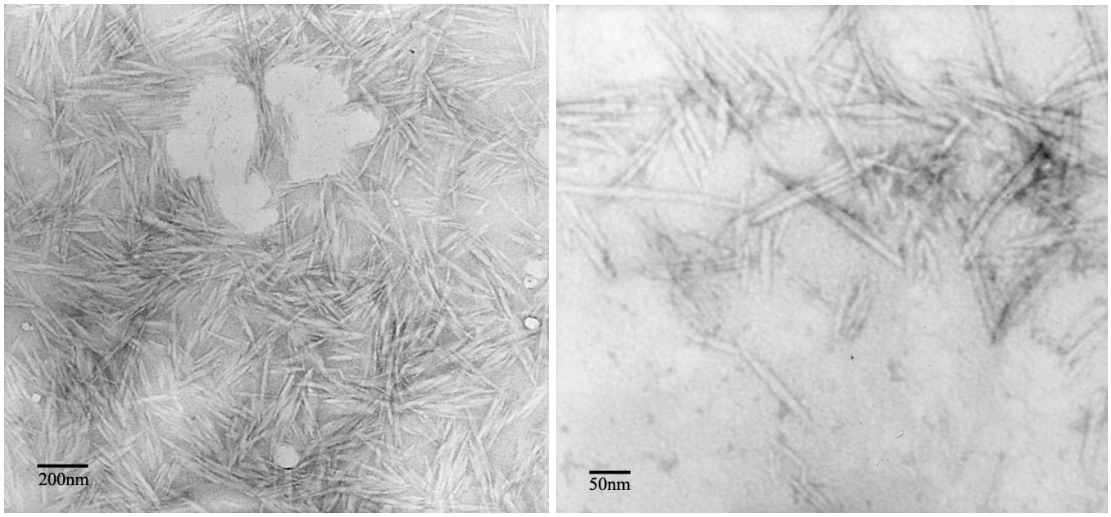

Figure 4.5 Cellulose nanowhiskers isolated from cotton (Whatman No.1 filter paper)

4.4.2 Surface modification of CNW with methacrylated hemicellulose

"Grafting from" approach on cellulose nanowhiskers was carried out to synthesize nanoreinforced hydrogels. This method has been recently reported to make nanocomposite hydrogels by using inorganic clay nanoparticles on which initiators were immobilized and *in situ* polymerization of several hydrophilic polymers was performed.[10] In this way, clay nanoparticles acted as highly multifunctional crosslinking agents and long highly extensible polymer chains connecting each nanoparticle could be formed. In this study, instead of the initiator, monomers (HEMA) were immobilized onto cellulose nanowhiskers and *in situ* free radical polymerization was performed to synthesize PHEMA hydrogels.

In order to immobilize the HEMA monomer on CNW, a new biomimetic approach was introduced instead of direct surface chemical modification of the hydroxyl groups on CNW. This approach was based on the surface modification of cellulose

substrates through utilization of the intrinsic affinity of hemicelluloses (e.g., xyloglucans and glucorunoxylans) to cellulose in the plant cell wall.[6] The strength and interfacial stability of plant cell wall is due to the unique network structure of cellulose microfibrils coated with other matrix poly- and hetero-saccharides.[24] It was proposed that hemicelluloses self-assemble onto cellulose microfibrils and form interconnecting networks with other cell wall polymers (lignin, pectin), which is responsible for the load-bearing ability of the plant cell wall.[25] A schematic of a proposed cell wall structure is given in Figure 4.6.

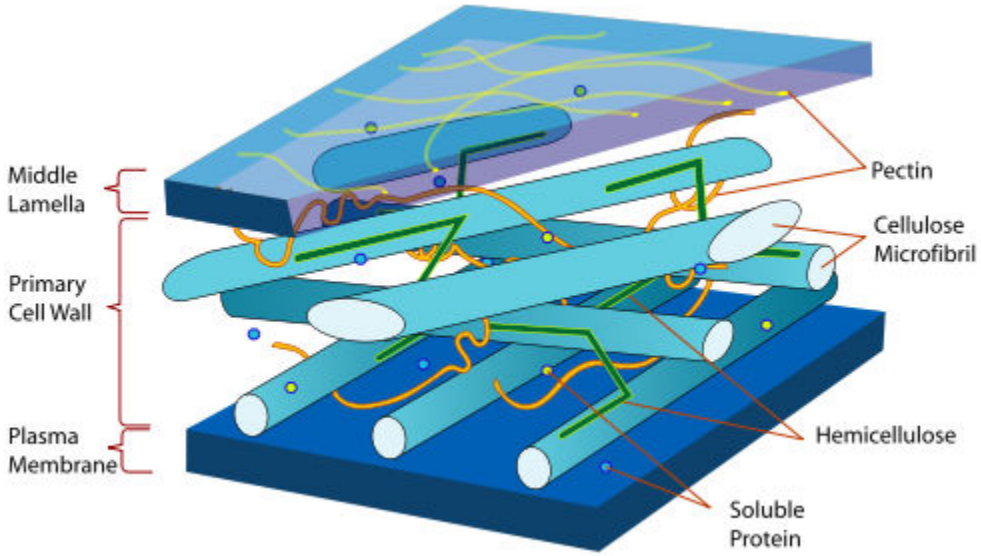

Figure 4.6. A model of a primary cell wall showing the network of hydrogen bonded hemicellulose on cellulose microfibrils and other cell wall matrix poly- and hetero-saccharides such as pectin or lignin. (Reprinted from Ref. [49])

Inspired by the network structure of the plant cell wall and the affinity of hemicellulose to cellulose, several research groups investigated the surface modification

of cellulose substrates (e.g., microfibers, bacterial cellulose, pulp etc.) by coating their surface with native or chemically modified hemicelluloses as molecular anchors to attach functional groups.[6, 26] As an alternative to direct chemical modification, the biomimetic modification by coating the surface with hemicelluloses has been reported to prevent the deterioration of the native structure, bulk morphology and mechanical stability of cellulose substrates.[24, 27]

To attach methacrylic functionality, aspen wood hemicellulose was chemically modified according to Lindblad et al.[22, 27] Methacrylation of the aspen hemicellulose was confirmed by FT-IR analysis (see Figure 4.7). In their study, a low molecular weight (below 3000) oligomeric hemicellulose, O-acetylgalactoglucomannan extracted from spruce softwood, was converted to its methacrylated derivative and used to prepare PHEMA hydrogels. The degree of modification determined by ^{1}H-NMR in hemicellulose was reported as 18-32% with 2-5 h reaction time. However, in this study it only was 8% and 18% for MH-10 and MH-25, respectively (see Fig. 4.8 for ^{1}H-NMR spectra). This might be due to the higher molecular weight of aspen wood hemicellulose ($MW_p \approx$ 401,000, and 391,000). Both methacrylated hemicelluloses MH-10 and MH-25 were water-soluble which was advantageous for the adsorption experiments performed in the presence of aqueous cellulose nanowhisker dispersion.

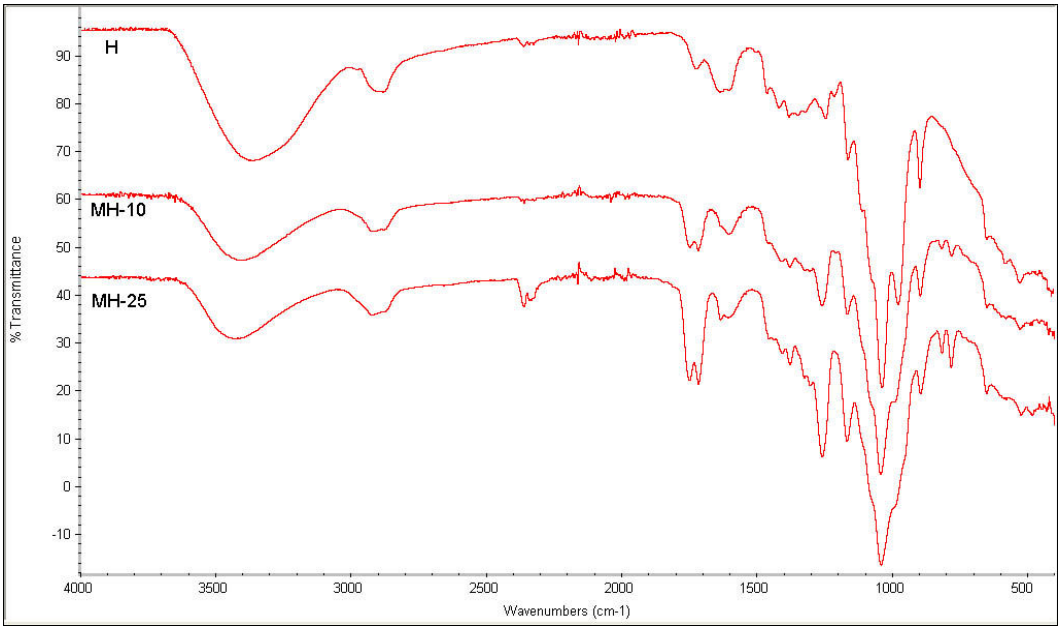

Figure 4.7 FTIR spectra of hemicelluloses (H: unmodified, MH-10 and MH-25: methacrylated for 10h and 25h) New peaks appeared: 1751cm^{-1}(carbonate C=O), 1713cm^{-1} (methacrylic ester C=O), 1635cm^{-1}(methacrylic C=C).

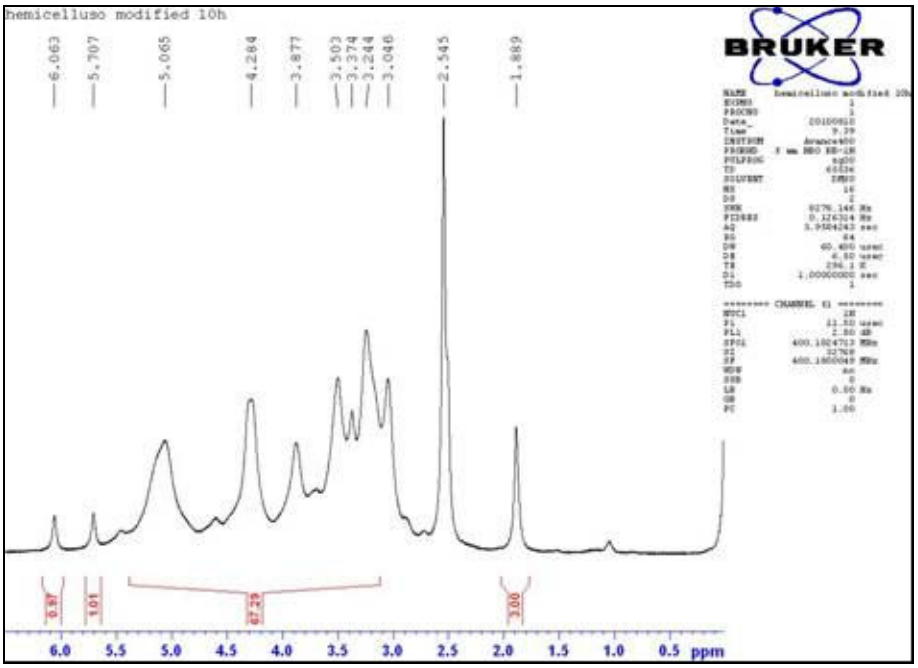

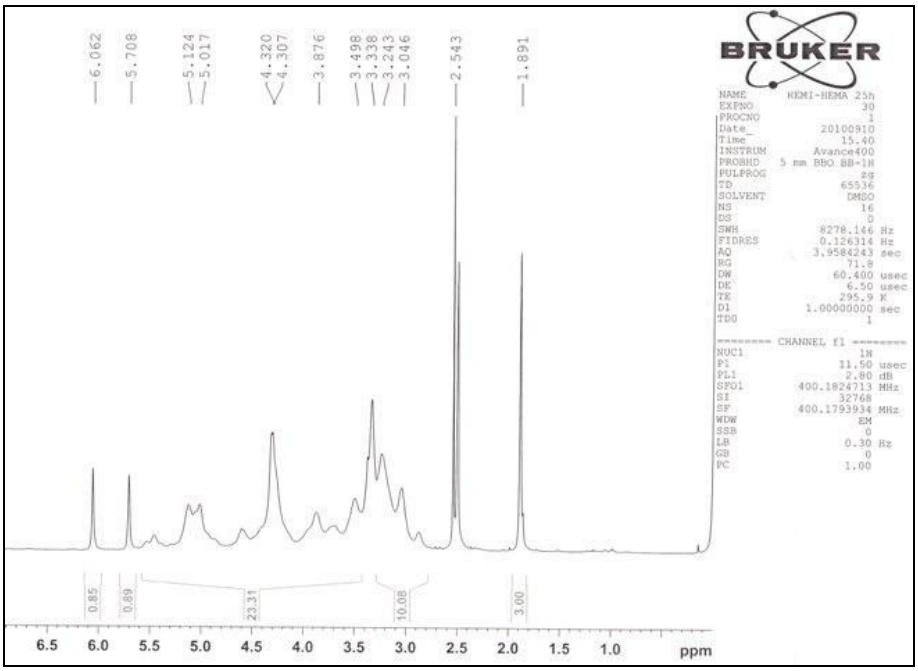

Figure 4.8 ^{1}H-NMR spectra of methacrylated hemicelluloses a) MH-10 b) MH-25. New peaks appeared: 6.06 ppm (s, 1H, vinyl C-H); 5.70 ppm (s, 1H, vinyl C-H); 4.31 ppm (m, 4H, CH_2O); 1.89 ppm (s, 3H, CH3)

4.4.2.1 Adsorption of methacrylated hemicellulose to CNW

Adsorption of hardwood hemicelluloses (glucoronoxylans) onto cellulose substrates are shown to be dependant on several parameters, such as xylan molecular structure, xylan concentration, crystallinity and the surface area of cellulose substrate, time, temperature, pH of the solution.[28] High xylan concentration in the solution, low xylan substitution pattern (branching), high cellulose crystallinity, large surface area of the cellulose substrate, high temperatures and the prolonged processing time have been reported to increase the hemicellulose adsorption. [29] To date, most of the adsorption experiments were conducted under autoclave conditions at high temperatures and alkaline

pH.[30] Moreover, the number of studies on the adsorption of hemicelluloses to cellulose nanocrystals has been very limited.[31, 32]

In this study, the adsorption of methacrylated hemicellulose on cellulose nanowhiskers was performed under mild conditions (45ºC for 24h) in order to prevent the possible cleavage (de-esterification) of surface sulfate groups on CNW. It has been reported that sulfate groups on CNW surface are stable up to 50ºC but susceptible to detach at higher temperatures which results in further degradation/hydrolysis of the CNW.[33]

At the end of the adsorption experiments, to remove unadsorbed hemicelllulose and to isolate modified CNW from the solution, a solvent exchange procedure was performed. This method has been described by Capadona et al.[20] to prepare CNW acetone gels (organogels) from CNW aqueous dispersions, which was further used as three dimensional percolating network of self-assembled CNW templates for nanocomposite production. By exchanging water with acetone, hydrogen bonds among whiskers could be switched on and well-individualized network could be formed. It has been shown that a polymer solution which is normally immiscible with CNW could be filled in the solvent-exchanged CNW network. Moreover, the CNW organogel could be easily redispersed in water without forming CNW aggregates.[20]

Preliminary studies showed that solvent exchange method was superior to other isolation methods such as centrifugation and freeze drying. Centrifugation was unsuccessful because of the tendency of hemicellulose to precipitate from its aqueous solutions even at low speeds (<4000 rpm). However, higher speeds (>10,000 rpm) were required to isolate CNW. With freeze-drying, water could be easily removed, however cellulose nanowhiskers were assembled into an architecture including self-supporting thin layers and microfibrils. This structure consisting of strongly hydrogen bonded CNW/hemicellulose aggregates was susceptible to completely redisperse in water (requiring extensive ultrasonication) without deforming the CNW/hemicellulose structure.

The adsorption of methacrylated hemicellulose (MH) was verified by FT-IR analysis (See Figure 4.9). In addition to characteristic cellulose peaks, new peaks appeared at 1751cm^{-1} (carbonate C=O), 1713cm^{-1} (methacrylic ester C=O) and 1635cm^{-1} (methacrylic C=C) belonged to MH and indicated that methacrylic functionality attached onto cellulose nanowhiskers.

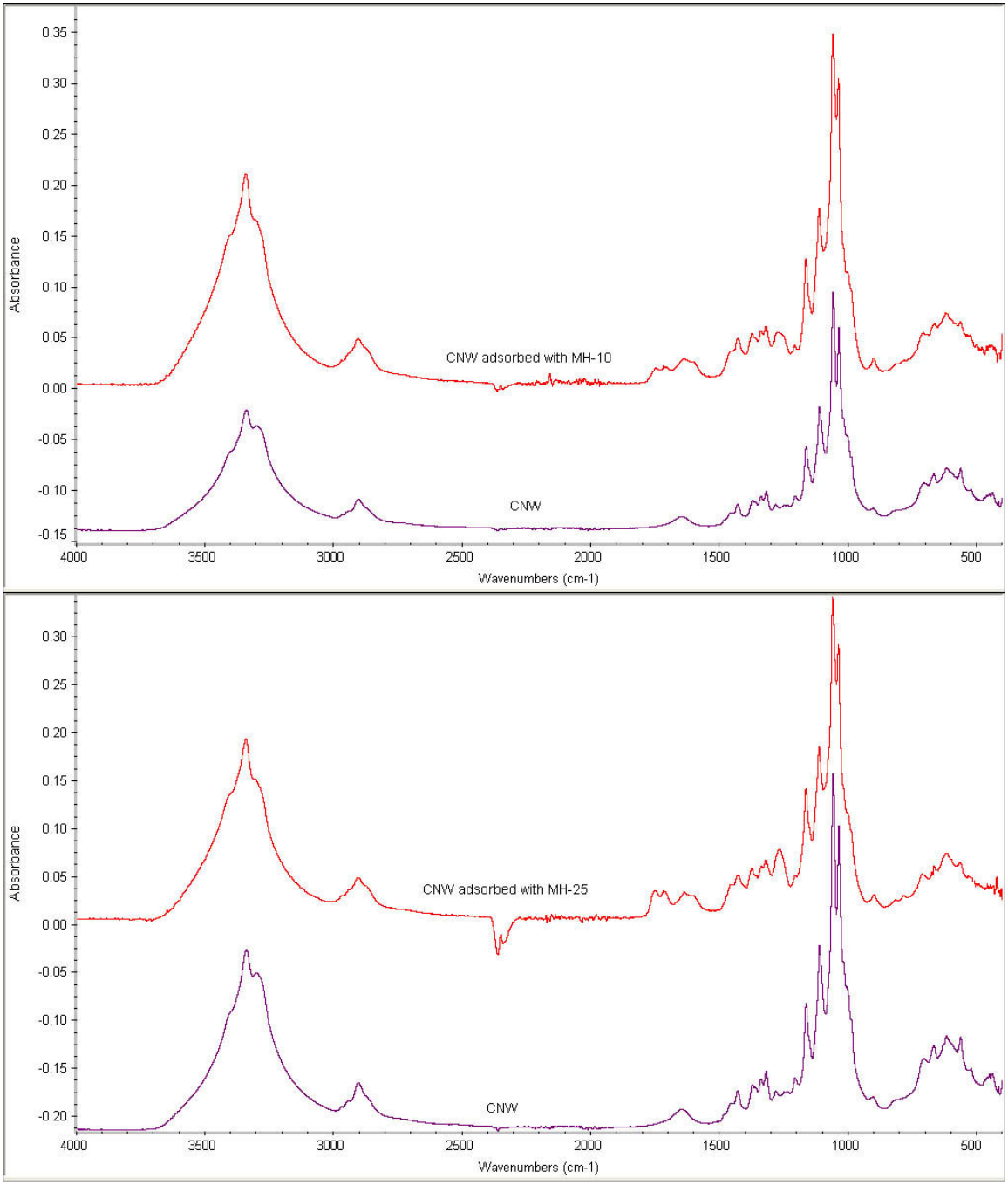

Figure 4.9 FT-IR spectra of CNW before and after adsorption with a) MH-10 b) MH-25

The adsorbed amount of MH was determined by colorimetric iodine-complexation method. The initial ratio of MH to CNW in the aqueous dispersion before the adsorption experiment was adjusted to 200mg MH per gram CNW. Results showed

that 70% and 74% of the added MH was adsorbed to CNW for MH-25 and MH-10, respectively. Compared to the given results in literature, [28, 29] the percentage of adsorbed hemicellulose was relatively high with respect to the processing temperature. This can be explained by the larger surface area and the higher crystallinity of CNW as compared to other cellulose substrates such as fibers and pulp. Specific surface area of CNW has been reported as 170-300 m^2/g and the degree of crystallinity up 95% depending on the source and processing conditions.[34-36] Degree of crystallinity of CNW used in this study was calculated as 83%.

The adsorbed amount of MH-10 was slightly higher than that of MH-25. This result was consistent with the fact that the hemicellulose molecules with longer unsubstituted segments were preferentially adsorbed on cellulose surfaces.[19, 21] MH-10, which had lower degree of modification than that of MH-25 and therefore probably had less branching on the hemicellulose backbone, adsorbed slightly more in comparison to MH-25. In addition, it has been reported that the increased amount of branching on the hemicellulose backbone reduced the reaction of iodine with hemicellulose and resulted in less coloration.[19, 21] This fact was also in agreement with the reduced slope of standard curves (A610 vs. hemicellulose concentration) as the degree of modification increased (See Fig. 4.10).

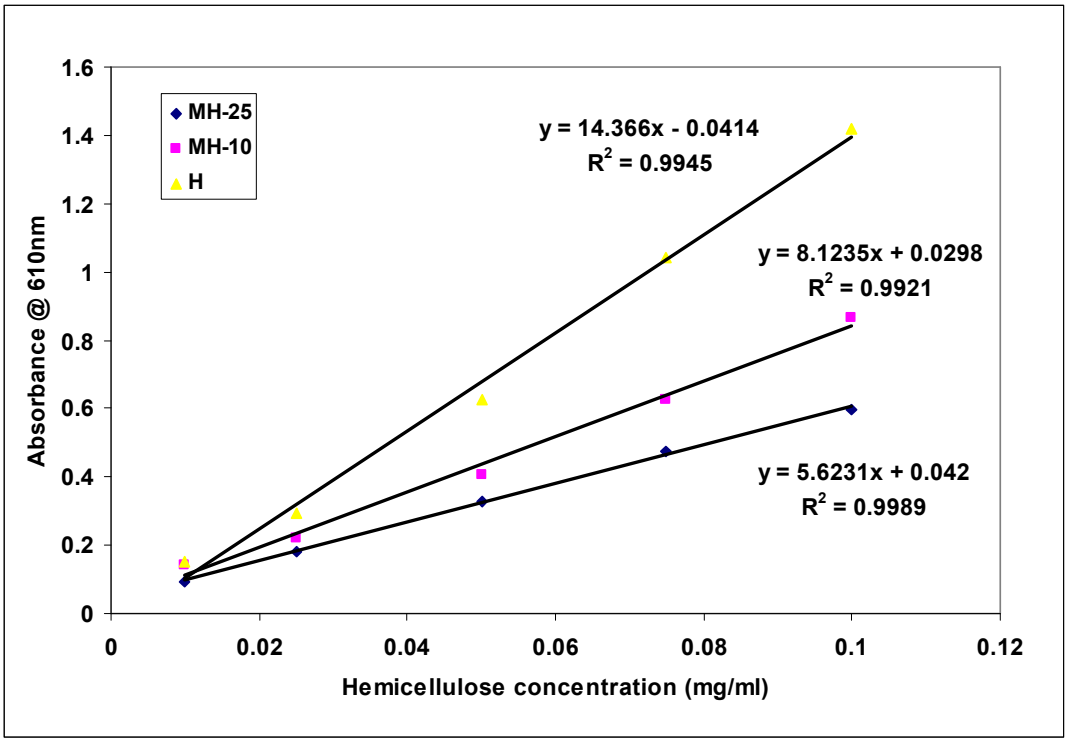

Figure 4.10 Standard curves of hemicelluloses determined by iodine complexation method (H:hemicellulose raw, MH-10 and MH-25: methacrylated for 10h and 25h)

Transmission electron microscopy images of the modified CNW with MH-10 and MH-25 are shown in Fig. 4.11 and Fig. 4.12. Coating with MH did not significantly influence the morphology and the dispersion of modified CNW as compared to unmodified CNW (Fig.4.4). Considering the adsorbed amount of MH, which is about 140-150 mg/g, the thickness of coating layer was difficult to measure with TEM analysis. For a more detailed analysis, AFM (atomic force microscopy) might be beneficial.

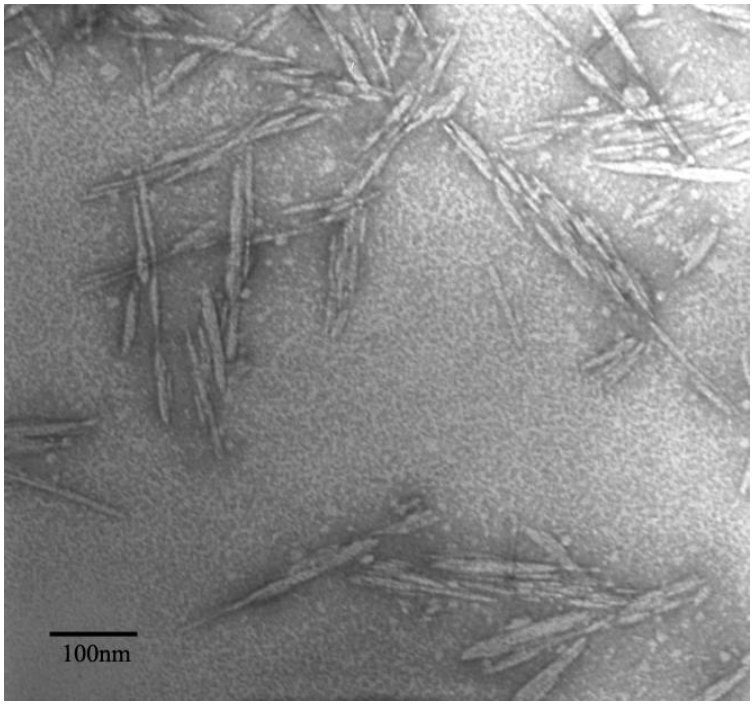

Figure 4.11 TEM image of aspen CNW after adsorption test with MH-10

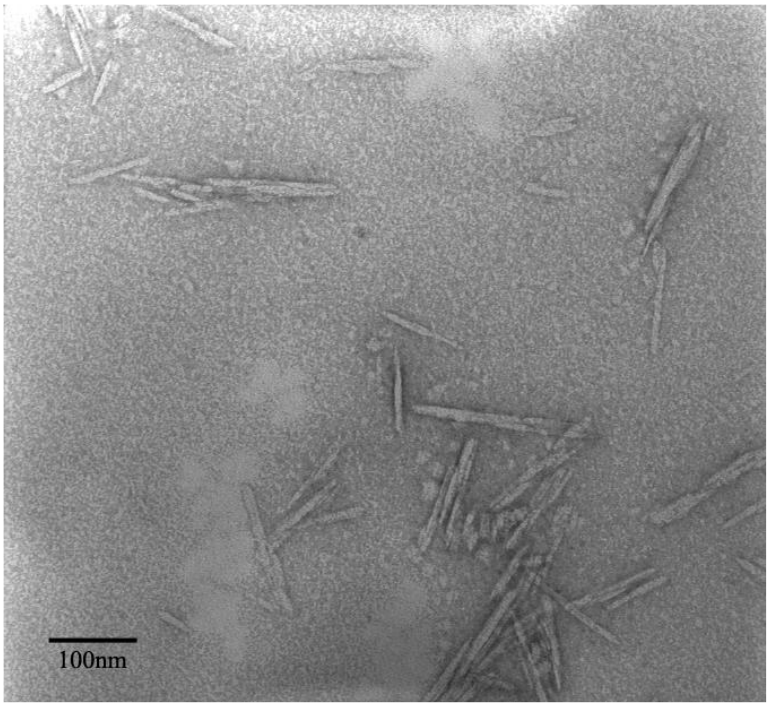

Figure 4.12 TEM image of aspen CNW after adsorption test with MH-25

4.4.2 Synthesis and network structure of nanoreinforced hydrogels

Nanoreinforced PHEMA hydrogels (NR-PHEMA gels) were prepared by *in situ* free radical polymerization of 2-hydroxyethyl methacrylate (HEMA) monomer in the presence of aqueous dispersion of MH coated CNW. Similar to the nanocomposite hydrogels (NC gels) composed of clay nanoparticles and MMC hydrogels composed of macromolecular microspheres,[10, 11] no chemical crosslinking agent has been used to prepare NR-PHEMA gels.

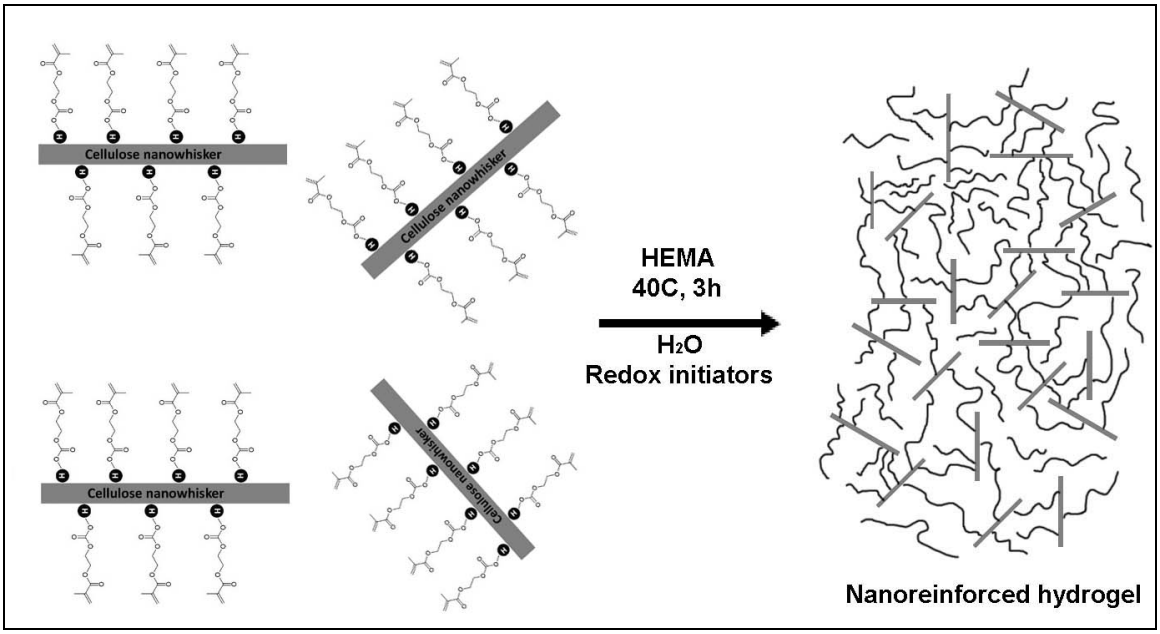

Figure 4.13 Proposed mechanism for the formation of nanoreinforced PHEMA hydrogel.

The hypothesis was to use MH coating on CNWs as the uniformly distributed highly multifunctional crosslinking points and to grow linear PHEMA polymer chains in between them. Uniform dispersion of CNWs in aqueous medium could be achieved by the repulsion of negatively charged surface sulfate groups. The double bonds at the surface of CNWs introduced through methacrylic functionality of MH layer are proposed

to be possible grafting sites for PHEMA polymer chains. The proposed mechanism for the formation of the hydrogel is given in Figure 4.13.

In the proposed hydrogel network structure, the formation of PHEMA polymer chains might be as follows;

- Crosslinked chains; a chain initiated from the surface of a CNW and terminated on the surface of the adjacent CNW, connecting two CNW to each other.
- Short polymer chains with one end attached to the surface of a CNW and the other chain end moving freely.
- Looped chains; grafted polymer chains with both end terminating on the surface of the same CNW.
- Entangled chains; grafted polymer chains with free chain ends which are longer than half of the distance between two CNWs.
- Free chains; polymer chains with two ungrafted free chain ends.

It has been shown that the excellent mechanical properties of NC and MMC gels are predominantly determined by the number of crosslinked chains per unit volume. [10, 11, 37] Therefore, the number of crosslinked PHEMA chains that are connecting two adjacent CNWs is expected to be responsible for improved mechanical properties of nanoreinforced PHEMA (NR-PHEMA) gels as well.

4.4.3 Mechanical properties

Compressive mechanical properties of fully water-swollen NR-PHEMA hydrogels were determined by using parallel-plate geometry of DMA. Figure 4.14 shows the stress-strain curves obtained from uniaxial unconfined compression tests of NR-PHEMA hydrogels including CNWs coated with MH-10 and MH-25, respectively. For comparison, the stress-strain curve of normal structure (NS) PHEMA hydrogel crosslinked with 1% w/w conventional chemical crosslinking agent EGDMA is shown as well.

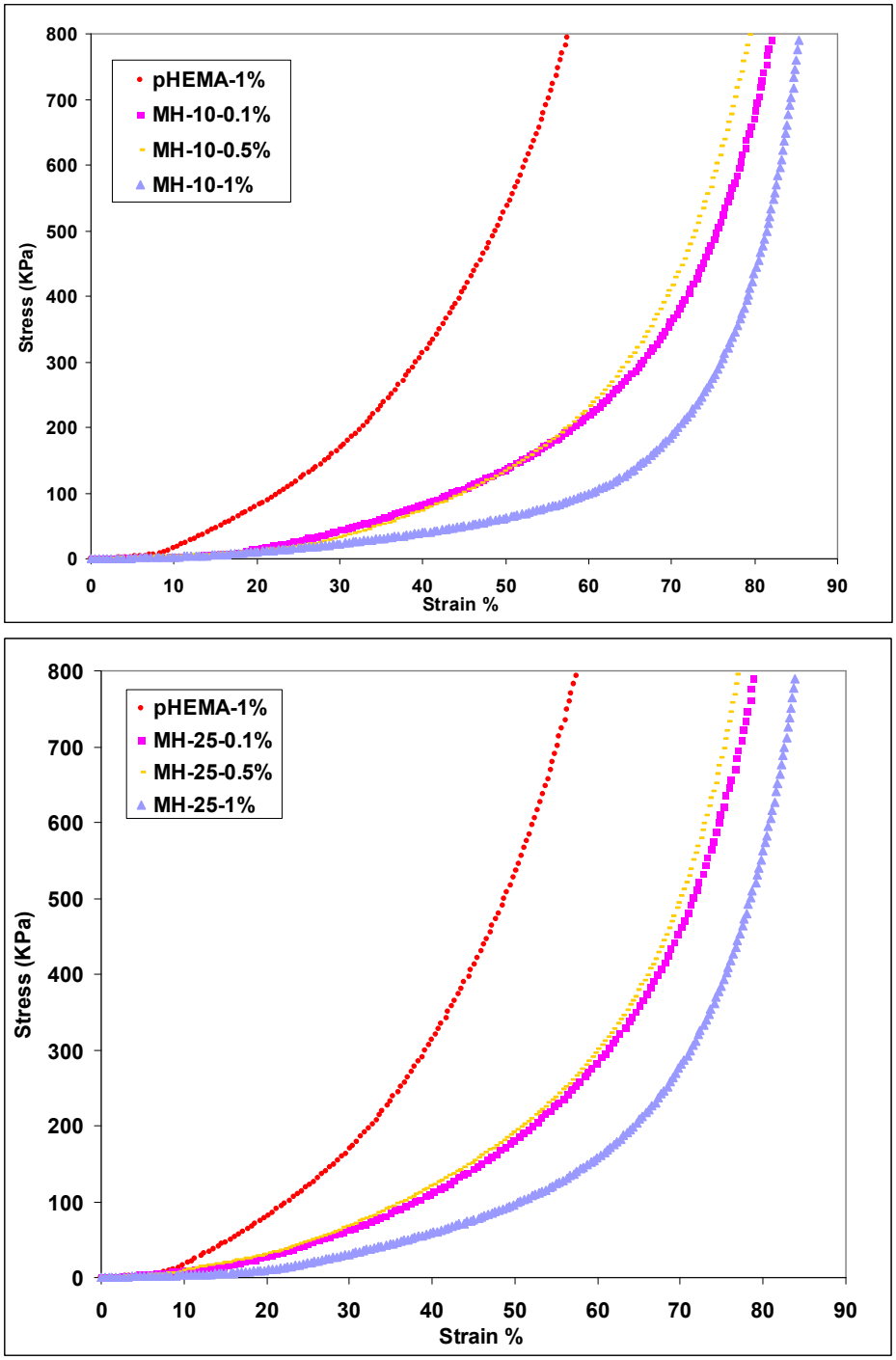

Figure 4.14 Stress strain curves of NR-PHEMA hydrogels reinforced with different weight fractions (0.1%, 0.5% and 1% w/w) CNW a) coated with MH-10 b) coated with MH-25. Control sample is NS-PHEMA hydrogel with 1%w/w EGDMA.

The DMA instrument used for the uniaxial compression tests has a constant load cell that was able to measure forces up to 3.5 kg. Therefore, the maximum amount of stress (force per unit surface area) that can be applied to the cylindrically shaped hydrogel samples for the chosen sample dimensions (6.7 mm diameter) was about 800 KPa. At that stress level, no fracture or break was observed in any of the hydrogel samples. The breaking strength could not be obtained. The strain at equivalent stress level (800 KPa) and the elastic moduli calculated from the stress-strain curves are given in Table 4.1.

The elastic shear modulus of hydrogels (G) was determined by plotting σ versus $(\lambda - \lambda^{-2})$ and calculating the slope from the linear region of these curves. Here, σ is the compressive force per unit of initial cross-sectional area of swollen gel and λ. is the deformation ratio (L/L_0) where L_0 and L is the thickness of the sample before and after the compression. In addition, to better evaluate the transition of the modulus (E) in the highly non-linear stress-strain curves (σ vs. ε), the average tangent slope at 10% strain increments from 10-90% strain was calculated.[38]

Table 4.1 Compressive mechanical properties of hydrogels

	ε (%) at 800 KPa	E (KPa) at ε=60%	E (KPa) at ε≥80%	G (KPa)
NS-PHEMA-1%	59±1.4	3434±239	-	156±5.3
NR-PHEMA-**MH-10-0.1%**	82±1.4	847±46	5661±135	27±4.0
NR-PHEMA -**MH-10-0.5%**	81±1.1	913±56	6593±65	31±3.5
NR-PHEMA -**MH-10-1%**	86±0.3	355±13	6791±51	16±0.8
NR-PHEMA -**MH-25-0.1%**	79±1.6	1023±44	5763	35±5.1
NR-PHEMA -**MH-25-0.5%**	78±2.0	1070±134	7199	40±7.3
NR-PHEMA **-MH-25-1%**	84±1.6	618±93	5956±208	19±4.3

The network parameters for each hydrogel were calculated according the rubber elasticity theory (see Table 4.2). The number of effectively cross-linked chains per unit volume (ν_e, effective crosslink density) was calculated by using Eq.4.2; [39]

$$\nu_e = \frac{RT\upsilon_2^{1/3}}{G} \tag{4.2}$$

where ν_e is the effective crosslink density in mol/cm^3, υ_2 is the polymer volume fraction at equilibrium swollen state (reciprocal of Q, volume swelling ratio), G is the shear elastic modulus, R is the gas constant, and T is the temperature in Kelvin. Q, volume swelling ratio, was calculated from the weight swelling ratio (S) by taking 1.27 g/cm^3 as the polymer density using the Eq.3.2 in the Chapter 3.

The relationship between number of effectively cross-linked chains per unit volume (ν_e) and the average molecular weight between crosslinks ($\overline{M_C}$, g/mol) can be defined by using Eq.4.3,

$$\frac{\rho}{\overline{M}_c}\left(1-\frac{2\overline{M}_c}{M_n}\right) = \nu_e\upsilon_2^{1/3} \tag{4.3}$$

where ρ is the density of the polymer in the swollen gel (1.27 g/cm^3) and M_n is the molecular weight of the linear polymer chains before crosslinking. The correction factor $\left\{1-2\overline{M_c}/M_n\right\}$ becomes negligible when $M_n \gg \overline{M_C}$ and the network is free of imperfections such as looped chains, chain entanglements and free chain ends that do not ideally contribute to the elastic stress.[39] Similar to NC gels, [9] considering the NR-PHEMA gels consist predominantly of crosslinked polymer chains rather than polymer chains with loops and free ends. The correction factor could be neglected.

Table 4.2 Network parameters and swelling ratios of hydrogels

c	$\overline{M_c}$ (g/mol)	ν_e (10^5.mol/cm^3)	S (%)
NS-PHEMA-1%	15,984	7.9	70±2.4
NR-PHEMA-**MH-10-0.1%**	87,210	1.5	92±2.6
NR-PHEMA -**MH-10-0.5%**	79,964	1.6	81±6.7
NR-PHEMA -**MH-10-1%**	139,822	0.9	128±8.4
NR-PHEMA -**MH-25-0.1%**	69,154	1.8	81±4.1
NR-PHEMA -**MH-25-0.5%**	61,717	2.1	80±4.6
NR-PHEMA **-MH-25-1%**	123,677	1.0	95±2.5

The shape of the strain-stress curves was similar to those reported in the literature.[10, 11] J-shaped curves indicating low modulus at low strains and high modulus at high strains with an instantaneous transition have been shown to be the result of increased toughness and strength in hydrogels designed for load-bearing applications. This behavior is also characteristic to many biological tissues that can be considered as natural gels. [40]

Compared to NS-PHEMA hydrogels, the transition from low modulus to high modulus was more pronounced for NR-PHEMA gels. Fig. 4.15 and Table 4.1 show the transition of compressive tangent modulus (E) with increasing compressive strain. Up to 60% strain, the modulus of NS-PHEMA gels was 3-5 fold higher than that of NR-PHEMA gels. In NS-PHEMA gels crosslinked with conventional crosslinkers, the distribution of chain lengths are broad because of the random distribution of crosslinking points. This might result in formation of large amounts of short chains with restricted mobility. Therefore, stress built up in NS-gels was higher than in NR-PHEMA gels in

this region. This phenomenon was in accordance with the average molecular weight between crosslinks ($\overline{M_c}$) calculated for NS-PHEMA gels which was 4-9 fold lower than that of NR-PHEMA gels (see Table 4.2). However, $\overline{M_c}$ values were rather high (up to about 130,000 g/mol) for NR-PHEMA gels.

Similar to the behavior of NC and MMC gels, the modulus values of NR-PHEMA gels were low compared to NS hydrogels because of the presence of very long flexible polymer chains between crosslinking points and the high mobility of these polymer chains in the water-swollen state. This was also the reason why NR-PHEMA gels were stretchable up to about 80% strains while the elongation of NS-PHEMA only amounted to 59% at the same applied stress level (see Table 4.1). However, the modulus values increased instantaneously when the strain was increased further. Surprisingly, tangent modulus values of NR-PHEMA gels above 80% strain were 5-19 times higher than values at 60% strain. Moreover, the modulus of NR-PHEMA gels ranged from 5.6 to 6.8 MPa which was significantly higher than NS- PHEMA (about 3.4MPa). A possible explanation for this sudden increase in modulus might be the restriction of the mobility of the long polymer chains in NR-PHEMA gels. At this strain region, the polymer chains between crosslinks were probably close to their full extension and their mobility was restricted because the water inside the hydrogels was squeezed out. It needs to be pointed out that no visible break or fracture was detected even at these high compressive strains and the samples recovered their original shape when the force was removed.

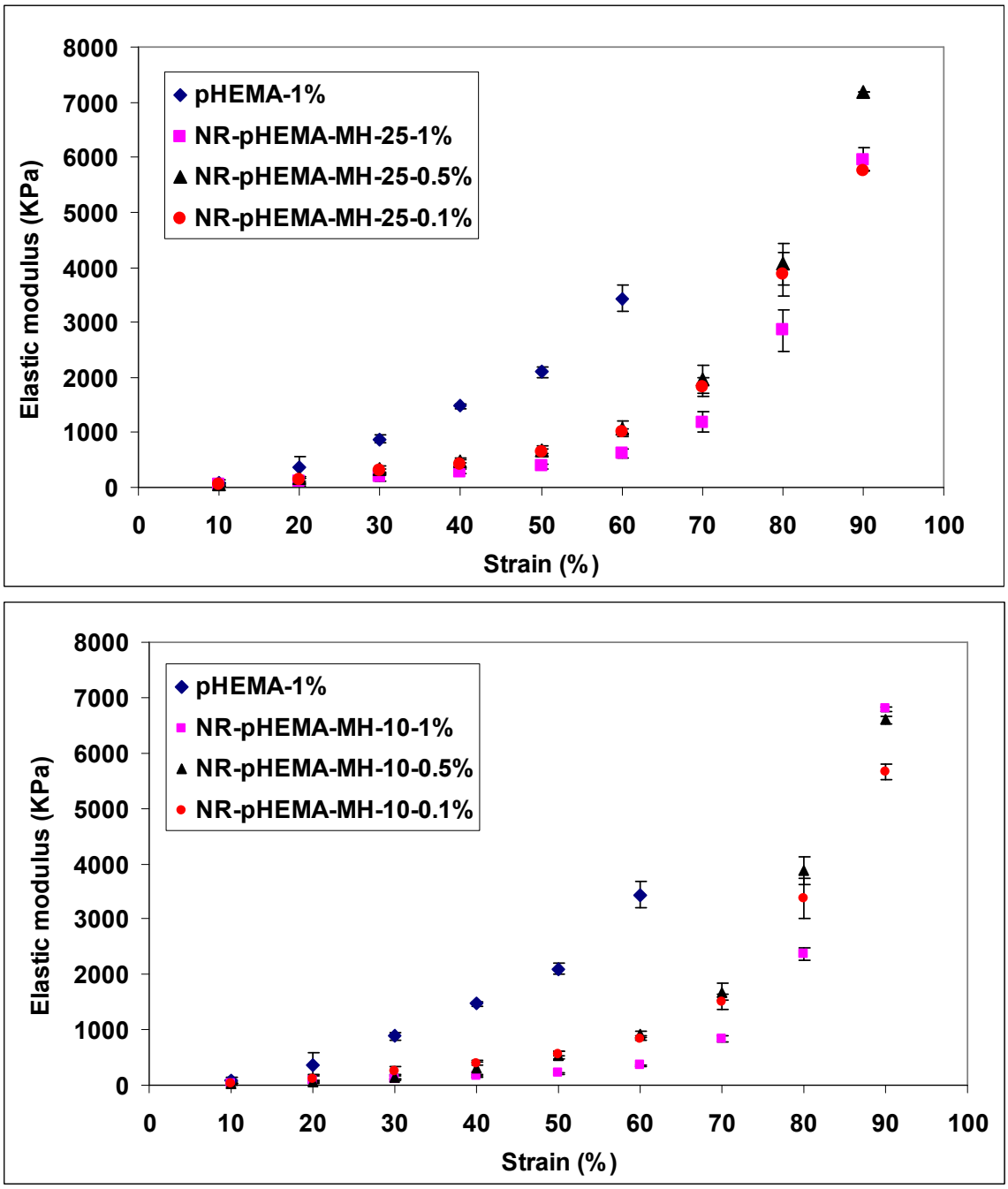

Figure 4.15 Tangent elastic modulus at 10% strain increments for NR-PHEMA hydrogels reinforced with different weight fractions of CNW a) coated with MH-10 b)coated with MH-25. Each data point represents the mean of triplicate values. Error bars represent the standard error. Control sample is NS-PHEMA hydrogel with 1%w/w EGDMA.

4.4.3.1 Effect of the degree of modification of hemicellulose

Assuming that the amount of methacrylated hemicellulose coated per unit gram of cellulose nanowhiskers (140-150 mg/g) was constant for MH-10 and MH-25, the influence of the degree of methacrylation on the mechanical properties of NR-PHEMA gels were evaluated. Tangent modulus values at 60% strain revealed that NR-PHEMA gels reinforced with MH-25 coated CNWs resulted in higher modulus compared to the gels reinforced with MH-10 coated CNWs. This result was consistent for each CNW weight fraction used in this study. Elastic shear modulus (G) values followed the same trend as well, even though the differences between data points were less pronounced.

One possible explanation for this trend might be the increase in the effective number of crosslinking chains (ν_e, crosslink density) with increasing methacrylic functionality at the surface of CNW. As can be seen in Table 4.2, for the same CNW weight fraction, ν_e values were high for samples loaded with MH-25 coated CNW. It is probable that with the increase in the amount of double bounds at the surface of CNW, the number of PHEMA polymer chains grafting from each CNW and the number of crosslinking chains connecting adjacent CNWs to each other increased. As a result, average length of the polymer chains between crosslinks decreased when the number of grafting sites on each CNW increased (see $\overline{M_c}$ values in Table 4.2). The main reason for enhanced modulus might be the denser network structure with shorter/more crosslinks formed in NR-PHEMA gels with MH-25 coated CNW.

4.4.3.2 Effect of CNW concentration

The concentration of MH coated CNW in the NR-PHEMA hydrogels were 0.1%, 0.5% and 1% w/w with respect to the amount of HEMA monomer used for the polymerization. The hypothesis was to decrease the average length of polymer chains between crosslinks ($\overline{M_c}$) by increasing the concentration of the CNW. Increasing the concentration of uniformly distributed nanowhiskers may reduce the distance between adjacent nanowhiskers, and therefore the average chain length of PHEMA chains that connect adjacent nanowhiskers may decrease proportionally. Another assumption was that the distribution of distance between individual nanowhiskers was quite narrow regardless of CNW concentration.

For both MH-10 and MH-25 coated CNW, as the CNW concentration increased from 0.1% to 0.5%, calculated $\overline{M_c}$ values decreased slightly which was in accordance with the outlined hypothesis. As a result, tangent moduli and shear moduli increased slightly with increasing CNW content. This was probably due to the formation of slightly shorter chains which had restricted mobility and easily reached their full extension. However, further increase in the CNW content to 1% w/w resulted in an unexpected increase in $\overline{M_c}$ and a decrease in modulus values. A possible reason for this may be the amount of water present inside the hydrogel during the compression testing. Since the polymer chains in NR-PHEMA gels are fairly large and mobile like in NC or MMS gels, it has been suggested that the influence of water content on hydrogels could be regarded as the effect temperature has on glassy polymers.[40] Therefore, flexible polymer chains of swollen hydrogels could behave like glassy polymers above their glass transition

temperature.[9] In NR-PHEMA gels with 1% CNW content, the swelling ratios were high probably due to the hydrophilic groups introduced through cellulose and hemicellulose (see Table 4.2). Higher water content resulted in lower modulus values and more rubbery like behavior. It could be expected that the assumed effect of CNW content of mechanical properties might be better evaluated when the water content in all NR-PHEMA hydrogels was comparable, for example, at higher compressive strains ($\varepsilon \geq 80\%$) when most of the water was squeezed out.

It needs to be pointed out that the CNW contents (0.1-1% w/w) used in this study was quite low compared to the nanoclay content in NC gels which ranged from 6.6% to 33% w/w with respect to amount of the monomer (N-isopropylacrylamide).[9,10] NR-PHEMA gels with higher CNW contents might be worthwhile to study in order to establish the accurate relationship between CNW content, network parameters and mechanical properties.

4.4.3.3 Stress relaxation

As mentioned in the previous sections, NR-PHEMA hydrogels did not fracture or break during the compression test despite the high compressive strains up to about 80%. One interesting observation was the almost complete recovery of these hydrogel to their original dimensions once force was released. This was probably due to the improved toughness or energy dissipation capability of these hydrogels. To further evaluate the time-dependant mechanical properties and the degree of the recovery of the hydrogels, stress relaxation tests were performed. Figure 4.16 shows the relative residual stress as a

function of time with respect to initial stress. Stress relaxation behavior of NS-PHEMA and NR-PHEMA hydrogels were significantly different. The relaxation rate of NR-PHEMA gels was apparently fast and the relative stress remaining after 20 min was quite low compared to that of NS-PHEMA gels. It took about 6-13 s for NR-PHEMA gels to relax 80% of the stress while it was about 460 s for NS-PHEMA gels (see Table 4.3). The residual stress of NS-PHEMA gels was about 77% of the initial stress and reached a plateau and without further decrease. However, in NR-PHEMA gels the residual stress could be as low as 11% and did not completely level off after 20 min. It has been shown that fast relaxation rate and low residual stress obtained from a stress relaxation test indicate high degree of recovery, good resilience and increased viscoelasticity.[41, 42] Good recovery properties of NR-PHEMA gels may be explained by the proposed network structure composed of long flexible PHEMA chains between uniformly distributed crosslinking points. In that manner the applied force could be easily distributed and the polymer chains were able return to their original conformations at a faster rate.

Table 4.3 Change in the relative residual stress during relaxation tests

	Time for 80% residual stress	Time for 50% residual stress	% Residual stress after 1200 s.
NS-PHEMA-1%	459	----	77
NR-PHEMA-**MH-10-0.1%**	6	43	15
NR-PHEMA -**MH-10-0.5%**	9	210	29
NR-PHEMA -**MH-10-1%**	6	32	8
NR-PHEMA -**MH-25-0.1%**	5	24	11
NR-PHEMA -**MH-25-0.5%**	13	240	31
NR-PHEMA -**MH-25-1%**	8	69	18

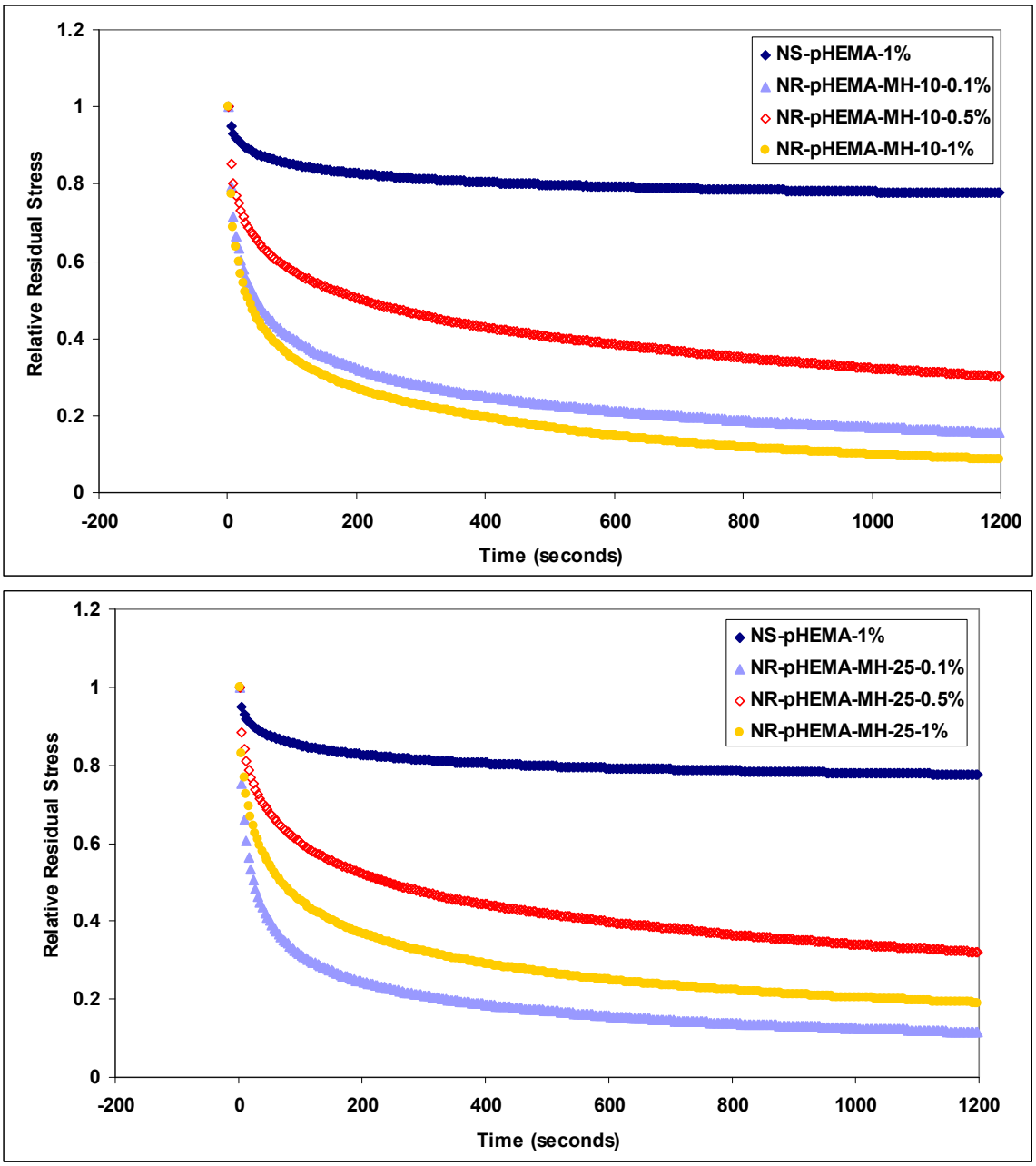

Figure 4.16 Change in the relative residual relaxation stress with time for NR-PHEMA hydrogels reinforced with different weight fractions of CNW a) coated with MH-10 b) coated with MH-25. Control sample is NS-PHEMA hydrogel with 1%w/w EGDMA.

4.4.3.4 Dynamic viscoelastic properties

Dynamical mechanical analysis is a nondestructive method used to characterize the viscoelastic properties of materials. An oscillatory strain or stress is applied to a material, resulting in stress or strain that can be measured. The response of a material to a sinusoidally varying force as a function of frequency or temperature is defined by the storage modulus, loss modulus and loss tangent. Storage modulus (E') represents the elastic response of a material and is proportional to the energy stored. Loss modulus (E'') represents the viscous response of the material and is proportional to the energy dissipated as heat. Loss tangent (tan δ) is the ratio of energy loss to energy stored (E"/E').[43]

NR-PHEMA hydrogels showed viscoelastic behavior evidenced by non-linear stress-strain response and time-dependant stress relaxation. To further study their viscoelastic properties, frequency sweep tests were performed to evaluate the dependence of modulus (E" and E') on loading frequency. Frequency was scanned between 0.1 to 80 Hz which has been reported to cover all physiological loading frequency in the human body during daily activities.[44] Figure 4.17 shows the viscoelastic behavior of NS-PHEMA gels with 1% crosslinker and NR-PHEMA gels, including 1% w/w CNW coated with MH-10 and MH-25. The E' and E" values of NS-PHEMA gels increased with increasing frequency and the value of E" came close to the value of E'. The increase in the value of E" means that the amount of energy dissipated as heat is significant due to the increased friction among polymer chains.[45] However, NR-PHEMA gels showed different viscoelastic behavior compared to NS-PHEMA gels. The value of E' slightly increased and reached a plateau at higher frequencies. The value of E" was much lower than the

value of E' over all frequencies and showed less dependency on frequency compared to that of NS-PHEMA gels. This result showed that more energy was stored in NR-PHEMA gels rather than was dissipated as heat which would be a characteristic behavior of an ideal elastomer in its rubbery state.[46] It is possible that there was less internal friction between polymer chains in NR-PHEMA gels as a consequence of its unique network structure and high water content. This might be the reason why NR-PHEMA gels relaxed at a faster rate to lower stresses and therefore had improved recovery.

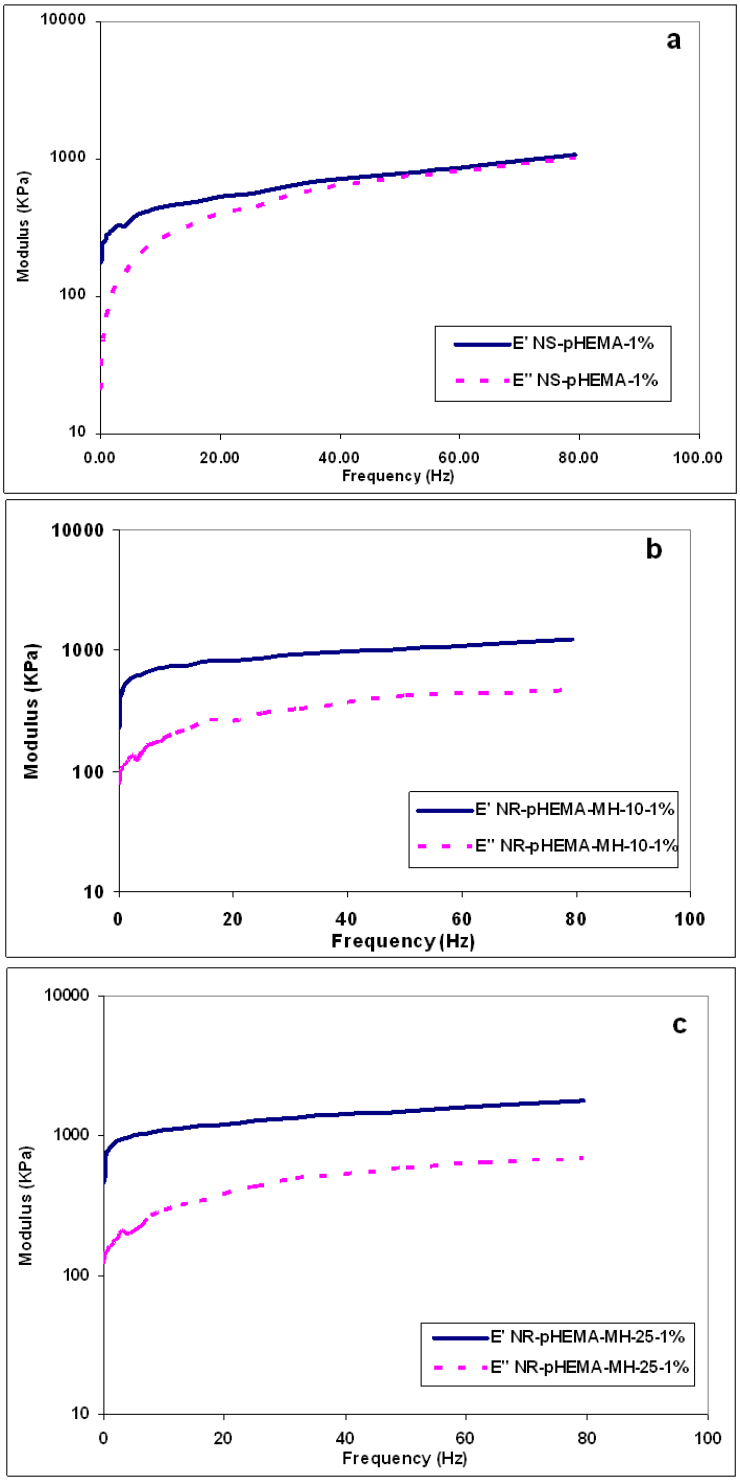

Figure 4.17 Storage (solid-line) and loss (dashed-line) modulus as a function of frequency for hydrogels a)NS-PHEMA-1% b)NR-PHEMA-MH-10-1% c)NR-PHEMA-MH-25-1%

4.4.4 Swelling

The water uptake of hydrogels in their equilibrium swollen state is shown in Table 4.2. NR-PHEMA gels had slightly higher swelling ratios (80-128%) compared to NS-PHEMA gels (70%). With the increase in the concentration of MH coated CNW, swelling ratio increased which might be as a result of the additional H-bounding between hydrophilic groups introduced by cellulose and hemicellulose. However, for the same CNW weight fraction, NR-PHEMA gels composed of MH-25 coated CNW had lower swelling ratios. Considering the average chain lengths between crosslinks and number of effective crosslinking chains given in Table 4.2, it might be suggested that the network parameters had a direct influence on the swelling ratios. With decreasing crosslink density and increasing $\overline{M_c}$, swelling ratios were high because more space was available for water molecules in the hydrogel network.

4.5 Conclusions

Cellulose nanowhiskers and hemicellulose extracted from renewable resources were used to prepare nanoreinforced hydrogels with unique network structure. Inspired by the plant cell wall matrix, intrinsic affinity of hemicellulose to cellulose was utilized for the surface modification of cellulose nanowhiskers. Chemically altered hemicelluloses carrying methacrylic functionality were adsorbed onto cellulose nanowhiskers in the aqueous medium. *In situ* radical polymerization of 2-hydroxyethylmethacrylate was carried out to synthesize nanoreinforced PHEMA hydrogels in the presence of surface functionalized cellulose nanowhiskers without using chemical crosslinking agents. Mechanical properties, swelling and viscoelasticity of

water-swollen hydrogels were investigated in regard to the hemicellulose degree of modification and cellulose nanowhisker content. Results showed that the number of effective crosslinks between polymer chains and the average chain length between crosslinking points had significantly different effects than crosslinked PHEMA hydrogels by conventional chemical crosslinkers. It was suggested that modified cellulose nanowhiskers acted like highly multifunctional crosslinking points. Uniform distribution of these large crosslinking sites allowed the formation of long crosslinks that increased the extensibility and toughness of the hydrogels. Non-linear J-shaped stress-strain curves obtained from uniaxial compression tests showed that nanoreinforced PHEMA hydrogels had potential to be used in load-bearing hydrogel applications. Stress relaxation and dynamical mechanical tests evidenced the increased viscoelasticity and enhanced recovery of as-synthesized PHEMA hydrogels.

One potential application of nanoreinforced PHEMA hydrogels prepared in this study would be human articular cartilage replacement. Articular cartilage is a load-bearing natural tissue within joints in the human body. To support and distribute loads and to provide lubrication in the diarthrodial joints are the main functions of the cartilage.[48] It is considered as a natural hydrogel reinforced with collagen fibrils and consist of 65-85% water in its structure. Hydrogels such as PVA have been suggested as biomaterials when the joint replacement is required in case of damaged or diseased cartilage tissue.[31] Articular cartilage is a viscoelastic material and shows non-linear strain response. Elastic modulus and fracture stress for human cartilage depend on its location in the body. It has been reported that elastic modulus of cartilage is in the range of 0.4-10

MPa and fracture stress is 78.6 MPa at 99.3% compressive strain.[11, 41] The fracture stress of hydrogels prepared in this study could not be determined because of the experimental difficulties. However, the other characteristics of nanoreinforced PHEMA hydrogels are similar to articular cartilage.

As a future work, it might be interesting to investigate the influence of higher cellulose nanowhisker contents (close its percolation threshold) on the network structure and mechanical properties of these hydrogels. In addition, the behavior of the hydrogels under cyclic compression tests and tensile tests would be worthwhile studying in order to match all of the properties of articular cartilage.

4.6 References

[1] Habibi, Y.; Lucia, L. A.; Rojas, O. J. Cellulose Nanocrystals: Chemistry, Self-Assembly, and Applications. *Chemical Reviews*. **2010**, 110 (6), 3479-3500.

[2] Lima, M. M. D.; Borsali, R. Rodlike Cellulose Microcrystals: Structure, Properties, And Applications. *Macromolecular Rapid Communications.* **2004**. 25, 771-787.

[3] Samir, M. A. S. A.; Alloin, F.; Dufresne, A. Review of Recent Research into Cellulosic Whiskers, Their Properties and Their Application in Nanocomposite Field. *Biomacromolecules*. **2005**, 6 (2), 612-626.

[4] Gatenholm, P.; Tenkanen, M. *Hemicelluloses: Science and Technology*, **2004**, 15-16. Oxford University Press.

[5] Ebringerova, A. Structural Diversity and Application Potential of Hemicelluloses. *Macromolecular Symposia.* **2006,** 232, 1-12.

[6] Zhou, Q.; Rutland, M. W.; Teeri, T. T.; Brumer, H.. Xyloglucan in Cellulose Modification. *Cellulose*. **2007**, 14, 625-641.

[7] Peppas, N. A.; Hilt, J. Z.; Khademhosseini, A.; Langer, R. Hydrogels in Biology and Medicine: From Fundamentals to Bionanotechnology. *Advanced Materials*, **2006**, 18, 1345.

[8] Slaughter, B. V.; Khurshid, S. S.; Fisher, O. Z.; Khademhosseini, A.; Peppas, N. A. Hydrogels in Regenerative Medicine. *Advanced Materials*, **2009**, 21, 1-23.

[9] Haraguchi, K.; Takehisa, T.; Fan, S. Effects of Clay Content on the Properties of Nanocomposite Hydrogels Composed of Poly(N-isopropylacrylamide) and Clay. *Macromolecules.* **2002,** 35, 10162-10171.

[10] Haraguchi, K.; Takehisa, T. Nanocomposite Hydrogels: A Unique Organic–Inorganic Network Structure with Extraordinary Mechanical, Optical, and Swelling/De-swelling Properties. *Advanced Materials.* **2002,** 14, 1120–1124.

[11] Huang, T.; Xu, H.; Jiao, K.; Zhu, L.; Brown, H. R.; Wang, H. A Novel Hydrogel with High Mechanical Strength: A Macromolecular Microsphere Composite Hydrogel. *Advanced Materials*. **2007**, 19, 1622–1626.

[12] Bryant, S.J.; Janet, L.C.; Hauch, K.D.; Ratner, B.D. Photo-patterning of porous hydrogels for tissue engineering. *Biomaterials.* **2007**, 28, 2978-2986.

[13] Karaaslan, M. A.; Tshabalala, M.; Buschle-Diller, G. Wood Hemicellulose/Chitosan-Based Semi-Interpenetrating Network Hydrogels: Mechanical Swelling and Controlled Drug Release Properties. *Bioresources*, **2010**, 5, 1036.

[14] Beck-Candanedo, S.; Roman, M.; Gray, D.G., Effect of Reaction Conditions on the Properties and Behavior of Wood Cellulose Nanocrystal Suspensions. *Biomacromolecules.,* **2005**, 6, 1048-1054.

[15] Dong, M.X.; Revol, J.F.; Gray, D.G. Effect of Microcrystallite Preparation Conditions On The Formation Of Colloid Crystals Of Cellulose. *Cellulose*. **1998**, 5, 19-32.

[16] Ranucci, E.; Spagnoli, G.; Ferruti, P., 2-[(1-imidazolyl)formyloxy]ethyl methacrylate as a new chemical precursor of functional polymers. *Macromolecular Rapid Communications.* **1998**, 20, 1-6.

[17] Lindblad, M. S.; Ranucci, E.; Albertsson, A. Biodegradable Polymers from Renewable Sources.New Hemicellulose-Based Hydrogels. *Macromolecular Rapid Communications.* **2001**, 22, 962-967.

[18] Gröndahl, M.; Teleman, A.; Gatenholm, P. Effect of acetylation on the material properties of glucuronoxylan from aspen wood. *Carbohydrate Polymers.* **2003,** 52, 359-366.

[19] Köhnke, T.; Brelid, H.; Westman, G. Adsorption of cationized barley husk xylan on kraft pulp fibres: influence of degree of cationization on adsorption characteristics. *Cellulose*, **2009**, 16, 1109-1121.

[20] Capadona, J.R.; Van Den Berg, O.; Capadona, L.A.; Schroeter, M.; Rowan, S.; Tyler, D. J.; Weder, C. A Versatile Approach for the Processing of Polymer Nanocomposites with Self-Assembled Nanofibre Templates, *Nature Nanotechnology*, **2007**, 2, 765-769.

[21] Gaillard, B.D.E.; Thompson, N.S. Interaction of Polysaccharides with Iodine. Part II. The Behavior of Xylans in Different Salt Solutions. *Carbohydrate Research*. **1971**, 18, 137–146.

[22] Lindblad, M.S.; Albertsson, A.C.; Ranucci, E.; Laus, M.; Giani, E. Biodegradable Polymers from Renewable Sources: Rheological Characterization of Hemicellulose-Based Hydrogels. *Biomacromolecules.* **2005,** 6, 684-690.

[23] Favier, V; Dendiel, R; Canova, G.; Cavaille, J.Y.; Gilormini, P. Simulation and Modelling of 3D percolating structures: Case of a latex matrix reinforced by a network of cellulose whiskers. *Acta Materilia*. **1997**, 45, 1557-1565.

[24] Teeri, T. T.; Brumer, H.. Daniel, G.; Gatenholm, P. Biomimetic engineering of cellulose-based materials. *Trends in biotechnology.* **2007**, 25, 299-306.

[25] Carpita, N. C.; Gibeaut, D. M. Structural Models of Primary Cell Walls in Flowering Plants: Consistency of Molecular Structure with the Physical Properties of the Walls during Growth. *The Plant Journal*. **1993**, 3, 1–30.

[26] Jean, B.; Heux, L.; Dubreuil, F.; Chambat, G.; Cousin, F. Non-Electrostatic Building of Biomimetic Cellulose−Xyloglucan Multilayers. *Langmuir.* **2009,** 25*,* 3920-3923.

[27] Zhou, Q.; Greffe, L.; Baumann, M. J.; Malmström, E.; Teeri, T. T.; Brumer, Harry. Use of Xyloglucan as a Molecular Anchor for the Elaboration of Polymers from Cellulose Surfaces: A General Route for the Design of Biocomposites. *Macromolecules.* **2005**, 38, 3547–3549

[28] Henriksson Å.; Gatenholm, P. Controlled Assembly of Glucuronoxylans onto Cellulose Fibres. *Holzforschung*. **2001**, 55, 494–502.

[29] Köhnke, T. Adsorption of Xylans on Cellulosic Fibres: Influence of Xylan Composition on Adsorption Characteristics and Kraft Pulp Properties. Dissertation, **2010,** Chalmers University of Technology. Göteborg,.

[30] Linder, Å.; Gatenholm, P. Effect of Cellulose Substrate on Assembly of Xylan, *ACS Symposium Series Vol.* 864, *Hemicelluloses: Science and Technology.* **2004**, 236–253.

[31] Bodin, A.; Ahrenstedt, L.; Fink, H.; Brumer, H.; Risberg, B.; Gatenholm, P. Modification of Nanocellulose with a Xyloglucan–RGD Conjugate Enhances Adhesion and Proliferation of Endothelial Cells: Implications for Tissue Engineering. *Biomacromolecules,* **2007**, 8, 3697-3704.

[32] Zhou,Q.; Brumer, H.; Teeri, T.T. Self-Organization of Cellulose Nanocrystals Adsorbed with Xyloglucan Oligosaccharide-Poly(ethyleneglycol)-Polystyrene Triblock Copolymer. *Macromolecules.* **2009**, 42, 5430–5432.

[33] Pranger, L.; Tannenbaum, R.Biobased Nanocomposites Prepared by In Situ Polymerization of Furfuryl Alcohol with Cellulose Whiskers or Montmorillonite Clay, *Macromolecules.* **2008**, 41, 8682-8687.

[34] Morandi, G.; Heath, L.; Thielemans, W. Cellulose Nanocrystals Grafted with Polystyrene Chains through Surface-Initiated Atom Transfer Radical Polymerization (SI-ATRP). *Langmuir.* **2009**, 25, 8280– 8286.

[35] Samir, M. A. S. A.; Alloin, F.; Dufresne, A. Review of Recent Research into Cellulosic Whiskers, Their Properties and Their Application in Nanocomposite Field. *Biomacromolecules*. **2005**, 6 (2), 612-626.

[36] Sturcova, A.; Davies Geoffrey, R.; Eichhorn Stephen, J. Elastic Modulus and Stress-Transfer Properties of Tunicate Cellulose Whiskers. *Biomacromolecules*. 2005, 6, 1055–1061.

[37] Haraguchi, K.,; Farnworth, R.; Ohbayashi, A.; and, Takehisa, T. Compositional Effects on Mechanical Properties of Nanocomposite Hydrogels Composed of Poly(N,N-dimethylacrylamide) and Clay. *Macromolecules.* **2003,** 36, 5732-5741.

[38] Stammen, J. A.; Williams, S.; Ku, D. N.; Guldberg, R. E. Mechanical Properties of a Novel PVA Hydrogel in Shear and Unconfined Compression. *Biomaterials.* **2001**, 22, 799-806.

[39] Anseth, K. S.; Bowman, C. N.; Bannon-Peppas, L. Mechanical Properties of Hydrogels and their Experimental Determination. *Biomaterials.* **1996,** 17, 1647-1657.

[40] Calvert, P. Hydrogels for Soft Machines. *Advanced Materials*. **2009**, 21, 743–756.

[41] Millon, L. E.; Oates, C. J.; Wan, W. Compression Properties of Polyvinyl Alcohol-Bacterial Cellulose Nanocomposite. *Journal of Biomedical Materials Research Part B: Applied Biomaterials*. **2009**, 90B, 922–929.

[42] Lv, S.; Dudek, D. M.; Cao, Y.; Balamurali, M. M.; Gosline, J.; Li, H. Designed biomaterials to mimic the mechanical properties of muscles. *Nature*. **2010**, 465, 69-73.

[43] Jones, D. S. Dynamic Mechanical Analysis of Polymeric Systems of Pharmaceutical and Biomedical Significance. International Journal of Pharmaceuticals. 1999, 179, 167-178.

[44] Meakin, J. R.; Hukins, D. W. L.; Aspden, R. M.; Imrie, C. T. Rheological properties of poly(2-hydroxyethyl methacrylate) (PHEMA) as a function of water content and deformation frequency. *Journal of Material Science: Materials in Medicine*. **2003**, 14, 783-787.

[45] Hafeman, A.E.; Li, B; Yoshii, T.; Zienkiewicz, K.; Davidson, J. M.; Guelcher, S. A. Injectable Biodegradable Polyurethane Scaffolds with Release of Platelet-derived Growth Factor for Tissue Repair and Regeneration. *Pharmaceutical Research*. **2008**, 10, 2387-99.

[46] Fulcher, G. R.; Hukins, D.W.L.; Shepherd, D. E. T. Viscoelastic Properties Of Bovine Articular Cartilage Attached To Subchondral Bone At High Frequencies. *BMC Musculoskel Disorders*. **2009**, 10, 61-68.

[48] Boschetti, F.; Pennati, G.; Gervaso, F.; Peretti, G. M.; Dubini,G. Biomechanical properties of human articular cartilage under compressive loads. *Biorheology*. **2004**, 41, 159-166.

[49] http://en.wikipedia.org/wiki/Cell_wall accessed on 04/05/2011)